

Worcester Polytechnic Institute

Digital WPI

Major Qualifying Projects (All Years)

Major Qualifying Projects

2020-05-07

Lignocellulosic Hydrolysate Detoxification for the Production of Second Generation Ethanol

Mackenzie Sarah Karnilaw
Worcester Polytechnic Institute

Follow this and additional works at: <https://digitalcommons.wpi.edu/mqp-all>

Repository Citation

Karnilaw, M. S. (2020). *Lignocellulosic Hydrolysate Detoxification for the Production of Second Generation Ethanol*. Retrieved from <https://digitalcommons.wpi.edu/mqp-all/7372>

This Unrestricted is brought to you for free and open access by the Major Qualifying Projects at Digital WPI. It has been accepted for inclusion in Major Qualifying Projects (All Years) by an authorized administrator of Digital WPI. For more information, please contact digitalwpi@wpi.edu.



WPI



UNICAMP

Lignocellulosic Hydrolysate Detoxification for the Production of Second Generation Ethanol

A Major Qualifying Project Report

Submitted to the Faculty of

WORCESTER POLYTECHNIC INSTITUTE

In partial fulfillment of the requirements for the
Degree of Bachelor of Science

May 7, 2020

Submitted by:

Mackenzie S. Karnilaw, Chemical Engineering

Submitted to:

Professor Michael T. Timko, Chemical Engineering

Abstract

Due to climate change and the depletion of fossil fuel-based energy, there is a growing need for alternative sources of energy. One growing alternative source of energy is second generation ethanol. Unlike fossil fuels, ethanol can be produced from lignocellulosic biomass and significantly reduces greenhouse gas emissions such as carbon dioxide. Before lignocellulosic biomass can be fermented to create ethanol, it undergoes hydrolysis to break down the coarse structure of the biomass. The main goal of this pretreatment step is to increase the surface area of carbohydrates while reducing the creation of ethanol production inhibitors, such as furanic compounds, phenols, and weak acids. Detoxification methods to remedy the lignocellulosic hydrolysate must successfully remove inhibitors without affecting the concentration of sugars. Activated carbon adsorption is currently the most common method used to detoxify lignocellulosic biomass. In a report by Heinonen et al., the saturation capacity of activated carbon was found to be 75 g/g for both HMF and furfural, while only being 4 g/g for glucose [48]. The goal of this project was to determine if biochar can replicate activated carbon adsorption to create a more environmentally and economically beneficial process. The experiment determined that biochar is not able to adsorb fermentation inhibitors at a large enough capacity to replace activated carbon. The found saturation capacity of all the biochars was less than 34 mg/g and 20 mg/g for 5-hydroxymethylfurfural and furfural respectively.

Acknowledgements

I would like to thank individuals at both Worcester Polytechnic Institute (WPI) in Worcester, Massachusetts, and the University of Campinas (UNICAMP) in São Paulo Brazil. I would like to extend gratitude to both Professor Tânia Foster Carneiro and Mauricio Ariel Rostango for helping to structure and complete my project while I was in Brazil. Also, I would like to thank both Tatiane Cristina Gonçalves de Oliveira and Paulo Cesar Torres Mayanga for taking the time to work with me in the lab every day, as well as for welcoming me into Brazil. I would also like to thank Daniel Lachos Perez, Maria Paula Jiménez Castro, and Larissa Castro Ampese for always helping me out in the lab whenever they could. Lastly, I would like to extend my gratitude to my professor Michael Timko for guiding me throughout the process of working in a lab abroad, advising me how to write a technical research paper, and for allowing me to take part in this amazing opportunity.

Table of Contents

Abstract	2
Acknowledgements	3
Table of Contents	4
List of Figures	7
List of Tables	9
1. Introduction	10
2. Background	12
2.1 Biofuel	12
2.1.1 First Generation Biofuel	12
2.1.2 Second Generation Biofuel	13
2.1.3 Third Generation Biofuel	14
2.2 Ethanol in Brazil	15
2.3 Sugarcane as a Feedstock	15
2.4 Lignocellulose Biomass	17
2.4.1 Cellulose	17
2.4.2 Hemicellulose	17
2.4.3 Lignin	18
2.5 Hydrolysis	18
2.5.1 Acid Hydrolysis	18
2.5.2 Enzymatic Hydrolysis	18
2.5.3 Subcritical Water Hydrolysis	19
2.6 Fermentation	19
2.7 Fermentation Inhibitors	19
2.7.1 Furfural	20
2.7.2 5-Hydroxymethylfurfural (5-HMF)	21
2.7.3 Other Fermentation Inhibitors	22
2.8 Detoxification Methods of Lignocellulose Hydrolysate	23
2.8.1 Vacuum Evaporation	23
2.8.2 Membrane Separation	23
2.8.3 Activated Carbon Adsorption	23
2.8.4 Solvent Extraction	24
2.8.5 Ion Exchange Resins	25
2.8.6 Overliming with Calcium Hydroxide	25
2.8.7 Enzymatic Detoxification	25
2.9 Biochar	25
3. Materials and Methods	27
3.1 Raw Materials and Chemicals	27

3.2 Characterization of Adsorbent: Total and Volatile Solids	27
3.3 Detoxification of the Lignocellulose Hydrolysates	28
3.3.1 Activating the Biochar	28
3.3.2 Continuous Fixed Bed Adsorption	28
3.4 Analysis of Purified Solution	31
3.4.1 PH	31
3.4.2 High Performance Liquid Chromatography (HPLC) for Sugars	32
3.4.3 HPLC for Inhibitors	32
3.4.4 Deciphering HPLC Results	33
3.4.5 Determining Saturation Capacity from a Breakthrough Curve	34
3.4.6 Determining Breakthrough Capacity from a Breakthrough Curve	35
4. Results and Discussions	37
4.1 Characterization of the Biochar	37
4.1.1 Physical Characteristics of the Biochar	37
4.1.2 Total and Volatile Solids Analysis	38
4.1.3 pH Analysis	40
4.2 Analysis of Effluent	40
4.2.1 Activated Carbon	41
4.2.2 Biochar 1	42
4.2.3 Biochar 2	44
4.2.4 Biochar 4	45
4.2.5 Biochar 5	46
4.2.6 Biochar 6	46
4.2.7 Activated Biochar 4	47
4.2.8 pH Analysis	48
4.3 Adsorption Characterization	50
4.3.1 Saturation Capacity	50
4.3.2 Breakthrough Capacity	51
4.4 Fermentation of Detoxified Lignocellulosic Hydrolysate	52
5. Conclusion and Recommendations	55
References	57
Appendix	63
Data 1: Total and Volatile Solid Percentage	63
Data 2: pH of the Adsorbent	64
Data 3: Positive Displacement Pump Raw Data for Weight of Adsorbent, Weight of Residue, and Time	65
Data 4: CO2 Peltier Pump Raw Data for Weight of Adsorbent, Weight of Residue, and Time	66
Data 5: HPLC Standard Curve for Carbohydrates and Inhibitors	67
Data 6: HPLC Raw Data for Trials with the Positive Displacement Pump	68
Data 7: Concentration Profile for Trials with the Positive Displacement Pump	69

Data 8: Positive Displacement Pump Cx/Co Values	70
Data 9: HPLC Raw Data for Trials with the CO2 Peltier Pump	71
Data 10: Concentration Profile for Trials with the CO2 Peltier Pump	72
Data 11: CO2 Peltier Pump Cx/Co and Normalized Cx/Co Values	73
Data 12: pH of the Collected Effluents for the Positive Displacement Pump	74
Data 13: pH of the Collected Effluents for the CO2 Peltier Pump	75
Data 14: Saturation and Breakthrough Capacity, Calculated from Results from the CO2 Peltier Pump	76
Data 15: Percent Ethanol Produced from Detoxified Lignocellulose Biomass	77
Appendix B: Sample Calculations	78
Sample Calculation 1: Total and Volatile Solid	78
Sample Calculation 2: Ratio of Adsorbent to Adsorbate	79
Sample Calculation 3: Ergun Equation	80
Sample Calculation 4: Interpretation of HPLC data of Glucose	81
Sample Calculation 5: Normalizing a Breakthrough Curve	82
Sample Calculation 6: Saturation Capacity	83
Sample Calculation 7: Breakthrough Capacity	84
Sample Calculation 8: Percent Ethanol Produced from Detoxified Lignocellulose Biomass	85
Appendix C: Images	86
Image 1: Biochar 1, Cool Terra	86
Image 2: Biochar 2, Blak 1	86
Image 3: Biochar 3, Rogue Biochar	87
Image 4: Biochar 4, Gold Standard	87
Image 5: Biochar 5, Art 1	88
Image 6: Biochar 6, Wakefield	88
Image 7: Photograph of the Supercritical Peltier CO2 Pump Display.	89

List of Figures

Figure 1. A flow chart of a typical process to produce ethanol from sugarcane bagasse.	10
Figure 2. The anatomy of a sugarcane plant.	16
Figure 3. Photograph of crushed sugarcane bagasse.	16
Figure 4. Degradation of lignocellulose biomass into its constituent monomers and oligomers.	20
Figure 5. Structure of furfural.	20
Figure 6. Ethanol produced from <i>S. cerevisiae</i> in the presence of 0.5, 1, and 2 g/L of furfural.	21
Figure 7. Structure of 5-Hydroxymethylfurfural.	21
Figure 8. Ethanol produced from <i>S. cerevisiae</i> in the presence of 1, 3, and 5 g/L of 5-HMF.	22
Figure 9. Photograph of the six biochar donated by NextChar.	27
Figure 10. Schematic of the continuous adsorption system.	29
Figure 11. Photograph of the continuous adsorption system.	29
Figure 12. The correct packing and orientation of the column and a photograph of the column.	30
Figure 13. Photographs of preparing the effluents for HPLC analysis.	30
Figure 14. Photograph of activated carbon and biochar after they were removed from the column.	30
Figure 15. Photograph of the experimental set-up with the supercritical Peltier CO ₂ pump.	31
Figure 16. Photograph of the HPLC unit.	32
Figure 17. Screen capture of the HPLC peaks for inhibitors.	33
Figure 18. Illustration of the definition of saturation capacity.	35
Figure 19. Illustration of the definition of the breakthrough capacity.	36
Figure 20. Photograph of biochar 2 and 5.	38
Figure 21. The pH of ultrapure water collected at the end of a fixed bed packed with biochar.	40
Figure 22. The breakthrough curves for sugars and inhibitors, when using the positive displacement pump and activated carbon as the adsorbent.	41
Figure 23. The breakthrough curves for sugars, when using the CO ₂ Peltier Pump and activated carbon as the adsorbent.	42
Figure 24. The breakthrough curves for sugars and inhibitors, when using the positive displacement pump and biochar 1 as the adsorbent.	43
Figure 25. The breakthrough curves for sugars, when using the CO ₂ Peltier Pump and biochar 1 as the adsorbent.	44
Figure 26. The breakthrough curves for sugars and inhibitors, when using the CO ₂ Peltier Pump and biochar 2 as the adsorbent.	44
Figure 27. The breakthrough curves for inhibitors, when using the CO ₂ Peltier Pump and biochar 4 as the adsorbent.	45

Figure 28. The breakthrough curves for inhibitors, when using the CO₂ Peltier Pump and biochar 5 46
as the adsorbent.

Figure 29. The breakthrough curves for inhibitors, when using the CO₂ Peltier Pump and biochar 6 47
as the adsorbent.

Figure 30. The breakthrough curves for inhibitors, when using the CO₂ Peltier Pump and activated 48
biochar 4 as the adsorbent.

Figure 31. pH of the effluent for each volume collected. 49

Figure 32. Percent of ethanol produced from lignocellulosic hydrolysate detoxified by biochar 2, 4, 53
5, 6, and activated biochar 4.

List of Tables

Table 1. HPLC retention times for all six compounds..	34
Table 2. Observable physical attributes of the six biochar.	37
Table 3. Percentage of total and volatile solids present in the biochar.	39
Table 4. pH of the hydrolysate mixture taken before the beginning of each trail.	49
Table 5. The saturation capacity of all adsorbents.	50
Table 6. The breakthrough capacity of all adsorbents.	52
Table 7. The concentration of 5-HMF and furfural, found in the effluent after detoxification.	53

1. Introduction

As developing countries become more industrialized, worldwide energy consumption will rise in unison. However, due to the irreversible environmental damage caused by the use of fossil fuels, alternative sources of energy are a necessity. These alternative energies must be sustainable, environmentally benign, and produced from renewable sources [51].

One alternative source of energy that has been growing in demand is ethanol. Unlike fossil fuels, ethanol can be produced from a variety of different biomass feedstock, and significantly reduces greenhouse gas emissions such as carbon dioxide. The environmental benefits of ethanol combined with the renewability of the fuel make it a preferred substitute for fossil fuels. However, there is one main drawback to using ethanol as a fuel source. Because ethanol is produced from biomass, land that is typically used to produce food must be allocated towards growing feedstock for ethanol production. This creates a conflict between the food and fuel industries leading to large socio-economic debates [51].

Therefore, it is crucial to develop a method for producing ethanol that does not directly compete with food sources. One possible approach to this method is the production of ethanol from industrial byproducts or lignocellulosic biomass. Currently, these feedstocks are underutilized and their production would not interfere with arable land needed for food production. Specifically, in Brazil there is an ample supply of sugarcane bagasse, therefore it has become a common feedstock for ethanol fermentation there.

However, before the sugarcane bagasse can be fermented it must undergo a pretreatment process. The fermentation process with pretreatment steps is shown in the flowchart below in Figure 1.

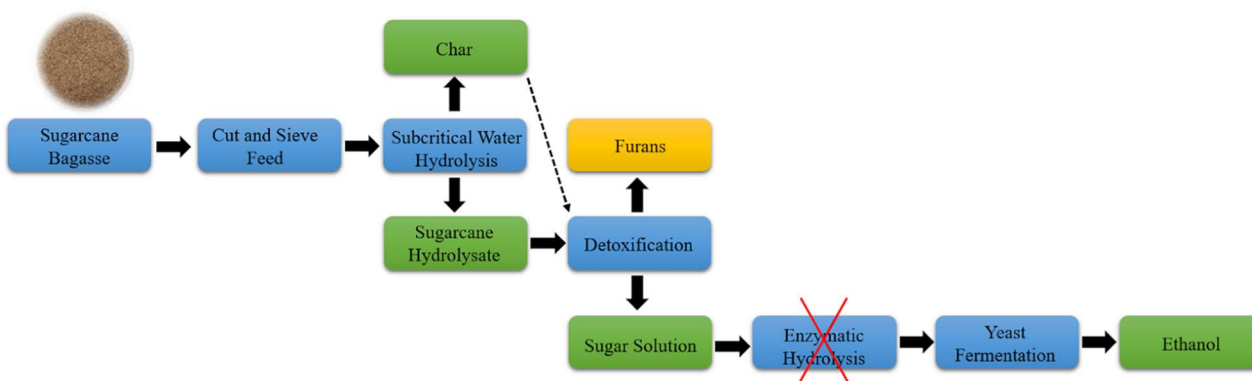


Figure 1. A flow chart of a typical process to produce ethanol from sugarcane bagasse. The blue rectangles show the normal pathway of the process, the yellow rectangles show the waste products, and the green rectangles show the preferred products. The sugarcane bagasse is cut to the appropriate size for subcritical water hydrolysis. The two byproducts of subcritical water hydrolysis are char and sugarcane hydrolysate; the char could be reused for detoxification but is most often a waste product. The hydrolysate is then detoxified, and the fermentation inhibitors are removed. The sugar solution then does not require enzymatic hydrolysis to be fermented and can be directly fermented to produce ethanol.

Pretreatment's main purpose is to break down the dense spatial structure of lignocellulosic material into its constituent monomers and oligomers. This step allows the yeast (*S. cerevisiae*) to then produce ethanol as

a metabolic byproduct. The process is typically mechanical, however, due to the strength and structure of lignocellulosic biomass, it must be pretreated chemically. During this process, the three structural components of lignocellulosic biomass: cellulose, hemicellulose, and lignin, are deconstructed.

Lignocellulosic biomass can be pretreated using a new method, subcritical water hydrolysis. Subcritical water is heated to its boiling point temperature but maintained at a high pressure, which prevents the water from transitioning to a gaseous state. Under these conditions, water gains unique properties that allow it to hydrolyze the biomass. However, subcritical water hydrolysis is a very uncontrolled process, so several degradation products are produced along with the desired sugar products. These degradation products are toxic to the yeast used for fermentation and are commonly referred to as fermentation inhibitors. The most common fermentation inhibitors are furfural, 5-hydroxymethylfurfural, phenol compounds, and organic acids.

Therefore, before fermentation can occur, the hydrolysate must undergo a detoxification process to remove the inhibitors without drastically affecting the sugar concentration. This step is either a physical, chemical, or biological process. The detoxification method depends not only on the lignocellulosic feedstock used but also on the yeast used for fermentation. One of the most common detoxification methods for sugarcane bagasse is an adsorption process using activated carbon adsorbent. Currently, activated carbon adsorption is a preferred method for detoxification because it is an environmentally benign process, is affordable, and has high selectivity.

Recently, there has been a rising interest in the use of biochar as an alternative adsorbent to activated carbon. Biochar is a pyrogenic, carbon product, synthesized through thermal degradation of biomass. Biochar contains many of the same characteristics as activated carbon and therefore could possess the same adsorption qualities as activated carbon, such as the ability to selectively remove fermentation inhibitors without affecting the concentration of sugars.

The main objective of this project will be to question whether biochar is able to adsorb inhibitor compounds from lignocellulosic biomass as efficiently or better than activated carbon. By calculating and testing the saturation capacity and breakthrough capacity of activated carbon and an assortment of biochars, concrete conclusions on the practicality of using biochar as a sorbent for detoxifying lignocellulosic biomass can occur. The implications of using biochar instead of activated carbon are endless. Biochar is not only easier produced than activated carbon, but it also releases less greenhouse gas emissions during production and is significantly cheaper. Therefore, the replacement of activated carbon with biochar is favorable not only for environmental reasons but also economical. In this paper, the results of the sorption properties of both biochar and activated carbon are reported and discussed.

2. Background

As of 2018, the world temperature has increased at an average rate of 0.07 °C per decade since 1880, totaling to an increase of about 1°C. Due to the vast size and heat capacity of the oceans, it requires a tremendous amount of heat energy to raise the temperature of the Earth [32]. The burning of fossil fuels and coal are attributed as the main reason there has been such a large increase in greenhouse gas emissions in the atmosphere. Once these gases are released into the atmosphere, they trap in the heat radiating off of Earth's surface, causing the Earth's temperature to gradually rise over time and thus producing irreversible damage to Earth's biosphere [65] [46]. Furthermore, due to the development and growth of the world's population the need for energy has also increased. This change in energy consumption and production spurs the need for the advancement of alternative resources to replace fossil fuels. These alternative energy sources are integral in limiting the amount of greenhouse gases produced [20].

2.1 Biofuel

The idea of sustainable development, or development that meets the current energy needs without hindering future generations from meeting their own energy needs, has led to the creation of energy sources that come from renewable feedstocks [44]. Biofuel, which are fuels derived directly from biomass, is a type of renewable energy source [56]. There are two main types of biofuel: ethanol and biodiesel, both of which can be used to meet transportation and fuel needs [66]. Because biofuels are regarded as a “cost effective environmentally friendly benign alternative” to fossil fuels and petroleum, their production and growth has increased rapidly, mainly in Brazil and the United States of America (USA) [56]. However, the growth of biofuels has had its share of controversy, particularly because they contribute to monoculture, rising food prices, and deforestation. Because of this, there has been a push to produce biofuels from non-food biomass. These biofuels are not only less water intensive, but they also utilize otherwise discarded agricultural residues [18]. These biofuels are commonly known as second generation biofuel.

2.1.1 First Generation Biofuel

Currently, there are three different classifications of biofuels. First generation biofuels refer to fuels which are created directly from biomass or edible sources. Both biodiesel and bioethanol (ethanol) can be created by means of first generation, however the feedstocks required to create the two differ vastly. Ethanol is commonly produced from sugarcane or corn, but can also be produced from whey, barely, potato wastes, and sugarbeets. Biodiesel on the other hand requires a feedstock of oily plants and seeds [55].

In addition, the processes used in the production of these two biofuels are very different. However, before either ethanol or biodiesel are created the crops must be harvested. Ethanol is produced by crushing sugarcane with water to remove any sucrose, thus producing a juice like substance. Then, the juice is purified to remove any unwanted organic compounds such as fructose and glucose [27]. Lastly, the juice is fermented to produce ethanol. If the feedstock is corn, the process is slightly more complex. Corn consists of starch and sugar, so it must be pretreated using hydrolysis to separate the sugars and starch. After the starch is pretreated it can be fermented into ethanol [55]. Ethanol is currently the largest biofuel produced worldwide and its production is led by both Brazil and the USA. Currently, these countries utilize corn and sugarcane as the main feedstock. Europe also produces ethanol, however their feedstock is potato, wheat,

or sugar beet [7]. The production of biodiesel varies vastly from the production of ethanol, in that it is a chemical process that utilizes transesterification. Transesterification works by breaking the bonds that connect the glycerol to the long chain fatty acids, and replacing the glycerol with methanol. This creates a methyl [55]. Most often the biodiesel must be distilled to remove the glycerol before the biodiesel can be used. Currently, biodiesel is mainly used for transportation and energy generation. Biofuel that is produced from biomass has gained popularity since the early 90s because of the simplicity of conversion technology and the greenhouse gas savings [34].

However, the success of first generation biofuels has also been met with wide opposition. The feedstock of first generation biofuels is primarily a source of food, thus resulting in food-fuel competition. This link between biofuel and food security has caused some developing countries such as China and India to prohibit the use of food crops towards biofuel production [55]. In 2005, when only 2% of the available arable land was being utilized for the production of biomass feedstock, there was still an increase in the commodity prices for food as well as animal feed [34]. This example highlights the need for a biofuel that does not utilize a food source as a feedstock or monopolize large plots of arable land.

2.1.2 Second Generation Biofuel

The second classification of biofuels are referred to as second generation biofuels. Unlike first generation biofuels, second generation biofuels are produced from an array of low-value feedstocks, such as lignocellulosic energy crops, agricultural residues, and municipal waste [18]. Additionally, these feedstocks are arranged into three different categories, the first category being homogenous. One example of homogenous feedstock is wood chips. The second category is quasi-homogeneous which encompasses all agricultural and forest residues. The last category is non-homogenous, which usually includes the lowest value feedstock, such as municipal waste [55]. All of these feedstocks either go through a thermo, bio, or physical pathway to be converted into second generation ethanol. However, before the biomass can be converted it must first be pretreated. This step is vital in ensuring that physical properties of the biomass, such as size, moisture and density, are suitable for conversion [25].

The thermo pathway heats the biomass or feedstock with trace amounts of oxidizing agents present. The biomass is then converted into three different substances: biochar, pyrolytic oil, and syngas. The relative amounts of conversion of each product is controlled by the processing temperature. At low temperatures of between 250 and 350 °C the main product is solid biochar [55]. The process of producing the biochar is termed torrefaction, or the heating of a mass to produce a brittle more hydrophobic solid [36]. At higher temperatures of 550 to 750 °C without the presence of air, pyrolysis, or the decomposition of the biomass, occurs to produce bio oil. The speed of pyrolysis dictates the percent composition of the phase of the biofuel created. Fast pyrolysis favors the production of oil or gaseous biofuel, while slow pyrolysis favors the production of solid biofuel. Lastly at high temperatures of 750 to 1200 °C, the main product is a combustible gaseous fuel called syngas, which is created through gasification. Additionally, for the gasification to occur, the biomass must be exposed to trace amounts of oxygen, steam, or air [55] [25]. Out of the three different substances, pyrolytic oil and syngas are the most favorable intermediaries for transportation fuel. To produce transportation fuel from pyrolytic oil four different chemical processes are commonly used: hydrodeoxygenation, catalytic cracking, steam reforming, and emulsification using diesel. These processes all aim to reduce the amount of oxygen content of the oil, allowing it to be a more favorable energy source [55]. To convert syngas, which is composed of mainly single carbon compounds and hydrogen, a complex

catalyst to encourage the creation of carbon-carbon bonds is required. An example of this is the Fischer-Tropsch process [54]. However, the efficiency and cost of the thermo pathway needs to be developed before processes like gasification can reach the commercial-scale [59].

Another method for producing second generation ethanol is through the bio pathway. The most common biochemical pathway is fermentation, which is an anaerobic process. During this process, glucose is converted into ethanol through a series of different chemical reactions. However, before fermentation can occur the feedstock must be pretreated and undergo enzymatic hydrolysis to increase the amount of ethanol created. Pretreatment of the biomass allows for the isolation of cellulose. Once the cellulose is isolated, it can be used for the saccharification of cellulose, either by enzymatic or chemical hydrolysis using acids. This causes the production of glucose. The glucose is then fermented using yeast and distilled water to produce ethanol [55] [25].

The last method for producing second generation biofuel is by physical conversion. The main three physical conversion processes are briquetting, pelletizing, and fiber extraction. Briquetting converts loose biomass into a uniformly shaped dense solid block using a considerable amount of pressure. The second physical conversion process, pelletization, creates dense solid pellets rather than a block under pressure. Lastly, fiber extraction, or the extraction of fibers from biomass residues, produces solids that can be used as a burning fuel [25].

However, the success of second generation biofuel is hindered by the cost of the pretreatment of the lignocellulosic feedstock. Due to the low conversion efficiencies of feedstock into biofuel, further optimization and improvements are required in order to ensure that second generation biofuel is economically competitive with fossil fuels. Despite these challenges, second generation biofuels are a promising alternative for fossil fuels due to the greenhouse gas savings and the lack of competition within the food industry [34].

2.1.3 Third Generation Biofuel

The last classification of biofuel is third generation biofuel. Third generation biofuel uses algal biomass as feedstock [55]. Up until recently, algal biomass was considered a second generation biofuel, but due to the ability of algal matter to produce much higher yields while also utilizing lower resource inputs, it was moved into its own classification [12]. Additionally, algae do not require any arable land to be cultivated and does not compete with food or other crops. Therefore, algae overcomes the disadvantages of both first and second generation biofuel. The success of third generation biofuels is attributed to algae's ability to accumulate lipids, be "grown in a controlled environment, and exploit CO₂ directly from industrial emissions" [25]. Thus, due to its versatility, zero food crop competition, ease of cultivation, and high growth rate, the use of algae as feedstock has grown in the research field. However, the conversion of algae to biofuel requires vast amounts of energy and water, and has therefore hindered the success of third generation biofuels [34]. Also, further research to improve both the amount of energy produced and its variability needs to be conducted before third generation ethanol can compete with first and second generation biofuel.

2.2 Ethanol in Brazil

Biofuel production is currently limited to regions where biofuel feedstock is capable of growing. Nonetheless, the production and consumption of biofuels has experienced global growth due to their link to producing cleaner renewable energy. Led by the United States and followed closely by Brazil, the production of biofuels, specifically ethanol has seen growth in its application as an additive for gasoline in motor fuel [71]. The feedstock for the production of ethanol vastly depends on the region and what is available, namely in Brazil the main feedstock is sugarcane due to large surpluses of the crop.

Originally as early as 1905, tests were being performed in Brazil to determine if ethanol could be used as an additive for fuel. These tests resulted in the Institute of Sugar and Alcohol (IAA) law in 1931, that required 5% of alcohol to be mixed with all gasoline in Brazil [8]. Furthermore, in 1975 Brazil began to aim at large scale ethanol generation to reduce its dependence on expensive imported petroleum. Brazil also sought to solve the issue of declining sugar prices in the international market with the ProAlcohol program [4]. The ProAlcohol program mandated that the production of engines must adapt to consume E20 (20% ethanol and 80% gasoline). However, in 1979 due to another oil crisis, Brazil began to refocus the ProAlcohol program to create the first car that can run only on ethanol. By 1980 almost 95% of all vehicles ran on ethanol. Nevertheless, with the drop in oil prices and the rise of sugar prices, the demand for ethanol run cars dramatically decreased. At the beginning of the 21st century, an increase in high oil prices as well as a rising concern for greenhouse gas emissions, caused ethanol to be used as an additive for fuel again. The reemergence of ethanol led to the creation of flex-fuel technology. Flex-fuel cars have the option to run on either 100% hydrous ethanol or a blend of gasoline and ethanol, thus allowing consumers to choose the cheaper and more convenient fuel option [10]. This made it easier for the government to mandate that all gasoline must contain a certain percentage of ethanol. As recently as of 2018, it was declared that 27.5% ethanol must be present in all gasoline [69].

2.3 Sugarcane as a Feedstock

Sugarcane was first introduced to Brazil in the 16th century by Portuguese colonizers, and today is one of Brazil's largest exports [8]. Sugarcane consists of three main parts: the leaves, the stalk, and the roots. The anatomy of the plant is labeled in the Figure 2 below.

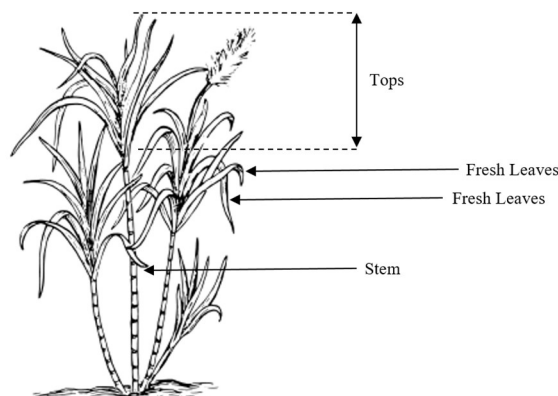


Figure 2. *The anatomy of a sugarcane plant.* The three main sections of the plant are the tops, leaves, and the stem [41].

Sugar, one of the main products of sugarcane, is produced from the juice located in the stalks of sugarcane. Due to the small amount of arable land that each stalk requires, the plant is able to be grown densely in fields and harvested by both mechanical and manual means. To extract the juice, the stalks must first be crushed in a sugarcane mill. The leftover dry fibrous remnants are commonly referred to as sugarcane bagasse [73] [62]. An image of crushed sugarcane bagasse can be seen in Figure 3 below.

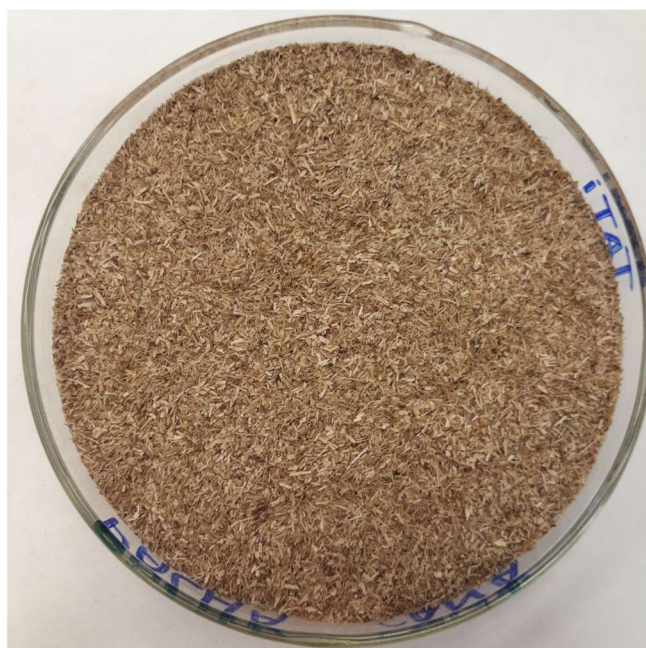


Figure 3. *Photograph of crushed sugarcane bagasse found in the BIOTAR lab.*

It was forecasted that in the crop year 2019-2020 Brazil would cultivate 643 million metric tons of sugarcane, a 23 million metric ton increase from the previous crop year [5]. This increase made Brazil the largest producer of sugar in the world. Brazil began the development of ethanol from sugarcane in the colonial periods when farmers would produce “cachaça” a sugarcane distilled spirit. However, in the beginning of the 20th century the use of ethanol switched from alcoholic beverages to energy sources [8]. In 2018 alone Brazil produced 36 million metric tons of sugar and 30 billion liters of ethanol fuel. Most of

the ethanol produced comes from the hydrolysis of the bagasse, but some fuel is fermented from the sugar itself [46]. The use of the bagasse for ethanol has grown in recent years due to legal statutes by Brazil (Brazil Federal Law 2661/98) which intend to prohibit the burning of sugarcane by 2031. This law makes finding alternate benefits of the bagasse essential [62].

2.4 Lignocellulose Biomass

Lignocellulosic biomass is a natural resource that is favored for the feedstock of transportation fuels due to its renewability and economic benefits. Lignocellulosic biomass refers to the bulk constituents of plant material. It includes agricultural residues such as rice husk, sugarcane bagasse, forest residues such as woods and woodchips, or energy crops such as energy cane or grass [2]. It is composed of hemicellulose, cellulose, and lignin, which together form a complex and rigid structure that helps maintain the integrity of the plant [68]. Lignocellulosic biomass is commonly used for soil treatment or for thermal energy due to its resistance to biological and chemical degradation into its useful monomers and oligomers. However, due to the low cost, abundance, and widespread availability of lignocellulosic material different methods that can successfully degrade the biomass into second generation ethanol are being researched [46].

2.4.1 Cellulose

Cellulose is the main component in most agricultural and forest residues. It resides in the plant cell wall and provides the structure of the plant. Cellulose comprises approximately 40-50% of sugarcane bagasse [2]. It is a linear polymer composed of D-glucose subunits connected by β -1,4-glycosidic bonds. Adjacent cellulose chains are coupled by both Van der Waals forces as well as hydrogen bonds allowing the chains to arrange in a crystalline structure [50]. The crystalline structure not only drives the difficulty in hydrolyzing the molecule, but also makes the substance insoluble in water and most organic solvents due to its hydrophilic nature. A cellulose chain consists of 500 to 25,000 glucose monomers. Cellulose is mainly used for the production of paper products such as cotton and linen, however it is emerging as a natural resource that can be utilized for the production of biofuels [33].

2.4.2 Hemicellulose

Hemicellulose is an amorphous heteropolysaccharide that also resides in the plant cell wall [46]. It comprises around 25-30 weight (wt)% of sugarcane bagasse [42]. In contrast to cellulose, hemicellulose is composed of different pentoses, such as xylose and arabinose, as well as hexoses, such as glucose, mannose, and galactose. The branches of hemicellulose are short lateral chains that are composed of the different carbohydrates. Hemicellulose chains typically consist of 80-200 monomers [23]. The branched and amorphous nature of hemicellulose allows it to easily be hydrolyzed into its monomer sugars [68]. Currently, there is increased interest in using hemicellulose as a raw material in the chemical industry as well as food and pharmaceuticals fields [67].

2.4.3 Lignin

Lignin is a large amorphous heteropolymer that comprises, on average, 14-25% of sugarcane bagasse [2]. It is also found in the cell wall and provides the plant with structural support, impermeability, and microbial resistance. Lignin is composed of three different phenylpropane units: p-coumaryl, coniferyl, and sinapyl. Lignin is unique in that its subunits are all linked differently. The amorphous heteropolymer is both water-soluble and optically inactive, so the degradation and associated hydrolysis of lignin is extremely difficult [50]. Today lignin is used in a wide array of opportunities such as derivatives in animal feed additives, textiles, and composites [19].

2.5 Hydrolysis

The dense spatial structure of lignocellulosic biomass requires a pretreatment step to break down the biomass into its constituent monomers and oligomers [23]. The four main goals of pretreatment are to reduce the crystalline structure of cellulose, increase the biomass surface area, eliminate hemicellulose and lignin, and increase the porosity of the material. By successfully completing these goals the structure of the lignocellulosic material will be altered, thus greatly enhancing downstream processing. Currently, one of the main industrial methods of pretreatment is through acid or enzymatic hydrolysis, however new methods such as subcritical hydrolysis are in the early stages of research [50].

2.5.1 Acid Hydrolysis

Acid hydrolysis is a straightforward method to prepare monosaccharides. Compared to other methods, acid hydrolysis has not only a higher sugar yield but also provides favorable reproducibility. Common acids that are used in this process are hydrochloric acid, sulfuric acid, and nitric acid. Acid hydrolysis can be performed using either strong or dilute acids. Although the acid catalyst is able to quickly break down the biomass, the process is extremely corrosive, toxic, and hazardous. Therefore, to ensure the success and economic feasibility of the process, the reactors must be resistant to corrosion and the concentrated acid must be recovered after the hydrolysis is complete. Additionally, when high acid concentration is used it is very difficult to recycle the acid, thus leading to environmental pollution. On the other hand, if dilute acid is used, some degradation products are formed that can inhibit subsequent processes [23].

2.5.2 Enzymatic Hydrolysis

Enzymatic hydrolysis occurs under mild conditions and uses highly specific cellulase enzymes to produce simple sugars. One of the main advantages of enzymatic hydrolysis over acid hydrolysis is that there are no issues with corrosion as well as no production of hazardous waste or degradation products. However, this process is more time intensive. In addition, the final product of enzymatic hydrolysis has adverse effects on the enzyme catalyst. To prohibit the final product from degrading the cellulase enzyme, the final product must be removed immediately after they are formed. The enzymatic catalysts are also extremely costly, and due to the difficulty associated with recycling these compounds a large cost investment is necessary. Moreover, enzymatic catalysts such as cellulases or xylanases have difficulty in destroying the crystalline structure of cellulose and struggles to reduce both hemicellulose and lignin. Therefore, before enzymatic hydrolysis can occur another pretreatment step is usually required [11].

2.5.3 Subcritical Water Hydrolysis

Subcritical water hydrolysis is a new method that is being researched for its use in the hydrolysis of lignocellulosic biomass. Subcritical water, or hydrothermal water, is liquid hot water that is maintained within a temperature range of 100-374 °C and a pressure higher than its saturation pressure to ensure the water remains liquid [42]. While under subcritical standards, the water molecules cleave apart much easier, thus greatly increasing the generation of ionic products by a magnitude of three. The increase in the formation of hydronium and hydroxide ions allows the water to act as either an acid or base catalyst [14]. Additionally, subcritical water has a multitude of unique properties, such as “temperature-tunable properties of density, viscosity, dielectric constant, ionic product, diffusivity, electric conductance, and solvent ability.” Due to the high density and the high temperature of the water, the environment required to convert lignocellulosic biomass to simple sugars is met. Furthermore, subcritical water as a catalyst is easy to produce, is non-toxic, requires minimal pretreatment, has shorter reaction times, and is less corrosive than other catalysts. However, in addition to being difficult to control, subcritical water hydrolysis can produce degradation products that will inhibit further processes such as fermentation [42].

2.6 Fermentation

Fermentation is a metabolic process which reduces simple sugars into target alcohols, gases, or organic acids, such as ethanol, in the absence of oxygen. The chemical formula below shows the main reaction of ethanol fermentation from cellulose [2].



Fermentation most often occurs in yeast, but can also occur in bacteria, or oxygen-starved muscle cells. When yeast is under anaerobic conditions it is able to convert glucose into pyruvic acid via the glycolysis pathways. The yeast then converts the pyruvic acid into ethanol and waste product: carbon dioxide [38]. Additionally, when glucose bonds are broken the energy from these bonds are used to form ATP and NAD⁺ which help to continue the process of glycolysis. However, a major problem that occurs during fermentation is the inhibition of the performance of yeast, caused by the presence of ethanol. Therefore, as the concentration of ethanol rises and the concentration of sugar diminishes, the efficiency of the yeast will greatly decrease, thus constructing a limit on the amount of ethanol that can be produced by fermentation [50].

2.7 Fermentation Inhibitors

As lignocellulosic biomass undergoes hydrolysis, degradation compounds such as furfural, 5-hydroxymethylfurfural (HMF), and phenolic compounds are also formed alongside the preferred carbohydrates. These degradation compounds not only reduce the activity of microorganisms used in fermentation, but also negatively affect cell growth, sugar uptake, and metabolic pathways. These compounds are mainly produced during acid hydrolysis but can also be produced during subcritical water

hydrolysis [40]. The degradation of lignocellulosic biomass into its constituent monomers and oligomers can be seen in Figure 4 below.

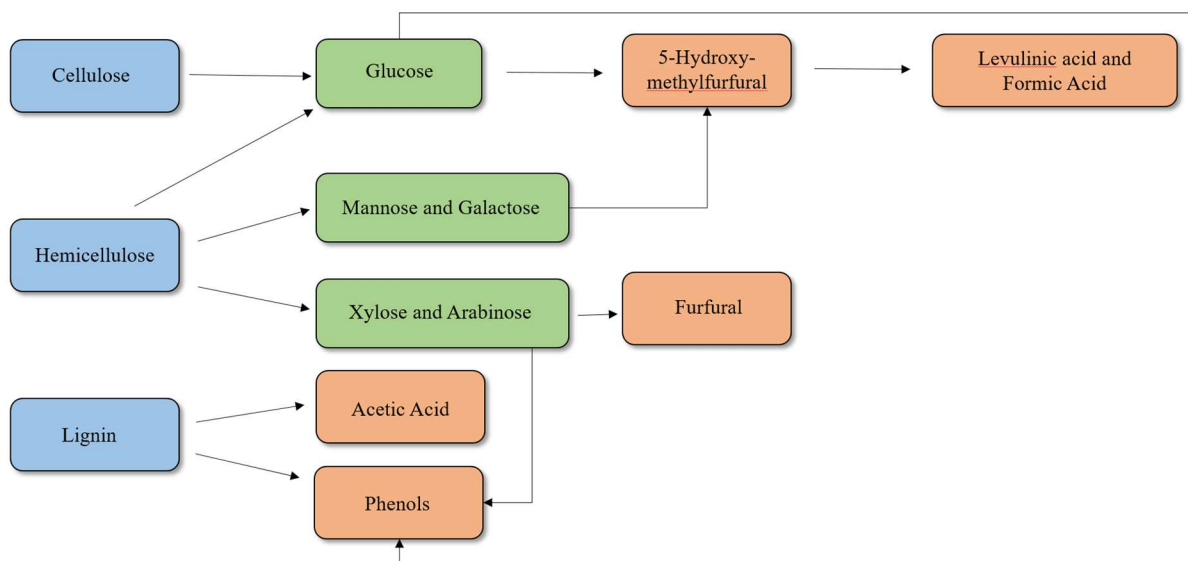


Figure 4. Degradation of lignocellulosic biomass into its constituent monomers and oligomers. In the flowchart blue rectangles indicate the three building blocks of lignocellulosic biomass, green rectangles indicate the carbohydrates formed from the degradation of lignocellulosic biomass, and the orange rectangles indicate the fermentation inhibitors formed [39].

2.7.1 Furfural

Furfural is the main degradation product of hemicellulose. More specifically, it is formed from the dehydration of xylose and arabinose that are located in the hemicellulose section of the lignocellulosic biomass. This organic compound consists of a furan ring with an aldehyde side group and is commonly known as “2-furancarboxyaldehyde, furaldehyde, 2-furaldehyde, fural, and furfuralaldehyde” [1]. An image of the structure of the compound can be seen in Figure 5 below.

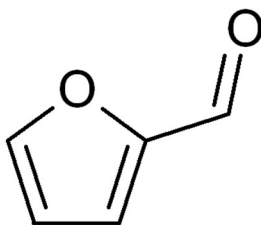


Figure 5. Structure of furfural [17].

Furfural is commonly used to make inks, plastics, fertilizers, and adhesives. It is also extremely helpful in producing other chemicals and is currently a major platform chemical. However, even though furfural is seen as a promising chemical, it is detrimental to ethanol production. Furthermore, the presence of furfural causes oxidative stress in yeast, thus reducing the activity of dehydrogenases in yeast cells and hindering the production of ethanol [1] [52]. In research performed by Delgenes et al., it was observed that when using yeast *P. stipitis*, furfural concentration below 0.5 g/L promoted cell growth, while furfural

concentration of 2 g/L and above severely constrained cell growth. A graph of the amount of ethanol that can be produced using yeast *S. cerevisiae* in the presence of varying amounts of furfural can be seen in Figure 6 below.

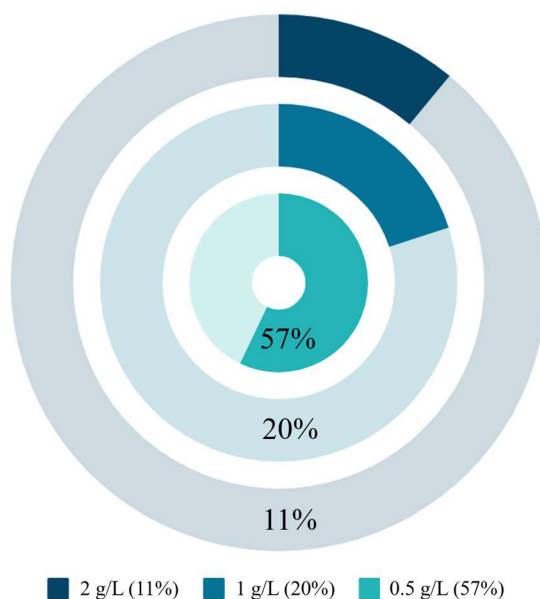


Figure 6. Ethanol produced from *S. cerevisiae* in the presence of 0.5, 1, and 2 g/L of furfural. Percentages are created by comparing the amount of ethanol produced with inhibitors present to the amount of ethanol produced without inhibitors [35].

As shown in Figure 6 at a concentration as low as 0.5 g/L of furfural, only 57% of the expected amount of ethanol can be produced. At concentrations of 1 and 2 g/L the amount of ethanol that can be produced is lowered to less than 20%. Indicating that any concentration of furfural above 0.5 g/L has adverse effects on the amount of ethanol that can be produced [35].

2.7.2 5-Hydroxymethylfurfural (5-HMF)

5-Hydroxymethylfurfural is a degradation compound produced from hexoses from cellulose, hemicellulose and lignin. It is a derivative of furan and contains both an aldehyde and an alcohol functional group. The structure of 5-HMF can be seen below in Figure 7.

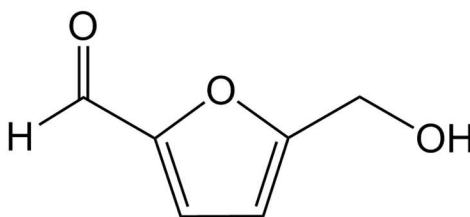


Figure 7. Structure of 5-Hydroxymethylfurfural [70].

5-HMF is an extremely versatile chemical. Its derived products are used in the pharmaceutical, food, fuel, plastics, and chemical industry. The molecule is a partially unsaturated aromatic compound, so it can easily be converted to fuel molecules via hydrogenation. The chemical versatility of 5-HMF makes the molecule

a promising renewable replacement to fossil-derived compounds. However, even with the benefits of 5-HMF, it still harms ethanol production in fermentation [1]. Although yeast cells are more sensitive to furfural than 5-HMF, 5-HMF still negatively affects the growth of yeast cells and thus the production of ethanol [52]. In research performed by Delgenes et al., it was found that at a concentration as low as 1 g/L of 5-HMF cell growth was almost completely constrained. A graph of the amount of ethanol that can be produced using yeast *S. cerevisiae* in the presence of varying amounts of 5-HMF can be seen in Figure 8 below.

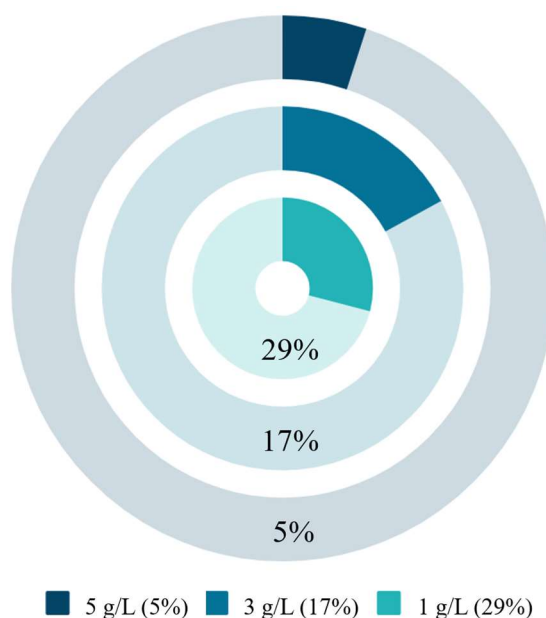


Figure 8. Ethanol produced from *S. cerevisiae* in the presence of 1, 3, and 5 g/L of 5-HMF. Percentages are created by comparing the amount of ethanol produced without inhibitors present to the amount of ethanol produced with inhibitors [35].

As shown in Figure 8 at a concentration as low as 1 g/L of 5-HMF, only 29% of the expected amount of ethanol can be produced. At concentrations of 3 and 5 g/L the amount of ethanol that can be produced is lowered to less than 17%. Illustrating that any concentration of 5-HMF above 1 g/L has adverse effects on ethanol production [35].

2.7.3 Other Fermentation Inhibitors

Phenolic compounds and weak acids, such as acetic acid, also contain synergistic inhibitory effects towards yeast cells [52]. These compounds are formed from the degradation of lignin, glucose, arabinose, and xylose. The type of phenol compound that is produced depends on the structure and type of the monomeric unit in the lignin or sugar [63]. Phenolic compounds affect yeast cells ability to act as a selective barrier and enzyme matrix, by dividing and limiting the integrity of the yeast cells. Consequently, the growth of yeast cells and the fermentation of ethanol is thus reduced. Additionally, phenols with the lowest molecular weight are the most harmful. On the other hand, the three main acids that inhibit fermentation are acetic, formic, and levulinic acid. The toxicity of the acid depends on the cultivation conditions used during fermentation. The main conditions that control the toxicity of the acids are their concentration, oxygen

concentration, and the pH of the medium. Although yeast cells are more sensitive to phenol compounds than acids, the acids still have a negative effect on the production of ethanol [64].

2.8 Detoxification Methods of Lignocellulose Hydrolysate

In an effort to achieve a higher concentration of sugars and increase the fermentability of lignocellulosic hydrolysate, a detoxification step is used to remove or eliminate all fermentation inhibitors from the lignocellulose hydrolysate. Detoxification methods can either be physical, chemical, or biological. The success of the different detoxification methods depends not only on the lignocellulosic feedstock being used but also on the microorganism used for fermentation. A detoxification method that has high selectivity, is environmentally benign, and requires a low amount of electricity is preferred [45].

2.8.1 Vacuum Evaporation

Vacuum evaporation is a physical detoxification method commonly used in the wastewater industry. It is predominantly used for its safe and clean technology [28]. Vacuum evaporation has been successful in reducing the concentration of volatile compounds, such as acetic acid, furfural, and vanillin, from lignocellulosic biomass. However, a disadvantage of this method is its ability to also increase the concentration of non-volatile toxic compounds such as extractives and lignin derivatives as well as its inability to remove phenolic compounds. Additionally, the energy required for this technology is costly. Therefore, for vacuum evaporation to be implemented successfully, a balance must be obtained between these two different consequences to ensure that an increase in the quantity of fermentation inhibitors does not occur, while also maintaining as an economically viable option [6] [60] [37].

2.8.2 Membrane Separation

Membrane separation is another physical detoxification method that has advantages over evaporation for a variety of reasons. One of the advantages of membrane separation is that the membranes are typically composed of standard units or are modular, thus scale up for industrial settings is relatively easy. Additionally, there are no toxic chemicals required for membrane separation, so waste disposal is not a large concern. One of the biggest advantages of membrane separation is that it is non-dispersive. Therefore, the organic phase or solvents which are toxic to fermentation are not mixed with the aqueous phase or the hydrolysate. Membrane separation works by using adsorptive micro-porous membranes with internal pores. The internal pores contain surface groups that eliminate fermentation inhibitors like acetic acid, 5-HMF, furfural, formic acid, and levulinic acid. One disadvantage that must be considered when implementing membrane separation in an industrial setting is that membrane fouling can occur. Additionally, a prefiltration step is needed to remove larger particles that have the capacity to clog the membrane pores. Therefore, the upkeep required for membrane separation might not make it an economic viable option [6] [60].

2.8.3 Activated Carbon Adsorption

Adsorption is a low-cost detoxification method that is mainly used in biorefineries to remove minor impurities. It is described as a process in which the atoms or molecules from a substance adhere to the

surface of an adsorbent. Adsorption has also found success in removing fermentation inhibitors, especially phenols and furans, with high efficiency. Some other benefits of adsorption are high selectivity, low cost, easy scale up, and simple design. Additionally, adsorption does not utilize any toxic substances and only causes small changes in the level of fermentable sugars. Nevertheless, the effectiveness of adsorption is mainly dependent on contact time, temperature, pH of the medium, and activated carbon concentration versus volume of hydrolysate [26] [22] [6].

The adsorption of inhibitors is extremely sensitive to any changes in pH. At low pH, weak organic acids in the non-ionized state are easily adsorbed [31]. However, at high pH the adsorption is poor because the phenols are in the form of anions rather than their non-ionic form. When the compounds are ionized, the physical and chemical properties are altered, affecting their adsorbability. However, weak basic compounds in the non-ionized state are more readily adsorbed at high pH. Another important factor affecting adsorption is contact time. As adsorption is occurring the carbons surface becomes saturated and is no longer able to adsorb any more compounds. Therefore, adequate contact time must allow for the carbon to reach equilibrium with the adsorbate or the hydrolysate. Another important factor that affects the rate of adsorption is temperature. At elevated temperatures the rate of diffusion is increased allowing the diffusion of molecules from the adsorbate to the adsorbent to be much faster. The last factor to affect adsorption is the ratio of adsorbate to adsorption. At higher concentrations of adsorbate to adsorbent, the sugar tends to be adsorbed along with the inhibitors. Therefore, a balance between the concentration of adsorbate and adsorbent must be achieved [64].

Activated carbon is one of the most common adsorbents due to its adequate porosity, large surface area, and positive chemical features. It is also a renewable and environmentally benign material. Some other common adsorbents are zeolites, diatomaceous earth, wood charcoal, and polymers. Each of the different adsorbents have unique benefits. Nevertheless, it has been concluded that carbon based adsorbents such as activated carbon are preferred for lignocellulosic hydrolysates [26]. Carbon based adsorbents are preferred because the surface of the material is hydrophobic, and requires minimal energy for regeneration. Additionally, carbon based materials can be used at atmospheric temperatures, have tailored surface chemistry, and are extremely stable [72].

Adsorption is a highly recommended method for the detoxification of lignocellulosic hydrolysate. However, it does possess some negative qualities. Activated carbon adsorption has not been successful in removing all acids, such as acetic and formic acid. Additionally, if the adsorbate is unable to be reused, the economic viability of the process can be jeopardized [26].

2.8.4 Solvent Extraction

Solvent extraction, also known as liquid-liquid extraction, is a common chemical detoxification method that has achieved success in removing fermentation inhibitors. Solvent extraction has been linked to the total removal of furfural and vanillin as well as the removal of over half the concentration of both acetic acid and phenolic compounds [22]. The success of the extraction depends on whether the solvent has a low boiling point, its partition coefficient of the solutes, and the miscibility of the feed with the solvent. Common solvents include ethyl acetate, chloroform, and trichloroethylene. Due to the low boiling point of these solvents they are easily recovered via evaporation, making their reuse quite simple. However, one

downside of solvent extraction is low selectivity, which causes small concentrations of the sugars to be extracted in addition to the inhibitors [6] [30] [26].

2.8.5 Ion Exchange Resins

Ion exchange resin is known for being one of the most efficient detoxification methods. Ion exchange resins can successfully remove lignin-derived inhibitors, acetic acids, and furfurals, thus significantly improving the production of ethanol. Another positive of this method is that the resins can be regenerated and reused without depreciating the efficiency of the process. However, even with this cost saving advantage, the overall process is not extremely viable and has a lot of downsides. One of these downsides is that media deformation causes the pressure drop across the bed to greatly increase during operation. Additionally, the binding sites for the target solutes are within the pores of the resin, making the pore diffusion sluggish and significantly prolonging the overall processing time. The ion exchange resin process also results in a sizable loss of fermentable sugars, making the system undesirable. These reasons, in addition to difficulties in scale up, deem this process to be sparsely used at the industrial scale [6] [60].

2.8.6 Overliming with Calcium Hydroxide

One of the most common methods used today for the detoxification of lignocellulosic hydrolysate is overliming with calcium hydroxide. Overliming is a chemical detoxification method known for its success in removing almost all fermentation inhibitors except for acetic acid [60]. Overliming occurs by increasing the pH and temperature of the hydrolysate using calcium hydroxide, then lowering the pH to a level susceptible to fermentation with sulfuric acid [49]. At higher pHs the toxic compounds are unstable and thus precipitate, allowing the toxic compounds to be removed via filtration. A downside of this method is that it causes a loss in the concentration of sugars from harsh conditions. Additionally, when the calcium hydroxide is added to the acidic hydrolysate it converts to gypsum, which is expensive to dispose of [45] [6] [22].

2.8.7 Enzymatic Detoxification

Enzyme detoxification is a common example of a biological detoxification process. Biological or enzymatic detoxification is preferred over chemical or physical detoxification methods because little waste is generated, few side reactions are present, and the process can occur in the same vessel as fermentation. It is also simple in nature, can be operated under mild conditions, and is environmentally friendly. However, the efficiency of the process is usually relatively low, it requires a long process time, and the enzymes are expensive. Two enzymes that are commonly used are laccase and peroxidase. Both of these enzymes have had success in removing phenolic compounds from the lignocellulosic hydrolysate [6]. Today enzymatic detoxification is mainly limited to laboratories as there are few industrial-scale investigations of enzyme detoxification for lignocellulosic hydrolysate [26].

2.9 Biochar

Biochar is commonly described as a pyrogenic stable carbon-rich by-product, synthesized through thermal degradation of biomass [3]. Distinguishable to charcoal only by its end use, biochar has been linked to

carbon sequestration, environmental management, soil fertility enhancement, and bioenergy production. Conversely, charcoal is mainly utilized to produce fuel and energy [16] [57]. Biochar, known for its porous structure, high organic carbon content, and fine-grained texture, can be produced through multiple thermochemical processes. These processes include slow pyrolysis, fast pyrolysis, flash carbonization, and gasification [61]. Currently, biochar is used in four different areas for environmental management: “soil improvement, waste management, climate change mitigation, and energy production” [3].

Biochar can also be used as a universal solvent. As mentioned before, carbonaceous materials are used as a common sorbent for both organic and inorganic contaminants due to their high porosity, and environmental benefits. Today activated carbon is the most common carbonaceous sorbent. By activating the charcoal, the surface area is consequently enhanced and expanded. Biochar has many similarities to activated carbon. Both are produced via pyrolysis, and have a relatively high surface area. One of the biggest differences between activated carbon and biochar is that biochar consists of a non-carbonized fraction. This fraction contains oxygen functional groups such as carboxyl, hydroxyl and phenolic surface groups. These additional traits of biochar could allow it to be a beneficial sorbent for inorganic and organic contaminants [3].

3. Materials and Methods

3.1 Raw Materials and Chemicals

Six different types of biochar were donated by NextChar (Amherst, Massachusetts, United States), an industrial manufacturing company of biochar. The six types of biochar provided were Cool Terra, Blak I, Rogue, Gold Standard, Art I, and Wakefield. All donated biochar were packed into a plastic bag and stored in the desiccator until needed. A picture of the donated biochar can be seen by Figure 9 below.

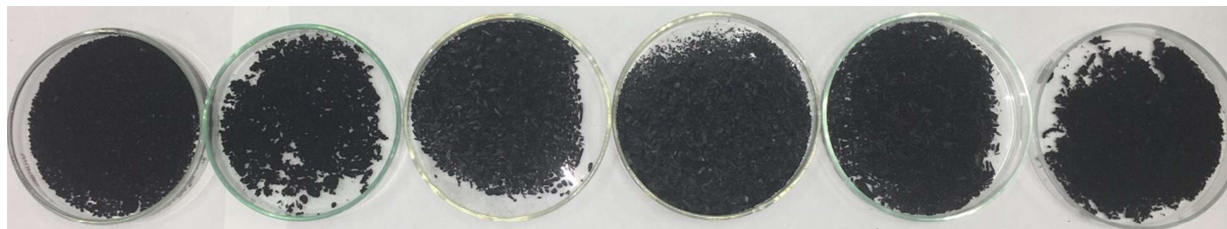


Figure 9. Photograph of six different biochars donated by NextChar. The names of the six different types of biochar, from left to right: Cool Terra, Blak I, Rogue, Gold Standard, Art I, and Wakefield. Picture was taken in the BIOTAR lab.

The synthetic sugarcane hydrolysate mixture was prepared by mixing one gram of each of the following compounds with one liter of ultrapure water: D-(+)-glucose, L-(+)-arabinose, D-(+)-xylose, acetic acid, furfural, and 5-hydroxymethylfurfural. All compounds except acetic acid were obtained from Sigma Aldrich (St. Louis, MO, USA). Acetic acid was acquired from Wako Pure Chemical Industries Ltd. (Osaka, Japan). The mixture was stored in a refrigerator at 10 °C for use later in the experiment.

In addition, the compounds were used to calibrate the high-performance liquid chromatography (HPLC) machine. HPLC grade acetonitrile from J.P. Baker (Darmstadt, Germany) and ultrapure water was used for the mobile phase of the HPLC machine analyzing the sugar compounds. Eighty-five percent phosphoric acid from Ecibra (São Paulo, Brazil), acetonitrile, and ultrapure water were used for the mobile phase of the HPLC machine analyzing the inhibitor compounds.

3.2 Characterization of Adsorbent: *Total and Volatile Solids*

The solid content of the six different biochars were measured to better understand the physical characteristics of each of the biochar. Before beginning, the weight of the crucible being used was weighed and recorded. Afterwards 1 gram of the biochar was placed in the crucible. To determine the total solid in each biochar, the moisture content of the residue was evaporated by drying out the sample at 105 °C in an oven for 12 hours. After twelve hours, the sample was removed and reweighed. Each test was performed in triplicate and then averaged. The equation used to determine the amount of total solids in the sample is shown by Equation 1 below.

$$TS = \frac{\text{mass of dry substrate}}{(\text{mass of wet substrate mix})} * 100 \quad \text{Equation. 2}$$

To determine the volatile solid composition of the biochar, the crucible containing the total solid residues was moved into a muffle furnace set to 550 °C. The crucible was left in the furnace for two hours to allow the solid residue to ignite. After two hours, the furnace was turned off and the sample was allowed to cool for two hours. The ignited crucible was then removed and reweighed. Each test was performed in triplicate and then averaged. The concentration of volatile solid was found by using Equation 3 shown below.

$$VS = TS - \left(\frac{\text{mass of incinerated substrate}}{\text{mass of dry substrate}} * 100 \right) \quad \text{Equation. 3}$$

3.3 Detoxification of the Lignocellulose Hydrolysates

3.3.1 Activating the Biochar

To activate biochar 4 (Gold Standard), five grams of the sample was separated and set aside. The biochar was then placed in an Erlenmeyer flask with a magnetic stir bar and filled with 10 mL of a 25% sodium hydroxide (NaOH) solution. The mixture was left in the Erlenmeyer flask on a magnetic stirrer for two hours. After two hours the biochar was saturated with the NaOH. The biochar was then filtered out using a vacuum filtration system. The solid remains were moved into the oven set at 105 °C, to remove all moisture content. Next, the biochar was left in the oven for twelve hours. After twelve hours, the biochar was moved into the muffler, an inert environment filled with nitrogen gas. The temperature of the muffler was allowed to rise to 700 °C by increasing the temperature by 20 degrees per minute. After ninety minutes the muffler was turned off, and the biochar was allowed to cool in the desiccator. After the biochar was activated, it was washed in a vacuum filter, by alternating between a 0.27 mM hydrochloric acid solution and distilled water. The pH of the liquid was tested in between washes with a universal pH indicator strip. Once the pH of the liquid was between seven or eight, the biochar was removed from the filtration system. The biochar was then allowed to continue drying in the oven for twelve hours at 105 °C. After the activated and washed biochar was dried it was ground using a mortar and pestle and stored in the desiccator until needed.

3.3.2 Continuous Fixed Bed Adsorption

Fermentation inhibitors were removed from the hydrolysates using a continuous fixed bed. The overall process of this system is shown in Figure 10 below.

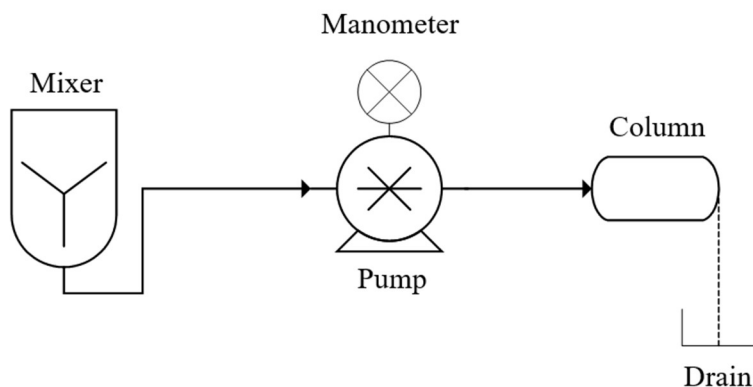


Figure 10. Schematic of the continuous fixed bed model used.

The experimental set-up used a magnetic stirrer from Fisatom (Model. 752, Series: 842646), a positive displacement pump from Eldex (Model. PN: 5976 - Optos 2SM), a metal column with an inner diameter of 2.1 cm, length of 8.5 cm, and an entrance of 1/16 cm, as well as a manometer. Figure 11 below, shows a photograph of the continuous adsorption system used.

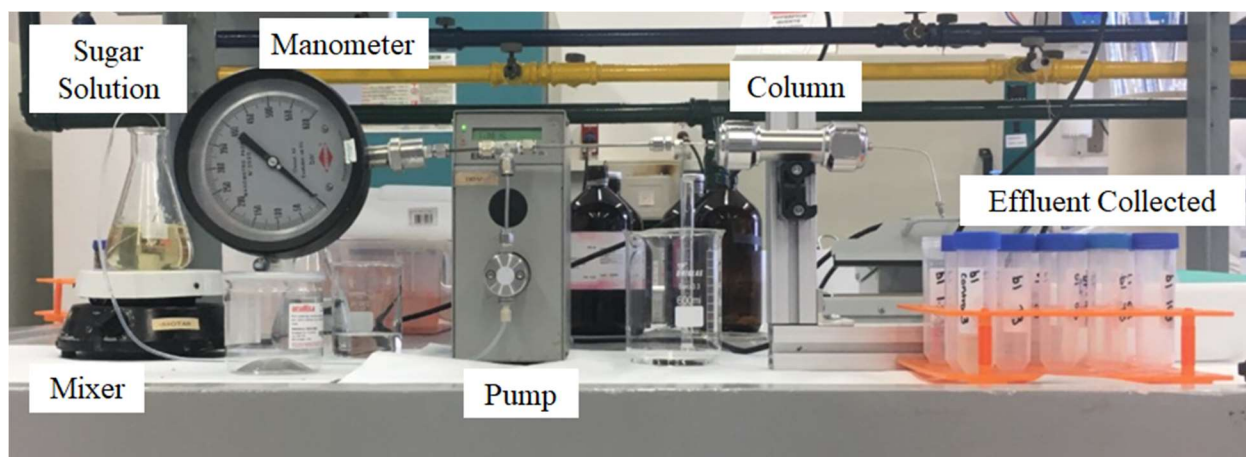


Figure 11. Photograph of the continuous adsorption system used. Photograph was taken in the BIOTAR lab.

Before the sugarcane hydrolysate entered the system, the hydrolysate was allowed to warm to room temperature (21 °C). Once the sugar solution reached ambient temperatures, it was placed in a 250 mL Erlenmeyer flask with a magnetic stir bar and put on the magnetic mixer set at level 4. The hydrolysate was then pumped through the column at a speed of 1.75 mL/min. The column was packed with cotton balls, 1 gram of adsorbent, and glass pearls, and sealed with thread sealing tape as shown by Figure 12 below.

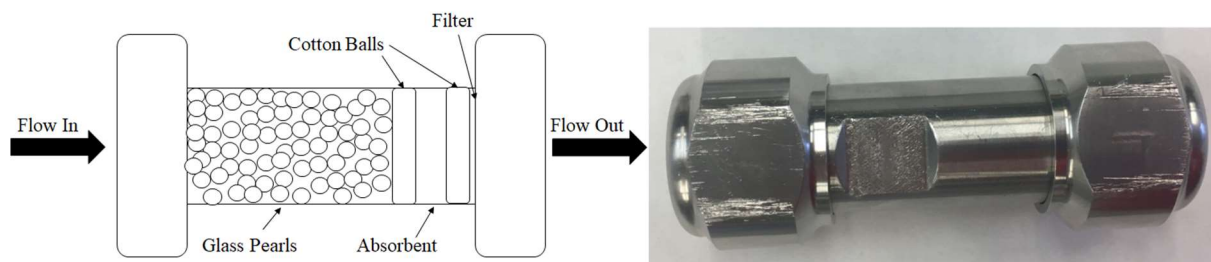


Figure 12. The correct packing and orientation of the column is seen on the left and a photograph of the column used in the experiment is seen on the right. The photograph on the right was taken in the BIOTAR lab.

Adsorption occurred as the hydrolysates moved through the column by gravitation [15]. The effluent was recovered in 5 mL or 10 mL segments in a falcon tube. Ten 5 mL effluents were collected before the pump was turned off. To prepare the collected effluents for analysis, 1.5 mL of each sample was moved into a small 2 mL vial with the aid of a 0.22 μm nylon syringe filter. The filters used to prepare the samples can be seen in Figure 13 below.

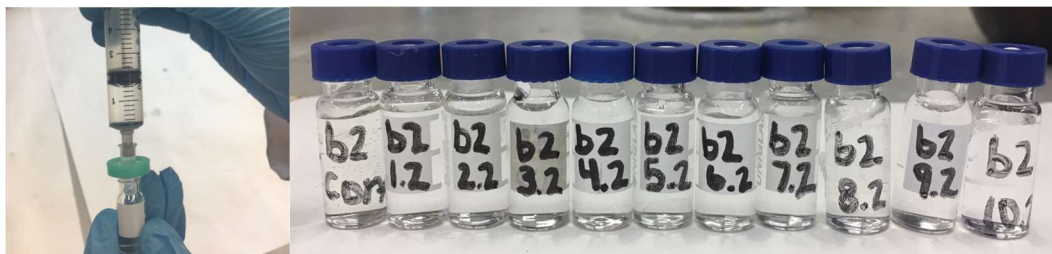


Figure 13. Photograph on the left is an example of moving the effluents into the 2mL vial with the aid of a nylon filter. The left image shows all the collected effluent for the second trial of Blak I biochar. Both photographs were taken in the BIOTAR lab.

All vials were placed in a freezer at $-18\text{ }^{\circ}\text{C}$ until needed for analysis. After all effluents were collected and the pump was turned off, the column was removed and the system was washed with ethanol and then water. The separated column was then emptied and the adsorbent was moved onto a petri dish. The adsorbent was then put in the oven at $105\text{ }^{\circ}\text{C}$ for twenty-four hours to remove any moisture. Photographs of the adsorbents after being removed from the column can be seen in Figure 14 below.

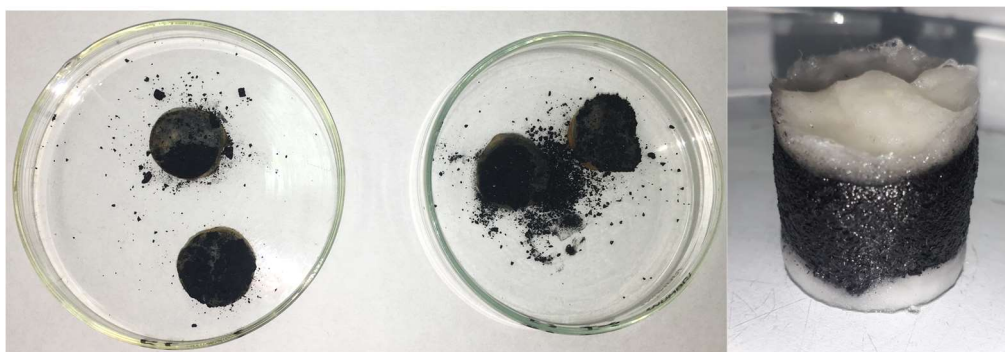


Figure 14. The photograph on the left is of activated carbon after it was removed from the column and dried in the oven. The image on the left is biochar after it was removed from the column. Both photographs were taken in the BIOTAR lab.

After twenty-four hours the adsorbent was reweighed and moved into a small bag for further analysis. Before the beginning of each trial, a sample of the hydrolysate was collected in a falcon tube to use as a

control. Also, the time for each effluent to be produced was measured using a stopwatch. To observe the efficiency of the apparatus, a control was performed with activated carbon as the adsorbent instead of biochar. Four trials were performed with the activated carbon before any trials with the biochar occurred. Duplicate or triplicate trials were performed for each type of biochar and the one activated biochar. Additionally, one trial was performed with each biochar while using ultrapure water as the adsorbate. For all of the trials performed with ultrapure water only the pH was recorded and no samples were prepared for the HPLC.

Due to the original pump being unable to maintain a constant flow rate, the pump used for the experiment was changed to a supercritical Peltier CO₂ pump (Jas.Co, PU-2080-CO₂ Plus). The updated experimental set-up can be seen by Figure 15 below.

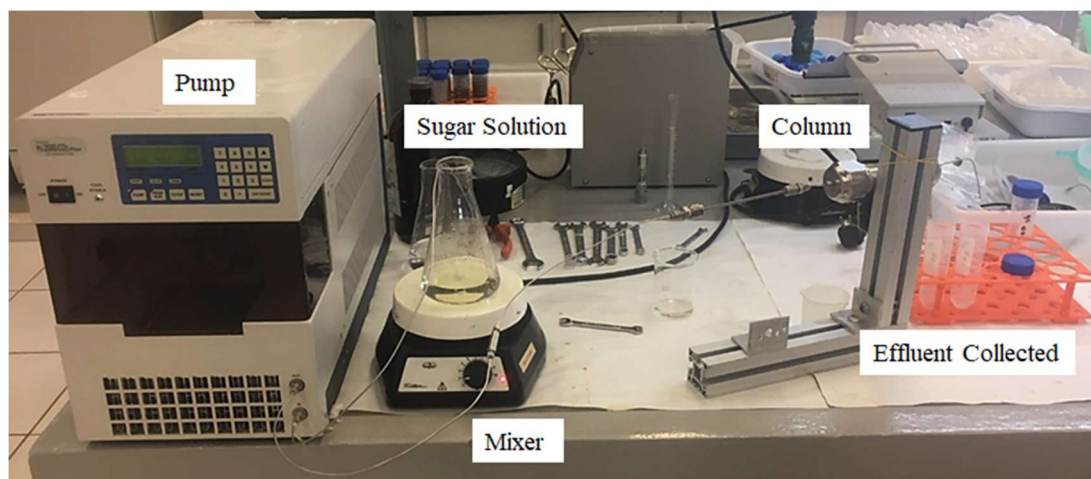


Figure 15. Photograph of the experimental set-up with the supercritical Peltier CO₂ pump. The picture was taken in the BIOTAR lab.

The alteration of the pumps changed the experimental set-up in that a manometer was no longer needed to monitor the pressure. The CO₂ Peltier pump contained a pressure sensor and was therefore able to record the change in pressure as the hydrolysate was pumped through the column. Additionally, while using the CO₂ Peltier pump effluents were collected in six 5 mL segments followed by four ten mL before the pump was turned off. In comparison to the positive displacement pump, the CO₂ Peltier pump was more successful in maintaining a consistent flow rate in between trials and was therefore used for most of the research.

3.4 Analysis of Purified Solution

3.4.1 PH

The pH was measured for each effluent and hydrolysate control at room temperature, by using a digital pH meter (Digimed, model DM-22, Brazil). The pH of the hydrolysate solution was typically 3.35 ± 0.0433 .

3.4.2 High Performance Liquid Chromatography (HPLC) for Sugars

To determine the concentration of standard compounds, such as arabinose, xylose, and glucose; in the effluent and sugar hydrolysate solution, an HPLC machine with a high-pressure isocratic pump (Waters 1515), a column heating model (Waters), and a refractive index detector (RI) (Waters 2414) was used. An image of the HPLC machine can be seen in Figure 16 below.



Figure 16. Photograph of HPLC unit used to determine the concentration of sugar in the effluent. The picture was taken in the BIOTAR lab.

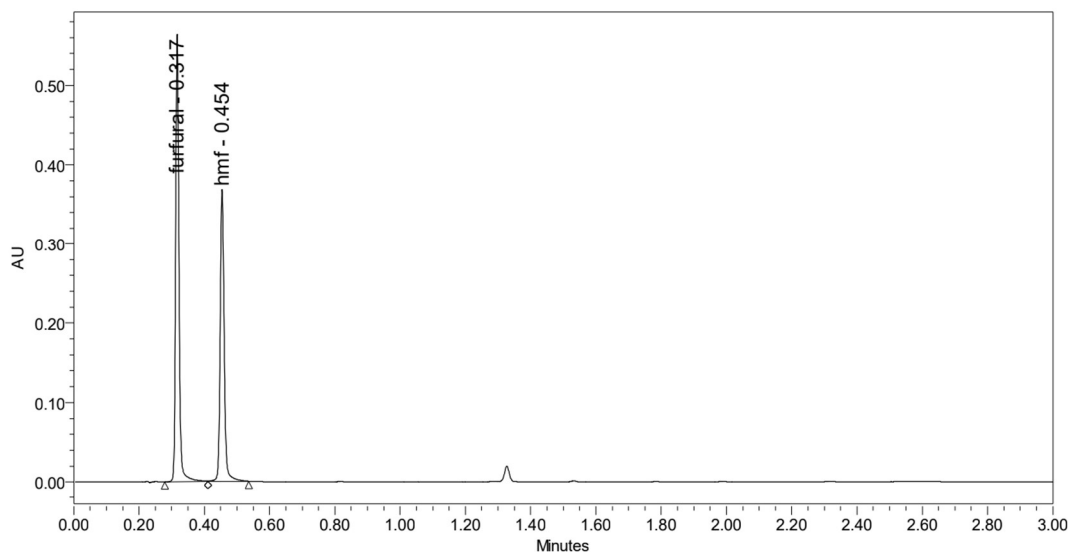
Chromatographic separation was performed using a 3.9×300mm carbohydrate analysis column maintained at 30 °C by a heating module. The flow rate for the column was 2 mL/min. Isocratic separations were achieved by using a mobile phase composed of an 80% aqueous acetonitrile solution (volume percentage). The total running time was ten minutes and the injection volume was 5.0 µL. By using standard solutions (solutions of pure xylose, arabinose, and glucose) both the calibration and retention times were determined; the concentration of these standard solutions ranged from 0.1 – 10 g/L.

3.4.3 HPLC for Inhibitors

To determine the concentration of 5-HMF and furfural, in the effluent stream as well as the sugar hydrolysate solution an HPLC with a liquid HPLC pump (PU-2080, Jasco, Japan), a ternary gradient unit (LG 2080-2, Jasco), a 3-line degasser (DG 2080-55, Jasco) and a UV-Vis detector (UV-7075 Jasco) were used. Chromatographic separation was performed with a Kinetex C18 column from Phenomenex (Torrance, CA, USA). The column was maintained at 40 °C with a flow rate of 1.1 mL/min. The mobile phase consisted of a mixture of water with 1% phosphoric acid and a mixture of acetonitrile with 1% phosphoric acid. The system operated by injecting 5 µL of sample and then allowing the system to run for thirteen minutes. The detector for this system operated at 270 nm. By using standard solutions of 5-HMF and furfural, both the calibration and retention times were determined; the concentration of these standard solutions ranged from 0.005 – 0.3 g/L.

3.4.4 Deciphering HPLC Results

After the HPLC unit was finished reading the samples, the connected computer would show something similar to Figure 17 seen below.



	Peak Name	RT	Area	% Area	Height
1	furfural	0.317	401506	56.33	563173
2	hmf	0.454	311275	43.67	368378

Figure 17. Screen capture of the HPLC peaks for inhibitors (specifically furfural and 5-HMF). Screen capture is from an analyte tested in Professor Mauricio Ariel Rostango's lab.

As shown in the image, each peak has a corresponding retention time and area. The time of occurrence for the peak indicates the compound in the solution, while the area under the peak dictates the concentration of the compound found. The specific retention times for each compound are found by analyzing pure solutions of all samples. The retention times for all studied compounds can be seen in Table 1 below.

Table 1. Retention times of all six compounds in the HPLC machines. Retention times were determined by analyzing known pure solutions of each compound.

Compound	Retention Time	Standard Deviation
Glucose	3.94	±0.003
Xylose	2.95	±0.003
Arabinose	3.21	±0.004
Furfural	0.32	±0.0007
5-HMF	0.45	±0.001

The retention time of the standard solutions was matched to the retention time of the peaks found in the analyte to identify the compounds present inside the effluent. Additionally, each peak had a certain detector response or area which relates to the concentration of that particular compound. To determine the concentration of each compound in the analyte, a calibration curve of all compounds was created using standard solutions of concentrations ranging from 0.1 - 10 g/L for the sugars, and 0.005 – 0.2 g/L for the inhibitors. The calibration curve was used to understand how the instrumental response changes with different concentrations of each compound in the analyte. Utilizing the slope and y-intercept of the calibration curves, the detector response results for the analytes could be used to determine the concentration of each compound. The calibration curve of each compound can be found in Appendix A5 .

3.4.5 Determining Saturation Capacity from a Breakthrough Curve

After the concentration of each molecule in the effluent was found, the mass transfer between the solid phase and the liquid phase could be quantitatively analyzed. A common method to analyze the mass transfer zone is through the construction of a breakthrough curve. A breakthrough curve is constructed by plotting the concentration in the effluent (C_x) divided by the initial concentration in the feed (C_o) versus time. A breakthrough curve is produced for every compound in the analyte and typically has an S shape. Instead of plotting C_x/C_o versus time, C_x/C_o versus volume will be graphed. Because time was not congruent between all tests, all graphs created will have volume on the x-axes thus creating consistency between all graphs. After the breakthrough curves are constructed, the saturation capacities can be calculated. The saturation capacity determines the maximum amount of adsorbate the adsorbent can retain. Figure 18 shown below illustrates the area on a breakthrough curve that refers to saturation capacity.

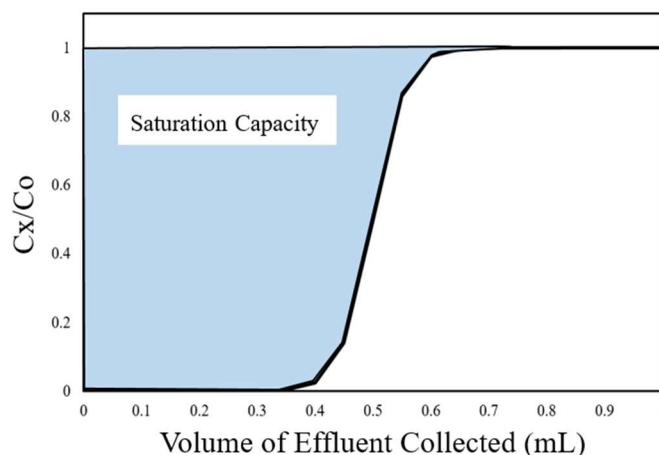


Figure 18. Illustration of the area that applies to saturation capacity on a graph of a breakthrough curve. The area of the graph that is blue illustrates the section of a breakthrough curve that is the saturation capacity. C_x/C_o stands for the concentration in the effluent over the initial concentration.

As shown in Figure 18, the saturation capacity refers to the area between the breakthrough curve and one, for the whole curve. Integrating the area between the breakthrough curve and one is the first step in finding the saturation capacity. After the area was found, the value is divided by the amount of adsorbent used and multiplied by the concentration of the compound being studied in the feed. The saturation capacity was calculated for each compound in each trial. A sample calculation of determining the saturation capacity from a breakthrough curve can be found in Appendix B6.

3.4.6 Determining Breakthrough Capacity from a Breakthrough Curve

Another analysis that is typically used to describe the capacity of adsorbents is breakthrough capacity. Breakthrough capacity in most cases is more important than saturation capacity. In most industrial situations the adsorbate flow is typically stopped or diverted before the breakthrough point, or point right before the breakthrough curve goes asymptotic. Therefore, breakthrough capacity refers to the maximum amount of adsorbate the adsorbent can retain before the breakthrough point. Figure 19 below illustrates the area on a breakthrough curve that refers to breakthrough capacity.

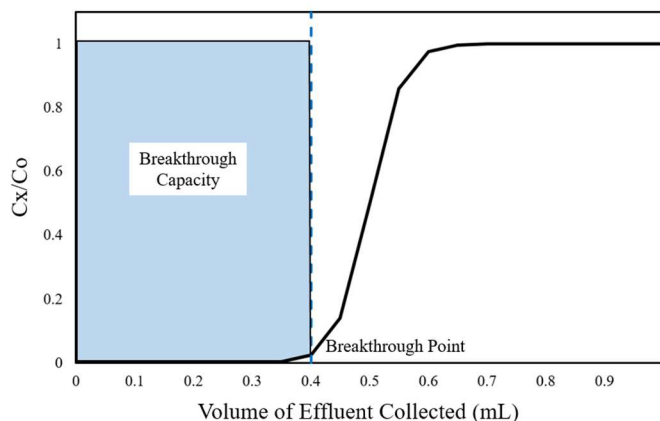


Figure 19. Illustration of the area that applies to breakthrough capacity on a graph of a breakthrough curve. The area of the graph that is blue illustrates the section of a breakthrough curve that is the breakthrough capacity. The dashed line indicates the breakthrough point. C_x/C_o stands for the concentration in the effluent over the initial concentration.

As shown in Figure 19, the breakthrough capacity refers to the area between the breakthrough curve and one, for the area before the breakthrough point. Integrating the area between the breakthrough curve and one up to the breakthrough point is the first step in finding the breakthrough capacity. After the area is found, the value is divided by the amount of adsorbent used and multiplied by the concentration of the compound being studied in the feed. Each compound in each trial has a breakthrough capacity. A sample calculation of determining the breakthrough capacity can be found in Appendix B7.

4. Results and Discussions

4.1 Characterization of the Biochar

Before beginning experimentation, characterization of the six different types of biochar was essential to understanding the chemical and physical attributes of each biochar. Each biochar was prepared under different conditions and was possibly produced from different feedstock materials. Therefore, the physical and chemical attributes of the six biochars likely differed. The results of the observed physical and chemical traits of the biochar is described below.

4.1.1 Physical Characteristics of the Biochar

Each of the six different biochars has slightly different observable physical characteristics. It was important to denote the physical characteristics of all six biochar before experimentation to ensure there was no confusion between them. For each biochar, the name, initial amount, relative particle size, and shape was noted. The results of the observable physical characterization of each biochar can be seen below in Table 2.

Table 2. *Observable physical attributes of the six different types of biochar.* Attributes noted in the table are name, amount, relative size, and shape.

Biochar	Name of Sample	Amount of Sample (g)	Relative Particle Size	Shape
Biochar 1	Cool Terra	84	Small	Angular
Biochar 2	Blak I	53	Medium	Sub-angular
Biochar 3	Rogue	13	Large	Elongated
Biochar 4	Gold Std.	31	Large	Elongated flakes
Biochar 5	Art I	22	Large	Elongated
Biochar 6	Wakefield	50	Small	Sub-angular

As can be seen by the table above, each of the six different biochars has slightly different physical characteristics. It was important to notate the starting amount of the different types of biochar, so we had an understanding of the possible number of tests that could be run with each adsorbent. The largest found physical difference between the six different biochars was the particle shape. Images of all biochars can be seen in Appendix C1-C6, and biochar 2 and 5 can be viewed in Figure 20 below.



Figure 20. *Photograph of biochar 2 and 5.* Biochar 2, on the left, has a sub-angular shape that can be contrasted with biochar 5 seen on the right, which has a more elongated shape.

As can be seen by Figure 20 and Table 2, the biochars supplied by NextChar had two main shapes: angular or elongated. Because each biochar has a slightly different shape, one gram of one type of biochar would fail to cover the same surface area as one gram of another type of biochar. This difference in surface area, shape, and particle size provides each biochar with slightly different adsorption abilities. However, further testing needs to be performed to understand the exact surface characteristics of each biochar. These tests will allow for concrete conclusions to be drawn between the physical characteristics of each biochar and its adsorption abilities.

4.1.2 Total and Volatile Solids Analysis

A more concrete characterization method that was performed on the six different biochar was the total and volatile solid analysis. Total solids tests show the concentration of moisture and other low boiling organic solvents, while volatile solid tests show the amount of organic material and the concentration of ash present in a sample of biochar. The total and volatile solid results for the six biochars are summarized in Table 3 below.

Table 3. *Analytical results of the percentage of total and volatile solids present in the six different biochars. Results are the average of three trials.*

Biochar	Total Solids	Standard Deviation	Volatile Solids	Standard Deviation
Biochar 1	76.5	±0.2	70.8	±0.3
Biochar 2	45	±10	19	±4
Biochar 3	90.3	±0.6	82.9	±0.4
Biochar 4	94.7	±0.1	89.3	±0.2
Biochar 5	88	±6	85	±8
Biochar 6	51	±8	46	±7

As shown in the table above, each biochar total and volatile solid percentage differ vastly. Biochar 4 had the largest percentage of both total solid and volatile solid (94.7% and 89.3% respectively), while biochar 2 was found to have the smallest (45% and 19% respectively). Overall the biochars had a relatively high total solid percentage, averaging out at around 75%. This indicates that all of the biochars had a relatively low percentage of moisture and organic material except for biochar 2. The low amount of moisture present is to be expected for two different reasons. During the production of biochar, especially if produced via gasification, drying procedures are incorporated to remove the high moisture content contained in the biomass feedstock. However, the type of production method used will determine how pertinent the drying process is, when it occurs, and for how long. For example, if biochar is produced via gasification, the drying process occurs before pyrolysis. Then after pyrolysis is complete, there is an oxidation/combustion step that will return some moisture to the biochar [20]. The second reason that the biochar has a relatively low moisture content is that most biochars are hygroscopic. Hygroscopic means that the biochar can attract and adsorb large content of moisture from the environment into its pores. Therefore, a temperature much higher than 105 °C is needed to remove the moisture. In regards to this study, high moisture content is not favorable. When the moisture content is high it signifies that the biochars adsorption sites are already engaged, meaning the biochar will be able to adsorb fewer inhibitors from the synthetic hydrolysate mixture.

Unlike the total solid percentage, the volatile solid percentage is much more spread out, averaging out at 65% of the mass. Typically, a low volatile matter percentage is beneficial in carbon sequencing and is preferred in biochars [1]. Additionally, the presence of volatile matter affects the stability of the material and implies that the surface of the biochar is already dominated by compounds making the pores inaccessible to new ions [13]. Therefore, a high percentage of volatile matter drastically lowers the sorption capacity of the biochar. Furthermore, as seen in the table above the six biochar we studied all had a relatively high volatile solid amount, with most being 70% or higher. Like total solids, the presence of volatile matter in biochar depends on the production method. Production methods like pyrolysis that occur at high temperatures tend to decrease the amount of volatile matter. Therefore, it is likely that all six biochars were produced from pyrolysis at low temperatures, and will have difficulty adsorbing new ions.

4.1.3 pH Analysis

Another determinant of the characterization of the biochars is the analysis of the biochar's respective pH. Biochar is typically known to be alkaline. The exact pH of each biochar is affected by the temperature at which the biochar underwent pyrolysis and the type of feedstock used to produce the biochar. At higher pyrolysis temperature the acidic functional groups such as carboxylic acid (COOH) and hydroxyl (OH) are removed. Therefore, increasing the ash content and making the biochar more basic [20]. The study of the pH of each of the biochars as ultrapure water moved through the fixed bed can be seen below in Figure 21 and Appendix A2.

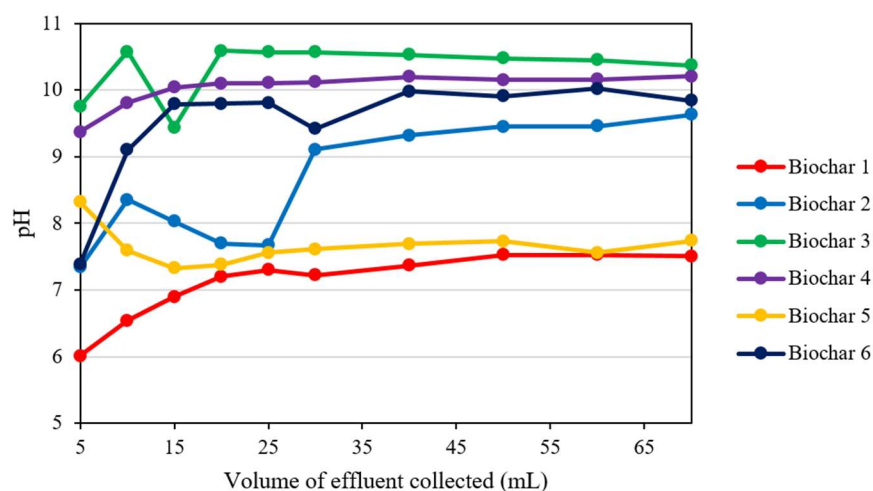


Figure 21. The pH of ultrapure water (average pH of 7.59) collected at set volumetric intervals from the end of a fixed bed packed with biochar. One trial was performed for each type of biochar.

Based on the figure shown above, it can be concluded that all six of the biochars have a basic pH, ranging from 7 to 10.5. Specifically, biochar 3 is seen to have the highest pH while biochar 1 and 5 are seen to have the lowest. Elevated pH levels are generally associated with a high pyrolysis temperature. Also, an elevated pyrolysis temperature is broadly associated with a larger pore size and thereby a larger surface area. In research conducted by Y. Chen et al., an increase of pyrolysis temperature of 500 to 900 °C increased the porosity of the biochar from 0.056 to 0.099 cm³g⁻¹, as well as the surface area of the biochar from 25.4 to 67.6 m²g⁻¹. However, Y. Chen et al. also noticed that in a few cases biochar produced at elevated temperatures was characterized by a lower porosity and surface area. They found that the increased temperatures destroyed or blocked the porous structure of the biochar with tar [24]. Nevertheless, since the exact pyrolysis temperature, production method, and feedstock of each biochar is unknown only a general assumption can be made about the physicochemical properties of each biochar.

4.2 Analysis of Effluent

As adsorption occurs and the hydrolysate moves through the adsorbent, the concentration of inhibitors in the fluid phase and solid phase changes. At the beginning of the adsorption process, most of the mass transfer occurs at the inlet of the fixed bed. Then, as the pores become saturated, the mass transfer zone moves closer to the outlet, until the end of the bed is reached. If the concentration gradient versus volume

of hydrolysate was graphed it would produce an S shape. However, it is extremely challenging to measure the concentration gradient throughout the fixed bed. Therefore, an effective method to record the mass transfer from the liquid phase to the solid phase is through a breakthrough curve. To obtain the values necessary to complete the breakthrough curve, HPLC analysis for glucose, xylose, arabinose, 5-HMF, and furfural was completed. The results of these analyses can be seen in the sections below as well as in Appendix A6-A11.

4.2.1 Activated Carbon

Before we began testing biochar as an adsorbent, we ran multiple preliminary trials with activated carbon. These trials served two main purposes. First, using the activated carbon allowed us to determine the functionality of the experimental setup. Second, because it is known that activated carbon is a successful adsorbent, trials using activated carbon were used as a comparison to determine the success of the biochars as an adsorbent. Trials with activated carbon were performed using both the positive displacement pump and the CO₂ Peltier pump. The results of the positive displacement pump are presented below because it provides a general idea of the success of the adsorbent. The breakthrough curves for a trial with activated carbon as the adsorbent in the positive displacement pump can be seen in Figure 22 below, additional results can be found in Appendix A8.

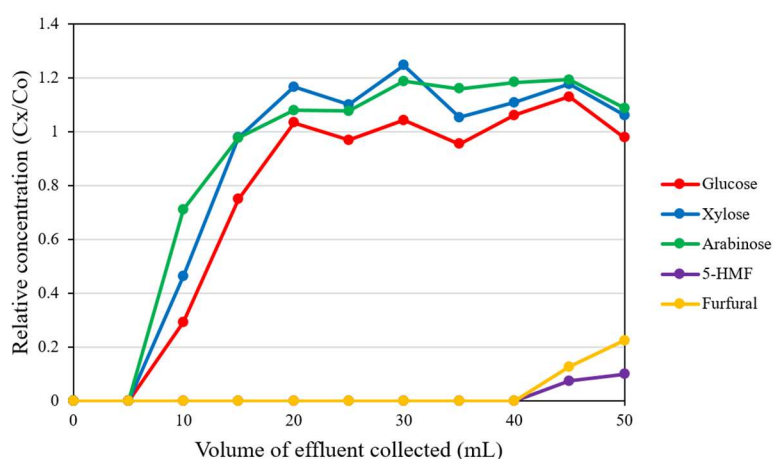


Figure 22. Breakthrough curves for glucose, xylose, arabinose, 5-HMF, and furfural, when activated carbon is the adsorbent. This trial occurred while using the positive displacement pump. The y-axis shows the concentration found in the effluent (Cx) divided by the concentration found in the control (Co). The x-axis shows the volumes of effluent collected.

As shown in Figure 22 above, activated carbon is a very successful adsorbent. It removed inhibitors (5-HMF and furfural), without adsorbing large amounts of the sugars (glucose, xylose, arabinose). However, it would have been beneficial if the volume of effluent collected was extended. By extending the volume of effluent collected a better understanding of whether the adsorption of these two compounds had a narrower or a wider mass transfer zone could occur. Additionally, by increasing the volume collected, all the breakthrough curves would be able to reach equilibrium. However, the sugar compounds did reach an equilibrium state during the collection period, and also broke through the column first. Even though the results are incomplete and based on the inconsistent pump, they do show that activated carbon has a strong affinity to the adsorption of inhibitors. Furthermore, upon analysis of Figure 22, it can be noted that over 97% of the inhibitors were removed from the hydrolysate. However, to gain a more definitive understanding

of the adsorption properties of activated carbon, duplicate trials were performed using the CO₂ Peltier pump. HPLC and graphical results of activated carbon adsorption in the CO₂ Peltier pump can be found in Figure 23 and Appendix A11.

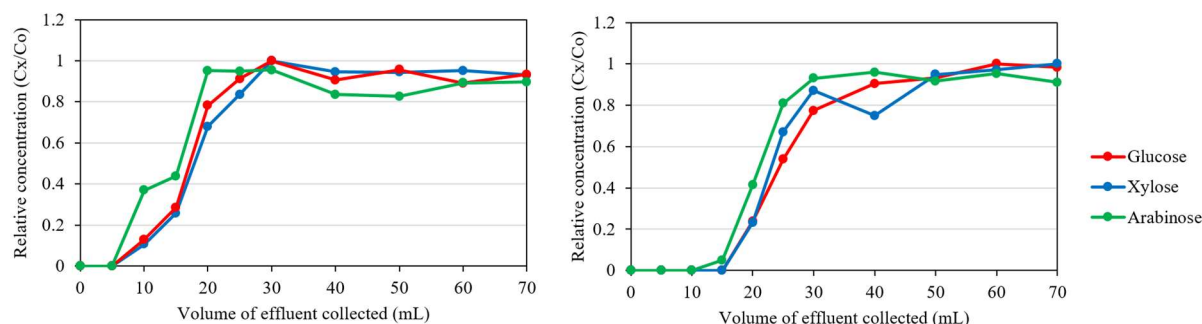


Figure 23. Breakthrough curves for glucose, xylose, and arabinose, when activated carbon is the adsorbent. These trials occurred while using the CO₂ Peltier pump. The curves for glucose and xylose were normalized on both graphs to disallow the relative concentration from exceeding one. The graph on the right is trial one, while the graph on the left is trial two.

Due to unforeseen circumstances, the results of the inhibitor compound were unable to be analyzed. Upon analysis of Figure 23, it appears that when the adsorption tests were moved from the positive displacement pump to the CO₂ Peltier pump, the activated carbon had a higher affinity for the carbohydrates. All three of the sugar compounds have very similar breakthrough curves and appear to reach equilibrium after 30 mL. This illustrates that the affinity activated carbon has for all the sugar compounds is similar. In the past researchers have been able to achieve high selectivity of inhibitors and low affinity for sugar molecules with activated carbon adsorption. Research by Chandel et al. (2007), observed that activated carbon treatment on sugarcane hydrolysate produced a 38.7%, 57%, and 46.8% reduction in furans, phenolics, and acetic acid respectively while having less than a 10% impact on the concentration of carbohydrates. The researchers also noted that the success of activated carbon adsorption is dependent on the ratio of hydrolysate to activated carbon [21]. In research cited by Mussatto et al., it was noticed that a proportion of 1% (w/w) activated carbon to hydrolysate was sufficient to remove 94% of phenolic compounds, with a sugar loss of only 0.47%. However, when a ratio of 30% (w/w) activated carbon to hydrolysate was used, a 31.3% reduction in the carbohydrates was found [64]. Therefore, the higher affinity for sugar seen above in Figure 23, is resultant of the 1.42% (w/w) ratio of activated carbon to hydrolysate. The ratio of adsorbent to adsorbent is worked out in Appendix B2. If a slightly lower mass of activated carbon was used, there would've likely been a decrease in the adsorption of sugar. However, manipulating the amount of activated carbon could have negative results on the adsorption of inhibitors. For this experiment, one gram of activated carbon was chosen, due to it being an adequate amount to completely cover the surface area of the column. If a lower weight is used there could be an insignificant amount of the adsorbent, therefore, creating pockets where the hydrolysate will flow through the column without interacting with the adsorbent at all. Overall, based on past research and the data available, it appears that activated carbon is a successful detoxification method due to its high selectivity for inhibitors.

4.2.2 Biochar 1

After the adsorption trends of activated carbon were understood, experiments were performed to test the ability and success of the different biochars as adsorbents. Biochar 1 was chosen to be tested first because

the initial supply of biochar 1, far exceeded the amount of the other available biochars. Therefore, multiple trials with biochar 1 could be run to understand the unique characteristics of the experimental setup that occur when biochar is used as the adsorbent. One of the main difficulties that occurred when we switched from activated carbon to biochar is the emergence of leaks in the column. The leaks can be attributed to two different features. The largest cause of leakage is the difference in particle size between biochar and activated carbon. Biochar's particle size is smaller allowing the biochar to pack more densely in the column. However, due to the dense compaction of the biochar, there is little to no void space for the liquid to flow through. The smaller void capacity of the biochar requires a larger pressure drop to propel the liquid through the biochar, thereby creating more leaks. The relationship between particle size and pressure drop through a packed bed is typically described by the Ergun Equation which can be seen in Appendix B3. The Ergun equation describes the pressure drop in a packed bed in relation to the packing or particle size, length of the bed, fluid viscosity, and fluid density. It effectively illustrates the inverse relationship between the pressure drop and the particle diameter or particle size. The second reason for the leaks is due to the pump having a poor or broken seal. The leaks happened more regularly in the positive displacement pump than in the CO₂ Peltier pump. The breakthrough curve for one trial of biochar 1 in the old pump can be seen in Figure 24 below, additional results can be found in Appendix A8.

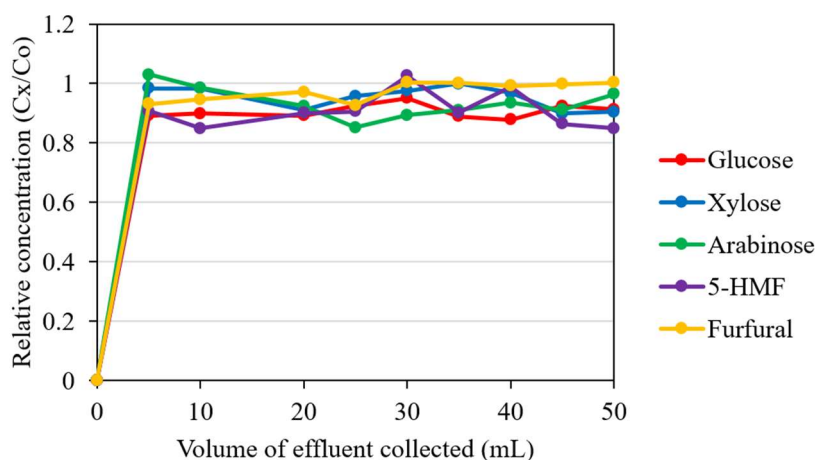


Figure 24. Breakthrough curves for glucose, xylose, arabinose, 5-HMF, and furfural, when biochar 1 is the adsorbent. This trial occurred while using the positive displacement pump.

Illustrated in the graph above, biochar 1 had no better or worse affinity for the inhibitor compounds than the sugar compounds. It almost appears as if the biochar adsorbed more sugars than inhibitors. This graph does illustrate that if any mass transfer did occur between the two phases it was in the first 5 mL of the liquid flowing through the bed. Therefore, to better understand if biochar 1 has an affinity for any compound, a sample should be taken every 1 mL for the first 5 mL. However, this data was unknown when we tested the biochar's adsorption ability in the CO₂ Peltier pump. The results of using biochar 1 as a sorbent in the CO₂ Peltier pump can be viewed below in Figure 25 and Appendix A11.

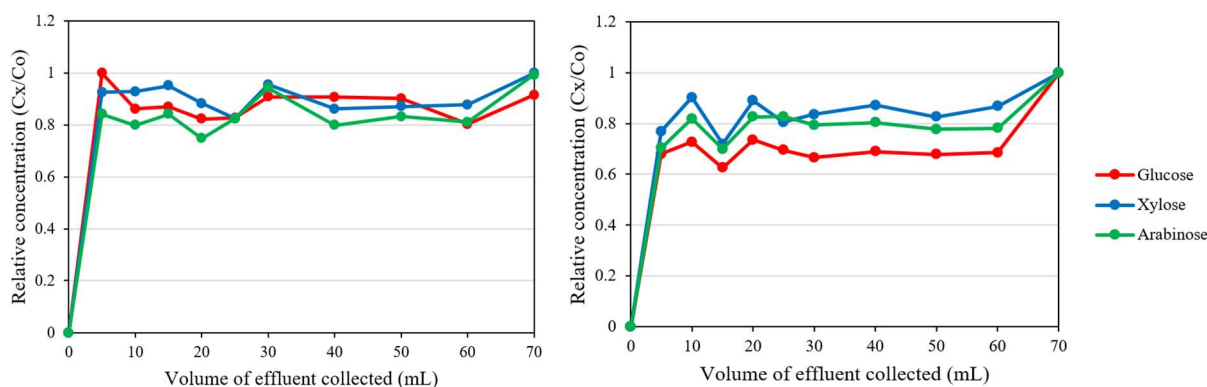


Figure 25. Breakthrough curves for glucose, xylose, and arabinose, when biochar 1 is the adsorbent. These trials occurred while using the CO₂ Peltier pump. The curves for glucose and xylose were normalized on both graphs, while the arabinose curve was normalized on the right graph. The graph on the left is trial one while the graph on the right is trial two.

Similar to the results of activated carbon, the results for furfural and 5-HMF in the CO₂ Peltier pump were unavailable due to unforeseen circumstances. One noticeable feature illustrated by Figure 25 above, is that slight affinity Biochar 1 has for the carbohydrates, shown by some sugars being adsorbed in the first 5 to 10 mL of effluent. Taking additional samples in the first 5 mL would have provided a clearer idea of the affinity between the sugar compounds and the biochar and allowed for a more typical breakthrough curve to emerge. Furthermore, to completely understand the adsorption properties of biochar 1 the breakthrough curves for both 5-HMF and furfural are necessary.

4.2.3 Biochar 2

After tests of the adsorption capacity of biochar 1 were completed, the experiment proceeded numerically through the remaining biochars. Biochar 2 was the last biochar to be tested in the positive displacement pump, although the data from these tests are currently unavailable. Even though the data from the positive displacement pump is unavailable, the results from biochar 2 in the CO₂ Peltier pump is available and can be viewed in Figure 26 below, and Appendix 11.

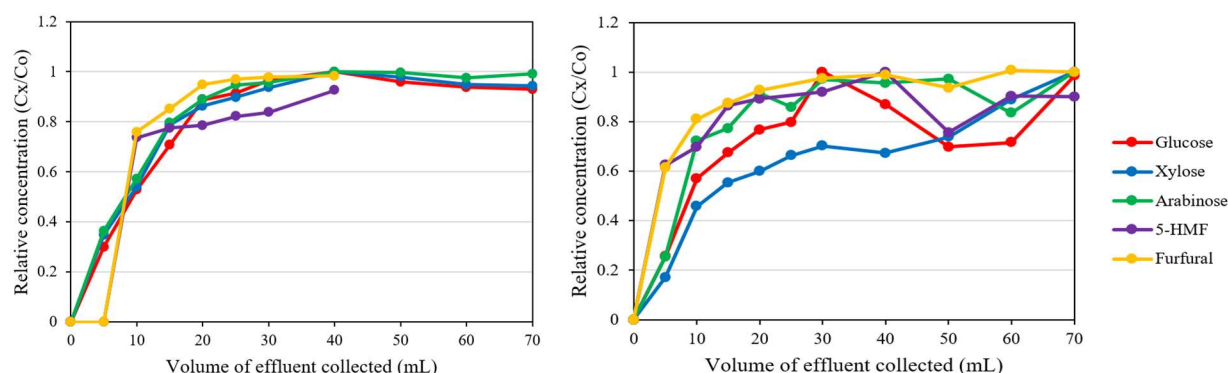


Figure 26. Breakthrough curves for glucose, xylose, arabinose, 5-HMF, and furfural when biochar 2 is the adsorbent. These trials occurred while using the CO₂ Peltier pump. The curves for glucose, xylose, and arabinose were normalized on both graphs, while the 5-HMF and furfural curve was normalized on the right graph. The graph on the left is trial one while the graph on the right is trial two.

Both trials performed with biochar 2 as the sorbent produced unfavorable results. In both trials, the biochar had a higher affinity for the sugar compounds than the inhibitors. In particular, trial two showed that biochar 2 adsorbs a relatively large amount of both xylose and glucose while adsorbing a minimal amount of 5-HMF and inhibitors. During both trials, all compounds reach their breakthrough point after only 5 mL of effluent collected. In the first trial, all the compounds have a narrow mass transfer zone while in the second trial the inhibitors have a narrow mass transfer zone while the sugar compounds specifically xylose and glucose have a wider mass transfer zone. Typically, a narrow mass transfer zone is preferred, due to the reduced use of the adsorbent and reduction in energy costs. Therefore, due to the mass transfer zone of biochar 2 being wider and having limited to no selectivity, biochar 2 is deficient in its ability to detoxify the synthetic hydrolysate solution.

4.2.4 Biochar 4

The next biochar studied was biochar 3, however, the data for biochar 3 was unavailable so a portion of the results for biochar 4 will be presented instead. All tests performed with biochar 4 used only the CO₂ Peltier pump. The results of biochar 4's inhibitor sorption capacity can be seen in Figure 27 below and Appendix A11.

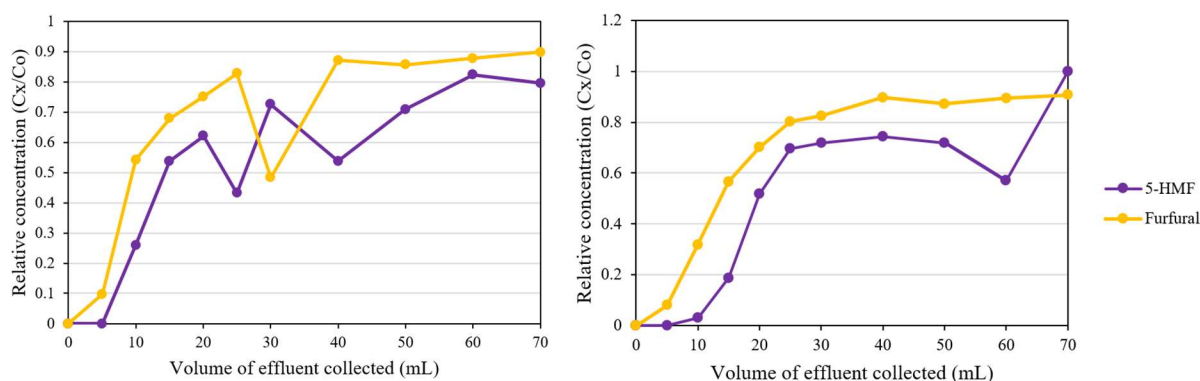


Figure 27. Breakthrough curves for 5-HMF and furfural, when biochar 4 is the adsorbent. These trials occurred while using the CO₂ Peltier pump. The curve for 5-HMF was normalized on the right graph. The graph on the left is trial one while the graph on the right is trial two.

Currently, only the breakthrough curves of 5-HMF and furfural are available for biochar 4. Other than activated carbon, biochar four appears to have the greatest affinity for inhibitors than any of the sorbents previously mentioned. In trial one, the breakthrough point for both 5-HMF and furfural occur after only 5 mL of effluent collected. However, in trial two the breakthrough point for furfural still occurs at 5 mL but the breakthrough point for 5-HMF occurs at 10 mL, allowing a larger volume of 5-HMF to be adsorbed. Larger adsorption of 5-HMF than furfural is a trend that has generally been observed in all sorbents previously studied. Separation occurs between the sorbent and adsorbate when differences in molecular weight, shape, or polarity occur thereby allowing certain molecules to be adsorbed more readily onto the pores of the adsorbent. This creates higher selectivity for one component. Because 5-HMF has a greater size and density than furfural, the adsorption of 5-HMF over furfural can't be due to the size of the compounds. Consequently, the adsorption of 5-HMF over furfural must be due to a molecular interaction between the adsorbent and 5-HMF. Another noticeable feature of the two trials shown above in Figure 27, is the shape of the breakthrough curves. All four breakthrough curves have a narrow mass transfer zone

illustrating the high efficiency of the adsorbent [47]. Concrete conclusions on the overall success of the adsorption properties of the biochar are dependent on understanding the selectivity of the biochar. The sugar breakthrough curves are currently unavailable, so the selectivity of the biochar is not yet determined. However, conclusions on the biochar's affinity for the inhibitor compounds are still beneficial in determining the biochar's ability to detoxify lignocellulosic biomass.

4.2.5 Biochar 5

The next biochar studied was biochar number 5. Similarly to biochar 4, all tests performed with biochar 5 used only the CO₂ Peltier pump. The results of biochar 5's inhibitor sorption capacity can be seen in Figure 28 below and Appendix A11.

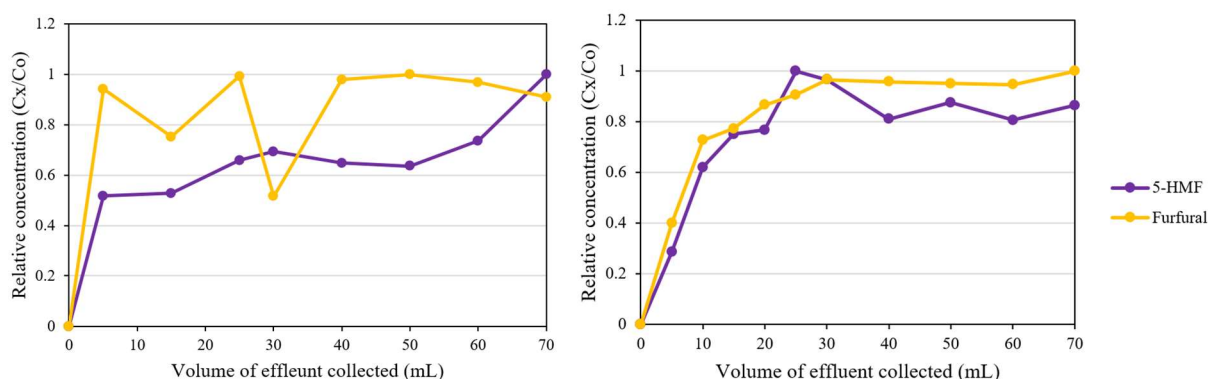


Figure 28. Breakthrough curves for 5-HMF and furfural, when biochar 5 is the adsorbent. These trials occurred while using the CO₂ Peltier pump. The curve for 5-HMF and furfural were normalized on both graphs. The graph on the left is trial one while the graph on the right is trial two.

Like biochar 4, the adsorption of 5-HMF was greater than the adsorption of furfural in both trials. The breakthrough point for all trials occurred at 5 mL, illustrating the limited mass transfer zone and inefficiency of biochar 5. Additionally, in trial one the biochar fails to follow a traditional breakthrough curve shape, hinting that the breakthrough point occurs at much lower than 5 mL, thus limiting the mass transfer zone further. Better results would emerge if additional tests were taken every mL during the first 5 mL of effluent collected. The additional tests would allow a more concrete breakthrough curve to emerge, thereby revealing a more accurate saturation capacity and breakthrough capacity. Based on the available results, it is possible to conclude that biochar 5 has a relatively low affinity for furfural and a higher affinity for 5-HMF. Yet, due to the large discrepancies between the two trials, an additional trial would need to be conducted to determine the exact relationship between 5-HMF and biochar 5.

4.2.6 Biochar 6

The next biochar to be investigated was biochar 6. Similarly to both biochar 4 and 5, all tests performed with biochar 6 used only the positive displacement pump. The results of biochar 6's inhibitor sorption capacity can be seen in Figure 29 below and Appendix A11.

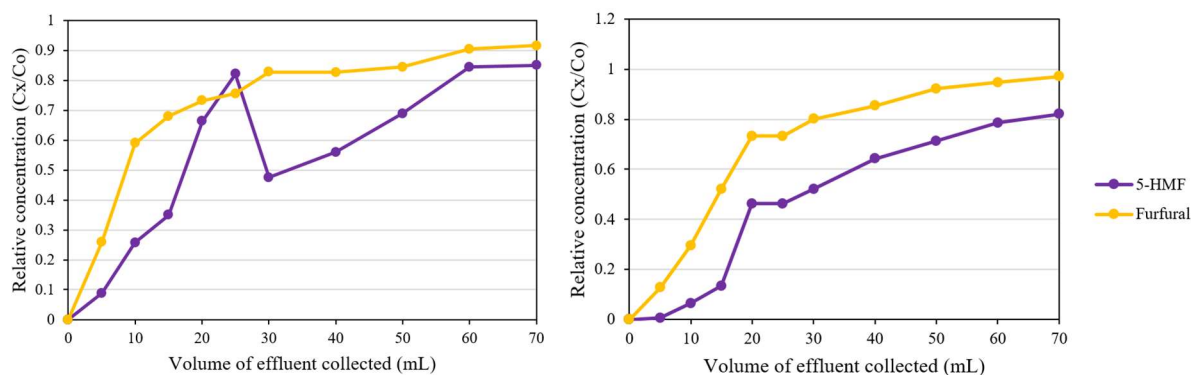


Figure 29. Breakthrough curves for 5-HMF and furfural, when biochar 6 is the adsorbent. These trials occurred while using the CO₂ Peltier pump. The graph on the left is trial one while the graph on the right is trial two.

Similar to both biochar 4 and 5, the adsorption of 5-HMF was greater than the adsorption of furfural. One aspect of biochar 6 that is unique is its breakthrough point for 5-HMF. In trial two the breakthrough point is at 15 mL, generally three times larger than the breakthrough point found for 5-HMF with any of the previously mentioned biochars. This indicates that biochar 6 had the largest mass transfer zone of all the biochars. Based on these preliminary results, it is possible to conclude that biochar 6 has one of the highest affinities for fermentation inhibitors. Yet, concrete conclusions on the sorption ability of biochar 6 depend on the results of the breakthrough curves for the carbohydrates. Therefore, the selectivity of biochar 6 is still unknown.

4.2.7 Activated Biochar 4

Activated biochar 4 was the last sorbent to be tested and analyzed. Biochar 4 was activated in hopes that the number of inhibitors adsorbed would increase due to an increased specific surface area and pore fraction on the biochar. In past research by Cha et al., when biochar was activated via a chemical activation agent such as sodium hydroxide (NaOH), the surface area and pore volume of the biochar increased with increasing doses of the activation agent. When the NaOH to char ratio was increased from 1:1 to 1:3 the specific surface area increased from 689 m²/g to 1,224 m²/g while the pore volume increased from 0.29 cm³/g to 0.44 cm³/g [20]. The ratio of NaOH to biochar used to activate biochar 4 was approximately 5:1. Therefore, it can be assumed that the surface of the biochar did not change favorably. The results of activated biochar 4's sorption capacity can be viewed in Figure 30 below and Appendix A11. It is important to note that all tests with activated biochar 4 occurred with the CO₂ Peltier Pump.

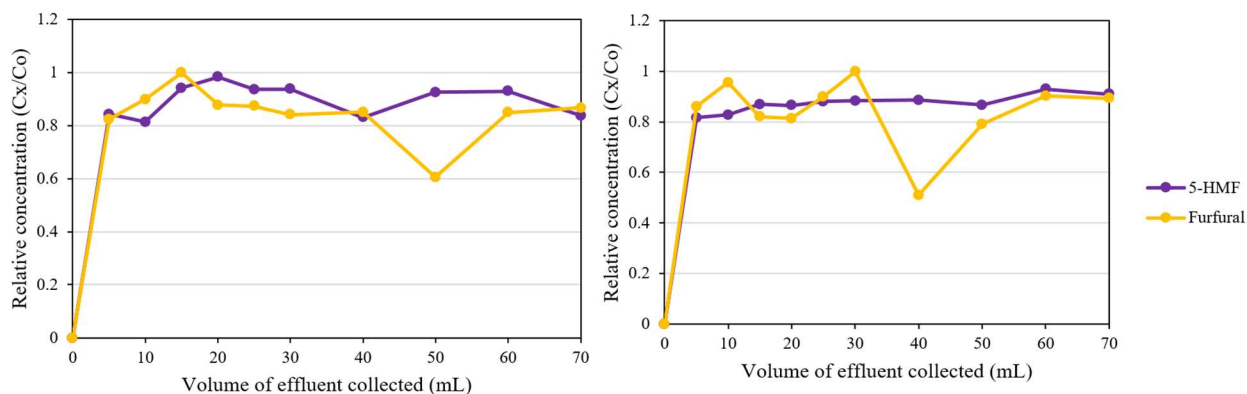


Figure 30. Breakthrough curves for 5-HMF and furfural, when activated biochar 4 is the adsorbent. These trials occurred while using the CO₂ Peltier pump. The curve for furfural was normalized on both graphs. The graph on the left is trial one while the graph on the right is trial two.

Upon activation, it appears that the sorption abilities of the biochar dramatically decreased. One issue with activating biochar is that it is possible to collapse and decrease the surface area of the biochar if inappropriate methods are followed. Activating the biochar for too long, and at too high of temperature have been linked to adverse effects on the surface area of the biochar. Additionally, due to the large amount of chemical agent used on the biochar, the biochar likely experienced adverse effects. However, until an analysis is performed on the change in pore size between biochar 4 and activated biochar 4, concrete conclusions cannot be made. Overall, upon the comparison of the breakthrough curves for furfural and 5-HMF, the mass transfer zone is extremely narrow and hits the breakthrough point at approximately 5 mL. However, because no tests were performed in the first 5 mL, the breakthrough point likely occurs at a much lower volume, signifying that the sorption capacity of the inhibitors is much lower than shown in Figure 30 above. Until additional tests can be performed it is impossible to conclude on the exact issues with activating the biochar, however, it is possible to note that activation had adverse effects on the sorption capacity of biochar 4.

4.2.8 pH Analysis

Inhibitor adsorption onto a sorbent is sensitive to any changes in the pH of the adsorbate. At the beginning of every trial, the hydrolysate pH was recorded. Then as effluents were collected the pH of the effluents was also noted. According to research performed by Mussatto et al., the adsorption of solutes is dependent on the pH of the medium. For example, if the solutes are acidic than a low pH favors adsorption. This happens because weak organic acids are the easiest adsorbed when they are in their non-ionized state. Therefore, an adsorbate with a low or acidic pH can adsorb phenols and anions, who are weakly acidic, more readily. Additionally, if weakly basic molecules are to be adsorbed, then an adsorbate with a high pH is preferred. In the case of the adsorption of lignocellulose degradation products, a major removal of the molecules was attained by Mussatto when the pH of the adsorbate was 2 [64]. The pH of the adsorbates we tested can be seen in Table 4 below, and Appendix A12-A13.

Table 4. The pH of the hydrolysate mixture taken before the beginning of each trial. All pHs were recorded at room temperature.

Trial	Activated Carbon	Biochar 1	Biochar 2	Biochar 3	Biochar 4	Biochar 5	Biochar 6	Activated Biochar 4
1	3.3	3.3	3.32	3.62	3.51	3.35	3.5	3.38
2	3.34	3.29	3.54	3.5	3.53	3.39	3.38	3.31

As seen by Table 4 above, the pH of the adsorbates fell into a range of 3.29 to 3.62 averaging out at around 3.41. This pH is slightly higher than the pH reported by Mussatto et al. and could be one of the reasons that limited inhibitor compounds adsorption. However, biochar 4 had some of the highest pH control recording and yet one of the largest sorption capacities. Therefore, concrete links between the influence of pH in the adsorption process are unknown based on the current data. In addition to recording the pH of the hydrolysate, all effluents collected were also analyzed via pH testing. The pH results of the effluents can be seen in Figure 31 below and found in Appendix A12-A13.

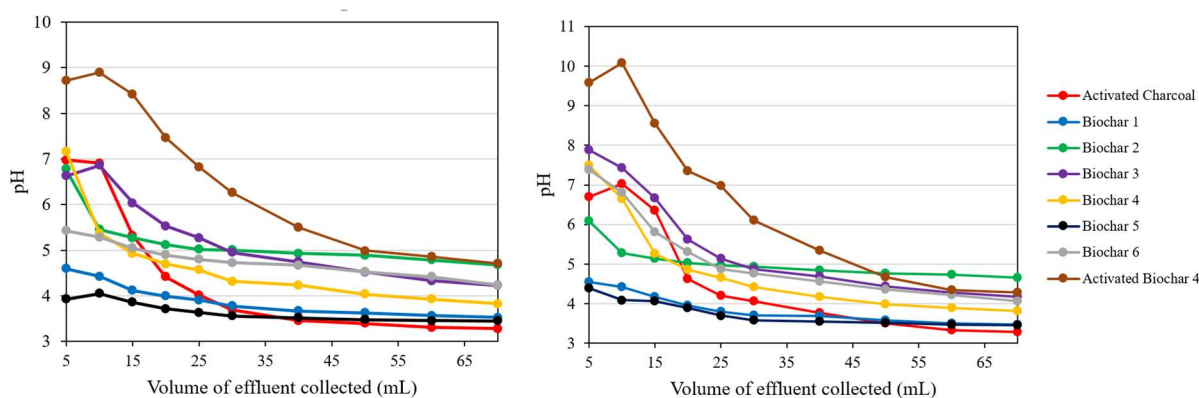


Figure 31. Results of the pH of the effluent for each volume collected. Results while using activated carbon, biochar 1-6, and activated biochar 4 as the adsorbent can be seen on each graph. The graph on the left is trial one while the graph on the right is trial two.

Each trial had a similar pH trend in that the early volumes tested had a much higher pH than the larger or later volumes tested. One reason the pH was higher in the beginning, was due to the pH of the biochar being much larger than the pH of the hydrolysate. Therefore, as the adsorbate moved through the biochar it would leach some molecules off of the biochar and increase the pH of the effluent. An example of this is shown by the results of activated biochar 4 who has much higher pH results than any other sorbent tested. One reason for this is that as the hydrolysate moved through the column, it interacted with the NaOH on the surface of the biochar which increased the pH of the effluent. Then as all the NaOH was leached off the surface of the biochar, the pH of the effluent began to approach the pH of the hydrolysate. Another reason the pH was larger at the onset of the trial, was the initial removal of some acids present in the adsorbate. Then as the adsorbent became saturated the adsorbate began to simply flow over the adsorbent, disallowing any inhibitors to be adsorbed and allowing the pH to approach the pH of the hydrolysate. A phenomenon noticed by Jameel et al. when studying the detoxification of lignocellulosic biomass, was a link between the removal of formic acid and acetic acid and a pH increase [53]. The analysis of the effluent's pH provides the ability to discern if additional chemical reactions are occurring as the adsorbate moves through the

adsorbent. However, due to the pH approaching the pH of the hydrolysate mixture in all trials it is safe to assume no additional reactions are occurring as the hydrolysate moves through the column.

4.3 Adsorption Characterization

Each compound's breakthrough curve shown above in section 4.2 has a unique saturation and breakthrough capacity that applies to it. Analyzing the saturation and breakthrough capacity of each adsorbent provides quantitative results of the success and efficiency of the sorbent. The saturation and breakthrough capacity for each adsorbent is discussed in the following section.

4.3.1 Saturation Capacity

The saturation capacity is a helpful tool in characterizing the success of each adsorbent because it illustrates the maximum amount of each molecule the adsorbent can hold. Therefore, a successful adsorbent will be characterized by a minuscule saturation capacity for all sugar molecules and a high saturation capacity for all inhibitors. The saturation capacity for each adsorbent can be seen in Table 5 below, and Appendix A14.

Table 5. *The saturation capacity of eight different adsorbents.* All capacities are recorded in mg/g and are the average of two trials from the CO₂ Peltier pump (dashed lines indicate unavailable data).

Adsorbent	Glucose	Xylose	Arabinose	5-HMF	Furfural
Activated Carbon	23.5	23.5	21.6	-	-
Biochar 1	16.3	10.9	14.6	-	-
Biochar 2	15.9	18.1	11.3	10.5	6.3
Biochar 3	-	-	-	-	-
Biochar 4	-	-	-	31.4	20.8
Biochar 5	-	-	-	20.9	10.4
Biochar 6	-	-	-	32.6	19
Activated Biochar 4	-	-	-	10	14.1

As seen in Table 5 above, there are some unknown saturation capacities. Yet, it is still possible to gain an understanding of the overall saturation capacity of each sorbent based on the material presented above. Biochar 4 and 6 have very similar saturation capacities, around 32 and 20 mg/g for 5-HMF and furfural respectively. This is the highest capacity seen for the inhibitors across the board. Additionally, biochar 4 and 6 had the second and third highest pH respectively, indicating that it is probable that these two biochars have the largest pore size and are therefore able to accommodate the largest amount of inhibitors. Another note of interest is the limited saturation capacity of activated biochar 4. This biochar only adsorbed 10 mg/g of 5-HMF and 14.1 mg/g of furfural. Activated biochar 4 had a lower saturation capacity for inhibitors than

biochar 1 and 2 did for sugars. Further, illustrating the deficiency of activated biochar 4 as an adsorbent. Also, activated biochar 4 adsorbed more furfural than 5-HMF indicating that the surface chemistry of this sorbent is different than any of the other sorbents.

Additionally, upon analyzing biochar 2 it is evident that the sorbent is not able to adsorb significant quantities of inhibitors. Specifically, biochar 2 adsorbed 10.5 mg/g of 5-HMF, 6.3 mg/g of furfural, and over 45 mg/g of carbohydrates. Indicating that biochar 2 has not only a low selectivity, it also has a low saturation capacity. Activated carbon known for its high adsorption capacity, was seen to adsorb relatively large amounts of sugar when compared to the saturation capacity of the biochars. However, the amount of inhibitors adsorbed for activated carbon is unknown, thereby, it is difficult to identify the amount of sugars adsorbed as relatively high or low. In a report by Heinonen et al., the saturation capacity of activated carbon was found to be 75 g/g for both HMF and furfural, while only being 4 g/g for glucose [48]. Indicating an approximately eighteen times larger affinity for inhibitors than sugars. Based on these trends the saturation capacity of activated carbon is much higher than the saturation capacity of any biochar tested in this study. If industries hope to use biochar as a sorbent instead of activated carbon, modifications to the surface chemistry of biochar must occur to allow it to be more susceptible to adsorption.

4.3.2 Breakthrough Capacity

Another method to quantitatively characterize the adsorption properties of each sorbent is through the breakthrough capacity. The breakthrough capacity indicates the amount of adsorbate the sorbent was able to adsorb before hitting the breakthrough point, or the amount adsorbed right before the breakthrough curve becomes asymptotic. In more industrial systems, the flow is either stopped or diverted right before the breakthrough point to allow the adsorbent to regenerate and remove adsorbed molecules. Additionally, by diverting the flow of adsorbate the detoxifying process is allowed to advance without ever reaching the saturation capacity of the adsorbent. Therefore, the breakthrough capacity indicates the optimum amount of inhibitors that can be removed by a certain amount of adsorbent. The breakthrough capacities for each adsorbent can be seen in Table 6 below and Appendix A14.

Table 6. *The breakthrough capacity of eight different adsorbents.* All capacities are recorded in mg/g and are the average of two trials from the CO₂ Peltier pump. For some capacities, the amount is lower than the value listed in the table below (dashed lines indicate unavailable data).

Adsorbent	Glucose	Xylose	Arabinose	5-HMF	Furfural
Activated Carbon	14.4	14.3	9.9	-	-
Biochar 1	< 2.9	< 2.9	< 3.1	-	-
Biochar 2	< 4.3	< 4.4	< 4.2	< 4.2	< 4.2
Biochar 3	-	-	-	-	-
Biochar 4	-	-	-	7.5	4.8
Biochar 5	-	-	-	< 4.0	< 3.3
Biochar 6	-	-	-	9.6	4.5
Activated Biochar 4	-	-	-	< 2.9	< 2.9

As seen in Table 6 above, the breakthrough capacity was significantly lower than the saturation capacity found in Table 5. Biochar 4 and 6 still exhibit similar adsorption characteristics however, biochar 6 has a slightly larger breakthrough capacity than biochar 4. This is specifically true when looking at the adsorption of 5-HMF. Biochar 4 adsorbed 7.5 mg/g while biochar 6 was able to adsorb 9.6 mg/g, approximately 2 mg/g more. Biochar 2 had very similar breakthrough capacities for both inhibitors and sugars, and both activated biochar 4 and biochar 5 had insignificant breakthrough capacities. The largest breakthrough capacity was seen when activated carbon was used as a sorbent. In research by Heinonen et al., a breakthrough capacity of 39 and 42 g/g was achieved for 5-HMF and furfural respectively while the breakthrough capacity for glucose was only 1.5 g/g [48]. Indicating that the inhibitor breakthrough capacity for activated carbon would be much larger than any results obtained with biochar. Overall the analysis of the breakthrough capacities reveals that the surface chemistry between the biochar and lignocellulosic hydrolysate is unsuitable for adsorption. Further research must be performed to understand the distinct difference between the surface chemistry of activated carbon and biochar before biochar can hope to replace activated carbon as an adsorbent.

4.4 Fermentation of Detoxified Lignocellulosic Hydrolysate

The purpose of detoxification is to reduce the concentration of inhibitors, thereby increasing the amount of ethanol that can be produced. In research by Delgenes et al., a concentration of 0.5 g/L of furfural and 1 g/L of 5-HMF is seen to have drastic effects on the percent of ethanol that can be produced using yeast strain, *S. cerevisiae* [35]. The amount of 5-HMF and furfural present in the hydrolysate after adsorption, using biochar 2, 4, 5, 6, and activated biochar 4 can be found below in Table 7. Activated carbon, biochar 1, 2, and 3 were not included in this study due to the unavailability of their inhibitor saturation capacity.

Table 7. The concentration of inhibitors (5-HMF and furfural) found in the effluents after detoxification. All concentrations are in units of g/L and are the average of two trials.

Adsorbent	5-HMF Concentration (g/L)	Furfural Concentration (g/L)
Biochar 2	0.85	0.91
Biochar 4	0.55	0.70
Biochar 5	0.70	0.85
Biochar 6	0.53	0.73
Activated Biochar 4	0.86	0.80

As seen by Table 7 above, the hydrolysate purified by activated biochar 4 had the largest amount of inhibitors still present in the effluent. Biochar 4 and 6 experienced a decrease in the concentration of inhibitors from the original amount of 1 g/L. The concentration of inhibitors present in the detoxified lignocellulosic hydrolysate was then used to calculate the percentage of ethanol that can be produced. A comparison of the amount of ethanol that can be produced from the lignocellulosic hydrolysates detoxified by biochar 2, 4, 5, 6, and activated biochar 4 can be seen in Figure 32 below and Appendix A15.

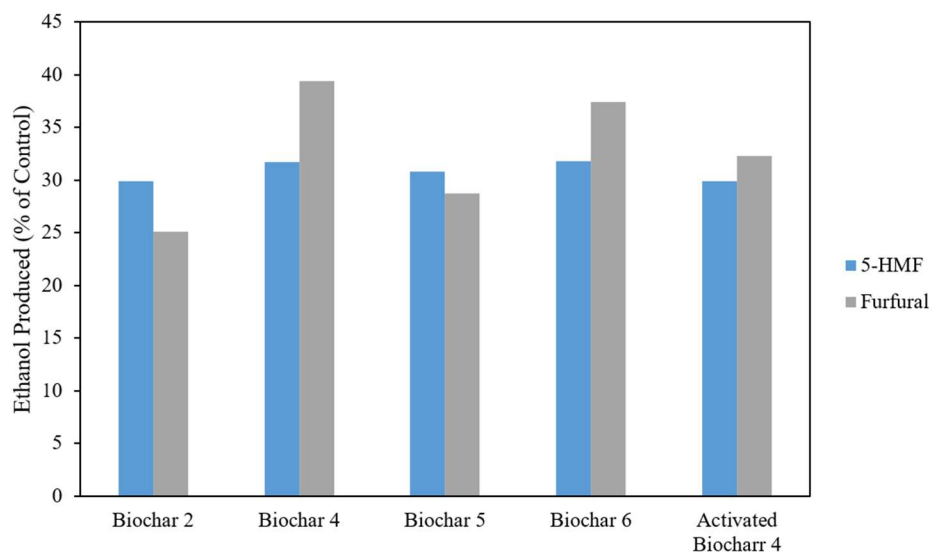


Figure 32. Percent of ethanol produced from lignocellulosic hydrolysate detoxified by biochar 2, 4, 6, and activated biochar 4. Percentages are calculated as the amount of ethanol produced as a percentage of the amount of ethanol produced by a control. The blue bars represent the percentage of ethanol produced in the presence of varying concentrations of 5-HMF, while the gray bars represent the percentage of ethanol produced in the presence of varying concentrations of furfural [35].

Figure 32, accounts for the percentage of ethanol that can be produced in the presence of only one inhibitor. In reality, the inhibitors have a synergistic effect on decreasing the amount of ethanol that can be produced. Therefore, if both inhibitors are present in large concentrations, the amount of ethanol that can be produced is much lower than noted in Figure 32. In research performed by Martinez et al., a furanic concentration above 0.9 g/L negatively affects the percentage of ethanol that can be produced. As seen by Table 7, all

collected lignocellulosic effluents had a concentration higher than 1.25 g/L of furanic compounds, with the average being 1.50 g/L [64]. Therefore, it can be concluded that the percentage of ethanol produced from the detoxified adsorbents is much lower than stated in Figure 32. Although Figure 32 fails to summarize the synergistic effect of the inhibitors, it does successfully summarize the ability of each hydrolysate to produce ethanol if only one inhibitors were present. The expected amount of ethanol produced was lower than 50% for all detoxified hydrolysates. The largest amount of ethanol produced was the hydrolysate detoxified by biochar 4, while the smallest amount of ethanol produced was the hydrolysate detoxified by biochar 2, 5, and activated biochar 4. The generally low percentages of ethanol produced from hydrolysate detoxified by biochar adsorption, illustrates the need for further testing on biochar's adsorption abilities.

5. Conclusion and Recommendations

The rapidly evolving environmental consequences of using fossil fuel-based energy have created a crucial need for cleaner, more environmentally friendly energy sources. In recent years, second generation biofuels, fuels derived from lignocellulosic biomass and industrial waste, have risen in popularity due to their reduced release of pollution, affordability, and high overall energy efficiency. Typically, second generation ethanol is produced through fermentation. Because of the rigid and coarse structure of lignocellulosic biomass, a pretreatment step is necessary to liberate the sugars before fermentation can occur. The most common pretreatment method is hydrolysis. During hydrolysis, the degradation of lignocellulose biomass produces fermentation inhibitors in addition to the desired simple sugars. Therefore, before fermentation can occur a detoxification step is necessary to strip the lignocellulosic hydrolysate of most of the inhibitor compounds. One of the most popular detoxification methods of lignocellulosic hydrolysate is through the use of activated carbon as an adsorbent. Due to the similarity between activated carbon and biochar, there has been an interest in whether biochar has the same adsorption properties as activated carbon. The affordability, relative ease of production, and environmental benefits of biochar make it a preferred adsorbent to activated carbon. However, the adsorption abilities of biochar are currently unknown, so it has not replaced activated carbon as an adsorbent.

Even though activated carbon and biochar are known to have similar methods of production, and thus similar composition, the surface chemistry of biochar and activated carbon are sufficiently different. Thereby, the adsorption characteristics of one do not apply to the other. Analyzing and quantitatively characterizing the HPLC results revealed that activated carbon could adsorb a significantly larger amount of molecules than biochar. However, two of the biochar, specifically biochar 4 and 6, showed promising results. Both biochars exhibited a similar saturation capacity for 5-HMF and furfural, which was found to be approximately 32 and 20 mg/g, respectively. Yet, when biochar 4 was activated in hopes of increasing the pore size, the saturation capacity significantly decreased from 31.4 and 20.8 mg/g to 10 and 14.1 mg/g for 5-HMF and furfural respectively. This indicated that to increase the adsorption properties of biochar, an activation method that enhances the surface properties instead of destroying the surface chemistry needs to be established. Overall, biochar does have benefits to being used as an adsorbent: it's not only renewable, but also affordable, and environmentally friendly. However, until the adsorption characteristics of biochar are greatly enhanced, it is unlikely it will be used at an industrial scale in the detoxification of lignocellulosic biomass.

Additionally, to better understand the results presented in this paper, some supplemental experiments and recommendations should be considered. One general recommendation that should be considered for the operation of the adsorption test, is to use glass wool instead of cotton balls. Cotton balls are made of glucose, so when the hydrolysate moves through the fixed bed, mass transfer occurs between the cotton ball and the hydrolysate. This accounts for why a slightly larger percentage of sugars were found in the effluent than in the control solutions. Additionally, the synthetic sugarcane hydrolysate that was produced contained equal parts of sugar and inhibitors, which is atypical of a hydrolysate mixture. If a higher percentage of carbohydrates than inhibitors were used, the adsorption of inhibitors would likely have been much larger. To test this theory, experiments should be conducted with varying concentrations of inhibitors and sugars present in the synthetic hydrolysate mixture. Also, to make the trials more realistic, a hydrolysate solution prepared from subcritical water hydrolysis should be used instead of a synthetic solution. Additionally, to

increase the accuracy of the results, more than two trials for each different adsorbent should be run. This applies to preliminary pH data as well as total and volatile solid data. Also, the physical and chemical attributes of the different adsorbents should have been studied, in particular, the pore size and functional groups present on the surface of the biochar. A better understanding of the different biochar properties would help determine an appropriate activation method to increase and enhance the surface chemistry of the biochar.

Furthermore, to better understand the surface chemistry of the sorbents, tests with biochars produced under known specifications should be used. If the feedstock material and production method of the biochar is known, clear links between the adsorption properties of the biochar and the physical and chemical properties of the biochar will become known. Also, testing the biochar adsorption isotherms will provide a clearer image of the adsorption characteristics. By performing different isotherm tests, different concentrations of adsorbent will be used, therefore determining a favorable ratio between adsorbate and adsorbent specific for biochar.

Before biochar can be negated as an adsorbent for lignocellulosic biomass, additional tests that more efficiently and effectively test the detoxification of lignocellulosic hydrolysate must occur. Until then, it is unlikely biochar will be able to be scaled-up for any industrial detoxification processes. However, any additional research performed on sustainable energy alternatives, whether they are successful or unsuccessful, will contribute to a cleaner and less polluted world.

References

1. Abraham, A., Mallapureddy, K. K., Mathew, A. K., & Sukumaran, R. K. (2018). Lignocellulosic biorefinery wastes, or resources? In T. Bhaskar, S. K. Khanal, D. Lee, S. V. Mohan, & A. Pandey (Eds.), *Waste biorefinery* (267-297). <https://doi.org/10.1016/B978-0-444-63992-9.00009-4>
2. Addy, M., Anderson, E., Chen, P., Cheng, Y., Ding, K., Fan, L., Lei, H., Li, B., Liu, P., Liu, Y., Peng, P., Ruan, R., Wang, Y., Zhang, Y., & Zhou, N. (2019). Biofuels: Introduction. In C. Dussap, E. Gnansounou, S. K. Khanal, C. Larroche, A. Pandey, & S. Ricke (Eds.), *Biofuels: Alternative feedstocks and conversion processes for the production of liquid and gaseous biofuels* (3-43). <https://doi.org/10.1016/B978-0-12-816856-1.00001-4>
3. Ahmad, M., Bolan, N., Lee, S. S., Lim, J. E., Mohan, D., Ok, Y. S., Rajapaksha, A. U., Vithanage, M., & Zhang, M. (2014, March). Biochar as a sorbent for containment management in soil and water: a review. *Chemosphere*, 99, (19-33). <https://doi.org/10.1016/j.chemosphere.2013.10.071>
4. Alchorne, J. A., Belincanta, J., & Teixeira da Silva, M. (2016). The Brazilian experience with ethanol fuel: Aspects of production, use, quality and distribution logistics. *Brazilian Journal of Chemical Engineering* 33(4). <https://doi.org/10.1590/0104-6632.20160334s20150088>
5. Alves, B. (2020, February 17). *Brazil: Sugar cane production volume 2010-2020*. Statista. <https://www.statista.com/statistics/742530/sugar-cane-production-volume-brazil/>
6. Antunes, F. A. F., Canilha, L., Chandel, A. K., Freitas, W. L. C., Milessi, T. S. S., & Silva, S. S. (2012, November 26). Bioconversion of sugarcane biomass into ethanol: An overview about composition, pretreatment methods, detoxification of hydrolysates, enzymatic saccharification, and ethanol fermentation. *Journal of Biomedical and biotechnology* 2012, 1-15. <https://doi.org/10.1155/2012/989572>
7. Aoki, K., Böttcher, H., De Cara, S., Fritz, S., Havlik, P., Kindermann, G., Kraxner, F., Leduc, S., Mosnier, A., Obersteiner, M., Schmid, E., Schneider, U. A., Skalsky, R., & Timm, S. (2011, October). Global land-use implications of first and second generation biofuel targets. *Energy Policy*, 39(10), 5690-5702. <https://doi.org/10.1016/j.enpol.2010.03.030>
8. Basso, L. C., Basso, T. O., & Rocha, S. N. (2011, September). Ethanol production in Brazil: The industrial process and its impacts on yeast fermentation. In M. A. Dos Santos Bernardes (Eds.), *Biofuel production recent developments and prospects* (85-100). Retrieved from https://www.researchgate.net/profile/Thiago_Basso/publication/221916714_Ethanol_Production_in_Brazil_The_Industrial_Process_and_Its_Impact_on_Yeast_Fermentation/links/552675660cf21e126f9db39c.pdf?sa=D&ust=1585532057737000&usg=AFQjCNFaCYLG9n0cZrN-LXILi8NnsL43FA
9. Bastidas-Oyanedel, J. R., Schmidt, J. E. (2018). Waste biorefinery in Arid/Semiarid Regions. In T. Bhaskar, S. K. Khanal, D. Lee, S. V. Mohan, & A. Pandey (Eds.), *Waste biorefinery: potential and perspectives* (605-621). <https://doi.org/10.1016/B978-0-444-63992-9.00020-3>
10. Bernardio, C. D., Cherubin, R. A., Cristina de Lima Paulillo, S., Giometti, F. H. C., Godoy, A., Lorenzi, M. S., Lopes, M. L., Neto, H. B. A. & Vianna de Amorim, H. (2016, October 25). Ethanol production in Brazil: a bridge between science and industry. *Brazilian Journal of Microbiology* 47, (64-76). <https://dx.doi.org/10.1016%2Fj.bjm.2016.10.003>
11. Binod, P., Janu, K. U., Pandey, A., & Sindhu, R. (2019). Hydrolysis of cellulosic and hemicellulosic biomass. In C. Dussap, E. Gnansounou, S. K. Khanal, C. Larroche, A. Pandey, & S. Ricke (Eds.), *Biofuels: Alternative*

- feedstocks and conversion processes for the production of liquid and gaseous biofuels* (447-460).
<https://doi.org/10.1016/B978-0-12-816856-1.00019-1>
12. Biofuel UK. (2010). *Third Generation Biofuel*. <http://biofuel.org.uk/third-generation-biofuels.html>
 13. Boguta, P., Sokolowska, Z., & Tomczyk A. (2020, February 5). Biochar physicochemical properties: pyrolysis temperature and feedstock kind effects. *Reviews in environmental science biotechnology* 19, 191-215.
<https://doi.org/10.1007/s11157-020-09523-3>
 14. Bowra, S., Cooper, H. J., & Powell, T. (2016, May 14). Subcritical water processing of proteins: An alternative to enzymatic digestion. *Analytical chemistry* 88(12), 6425-6432. <https://doi.org/10.1021/acs.analchem.6b01013>
 15. Calvo, L. F., García, A. I., Martín-Villacorta, J., Otero, M., & Rozada, F. (2003, May). Dye Adsorption by sewage sludge based activated carbons in batch and fixed bed systems. *Bioresource technology*, 87(3), 221-230.
[https://doi.org/10.1016/S0960-8524\(02\)00243-2](https://doi.org/10.1016/S0960-8524(02)00243-2)
 16. Cao, X., Gao, B., Inyang, M. I., Mosa, A., Ok, Y. S., Pullammanappallil, P., Xue, Y., Yao, Y., & Zimmerman, A. (2016). A review of biochar as a low cost adsorbent for aqueous heavy metal removal. *Critical reviews in environmental science and technology*, 46(4), 406-433. <https://doi.org/10.1080/10643389.2015.1096880>
 17. Capaccio. (2011, August 24). Netherlands: Furfural [Illustration]. Wikimedia Commons.
https://commons.wikimedia.org/wiki/File:Furfural_structuur.png
 18. Carriquiry, M. A., Du, X., & Timilsina, G. R. (2011, July). Second generation biofuels: Economic and policies. *Energy Policy*, 39(7), 4222-4234. <https://doi.org/10.1016/j.enpol.2011.04.036>
 19. Cayla, A., Giraud, S., Guan, J., Malucelli, G., Mandlekar, N., & Rault, F. (2018, March 21). An overview on the use of lignin and its derivatives in fire retardant polymer systems. In M. Poletto (Eds.), *Lignin-Trends and applications*. Doi: 10.5772/intechopen.72963
 20. Cha, J. S., Jeon, J., Jung, S., Park, S. H., Park, Y., Ryu, C., & Shin, M. (2016, August 16). Production and utilization of biochar: A review. *Journal of Industrial and Engineering Chemistry*, 40, 1-15.
<https://doi.org/10.1016/j.jiec.2016.06.002>
 21. Chandel, A. K., Kapoor, R. K., Kuhad, R. C., & Singh, A. (2007, July). Detoxification of sugarcane bagasse hydrolysate improves ethanol production by *Candida shehatae* NCIM 3501. *Bioresource Technology*, 98(10), 1947-1950. <https://doi.org/10.1016/j.biortech.2006.07.047>
 22. Chandel, A. K., Silvério da Silva, S., & Singh, O. V. (2011, September 15). Detoxification of lignocellulosic hydrolysates for improved bioethanol production. In M. A. D. S. Bernardes, *Biofuel production recent developments and prospects* (225-247). Doi: 10.5772/959
 23. Chen, H. (2015). Lignocellulose biorefinery feedstock engineering. In *Lignocellulose biorefinery engineering* (37-86). <https://doi.org/10.1016/B978-0-08-100135-6.00003-X>
 24. Chen, Y., De Oliveira, L., Dong, X., Li, H., Ma, L. Q., & Silva, E. Mechanisms of metal sorption by biochars: Biochar characteristics and modifications. *Chemosphere* 178, 466-478. [10.1016/j.chemosphere.2017.03.072](https://doi.org/10.1016/j.chemosphere.2017.03.072)
 25. Christoforou, E., & Forkaides, P. A. (2016). Life cycle sustainability assessment of biofuels. In J. Clark, C. S. K. Lin, R. Luque, & K. Wilson (Eds.). *Handbook of biofuels production* (41-60). <https://doi.org/10.1016/B978-0-08-100455-5.00003-5>

26. Cifirián, E., Coz, A., Llano, T., Maican, E., Sixta, H., & Viguri, J. (2016, July). Physico-chemical alternatives in lignocellulosic materials in relation to the kind of component for fermenting purposes. *Materials (Basel)* 9(7), 574. <https://dx.doi.org/10.3390%2Fma9070574>
27. Clifford, C. B. (2018). *Sugarcane ethanol production*. Pennsylvania State University College of Earth and Mineral Sciences. <https://www.e-education.psu.edu/egee439/node/647>
28. Condorchem envitech. *Introduction to vacuum evaporators*. <https://condorchem.com/en/vacuum-evaporators/>
29. Crawford, C. B., & Quinn B. (2017). The interactions of microplastics and chemical pollutants. In *Microplastic pollutants* (131-157). <https://doi.org/10.1016/B978-0-12-809406-8.00006-2>
30. Crus, J., Domínguez, H., Domínguez, J. M., & Parajó, J. C. (1999, November). Solvent extraction of hemicellulosic wood hydrolysates: a procedure useful for obtaining both detoxified fermentation media and polyphenols with antioxidant activity. *Food chemistry* 67(2), 147-153. [https://doi.org/10.1016/S0308-8146\(99\)00106-5](https://doi.org/10.1016/S0308-8146(99)00106-5)
31. Cuevas, M., Hodaifa, G., López, A. J. M., Quero, S. M., & Sánchez, S. (2014, July). Furfural removal from liquid effluents by adsorption onto commercial activated carbon in a batch heterogeneous reactor. *Ecological engineering* 68, 241-250. <https://doi.org/10.1016/j.ecoleng.2014.03.017>
32. Dahlman, L. & Lindsey R. (2020, January 16). *Climate change: Global temperature*. NOAA climate news. <https://www.climate.gov/news-features/understanding-climate/climate-change-global-temperature>
33. Dahman, Y. (2017). Smart nanomaterials. In *Nanotechnology and functional materials for engineers* (47-66). <https://doi.org/10.1016/B978-0-323-51256-5.00003-4>
34. Daverey, A., Dutta, K., & Lin, J. (2014, September). Evolution retrospective for alternative fuels: First to fourth generation. *Renewable Energy*, 69, 114-122. <https://www.sciencedirect.com/science/article/abs/pii/S0960148114001359#bib2>
35. Delgenes, J.P., Moletta, R., & Navarro, J.M. (1996, August). Effects of lignocellulose degradation products on ethanol fermentation of glucose and xylose by *Saccharomyces cerevisiae*, *Zymomonas mobilis*, *Pichia stipitis*, and *Candida shehatae*. *Enzyme and microbial technology*, 19(3), 220-225. [https://doi.org/10.1016/0141-0229\(95\)00237-5](https://doi.org/10.1016/0141-0229(95)00237-5)
36. Esweg, J. (2020). *Torrefaction*. Biomass technology group. <https://www.btgworld.com/en/rtd/technologies/torrefaction>
37. Evtuguin, D. V., Fernandes, D. L. A., Pereira, S. R., Serafim, L. S., & Xavier, A. M. R. B. (2012, February 1). Second generation bioethanol from lignocellulosics: Processing of hardwood sulphite spent liquor. In M. A. P. Lima (Eds.), *Bioethanol* (123-138). Doi:10.5772/850
38. Farabee, M. J. (2007). *Cellular metabolism and fermentation*. <https://www2.estrellamountain.edu/faculty/farabee/biobk/BioBookGlyc.html#Glycolysis>
39. *Figure 1*. Degradation of lignocellulosic biomass into its constituent monomers and oligomers. Adapted from “Formation of degradation compounds from lignocellulosic biomass in the biorefinery: sugar reaction mechanisms,” by Meyer, A. S., Rasmussen, H., & Sørensen, H, (2014, February 19), *Carbohydrate Research*, 385, 47. 2013 by “Elsevier Ltd.”

40. Floudas, C., Gounaris, C. E., Keitz, M., Ranjan, R., Thust, S., Tsapatsis, M., Valentas, K. J., Wei, J., Woo, M. (2009, June). Adsorption of fermentation inhibitors from lignocellulosic biomass hydrolyzates for improved ethanol yield and value-added product recovery. *Microporous and mesoporous materials* 122(1-3), 143-148. <https://doi.org/10.1016/j.micromeso.2009.02.025>
41. Foresman, P. S. (2007, December 2). w:Sugar cane [Illustration]. Wikimedia Commons. [https://commons.wikimedia.org/wiki/File:Sugar_cane_\(PSF\).svg](https://commons.wikimedia.org/wiki/File:Sugar_cane_(PSF).svg)
42. Foster-Carneiro, T., Jimenez, F. M., Lachos-Perez, D., Rezende, C. A., Timko, M., & Tompsett, G. (2016, February). Subcritical water hydrolysis of sugarcane bagasse: An approach on solid residues characterization. *The Journal of Supercritical Fluids* 108, 69-78. <https://doi.org/10.1016/j.supflu.2015.10.019>
43. Gasparatos, A., Stromberg, P., & Takeuchi, K. (2013, April 01). Sustainability impacts of first-generation biofuels. *Animal Frontiers*, 3(2), 12-26. <https://doi.org/10.2527/af.2013-0011>
44. Goldemberg, J. (2007, February 9). Ethanol for a sustainable future. *Science*, 315(5813), 808-810. doi: 10.1126/science.1137013
45. Hahn-Hägerdal, B., & Palmqvist, E. (2000, August). Fermentation of lignocellulosic hydrolysates. I: inhibition and detoxification. *Bioresource technology* 74(1), 17-24. [https://doi.org/10.1016/S0960-8524\(99\)00160-1](https://doi.org/10.1016/S0960-8524(99)00160-1)
46. Hanlon, K. E., & Interlandi, M. A., (2019). *Second generation ethanol production using subcritical water hydrolysis on sugarcane bagasse and straw*. [Undergraduate major qualifying project, Worcester Polytechnic Institute]. Digital WPI.
47. Harriot, P., McCabe, W. L., Smith, J.C. (1993). Gas Adsorption. In E. Castellano, & B. J. Clark (Eds.), *Unit operations of chemical edition: fifth edition* (686-736). New York: McGraw-Hill.
48. Heinonen, J., Sainio, T., & Turku, I. (2011, May). Adsorptive removal of fermentation inhibitors from concentrated acid hydrolyzates of lignocellulosic biomass. *Bioresource technology* 102(10), 6048-6057. <https://doi.org/10.1016/j.biortech.2011.02.107>
49. Helm, R. F., Jervis, J., McMillan, J. D., Ranatunga, T. D., & Wooley, R. J. (2000, August). The effect of overliming on the toxicity of dilute acid pretreated lignocellulosics: the role of inorganics, uronic acids and ether-soluble organics. *Enzyme and microbial technology* 27(3-5), 240-247. [https://doi.org/10.1016/S0141-0229\(00\)00216-7](https://doi.org/10.1016/S0141-0229(00)00216-7)
50. Hendriks, A. T. W. M., & Zeeman, G. (2009, January). Pretreatments to enhance the digestibility of lignocellulosic biomass. *Bioresource Technology* 100(1), 10-18. <https://doi.org/10.1016/j.biortech.2008.05.027>
51. Ingle, A. P., & Prasad, S. (2019). Impacts of sustainable biofuels production from biomass. In A. P. Ingle, & M. Rai (Eds.), *Sustainable bioenergy advances and impacts*, 327-346. <https://doi.org/10.1016/B978-0-12-817654-2.00012-5>
52. Iwaki, A., Izawa, S., Kawai, T., & Yamamoto, Y. (2013, March). Biomass conversion inhibitors furfural and 5-hydroxymethylfurfural induce formation of messenger RNP granules attenuate translation activity in *saccharomyces cerevisiae*. *Applied and environmental microbiology* 79(5), 1661-1667. <https://dx.doi.org/10.1128%2FAEM.02797-12>
53. Jameel, H., Kenealy, W. R., Lee, J. M., & Venditti, R. A. (2011, January) Detoxification of wood hydrolysates with activated carbon for bioconversion to ethanol by the thermophilic anaerobic bacterium

- Thermoanaerobacterium saccharolyticum*. *Biomass and bioenergy* 35(1), 626-636.
<https://doi.org/10.1016/j.biombioe.2010.10.021>
54. Jun, K., Kim, K., Lee, K., Roh, H., & Ryu, J. (2004, March). Catalytic investigation for Fischer-Tropsch synthesis from bio-mass derived syngas. *Applied Catalysis A: General*, 259(2), 221-226.
<https://doi.org/10.1016/j.apcata.2003.09.034>
 55. Lavoie, J., & Lee, R. A. (2013, April). From first- to third- generation biofuels: Challenges of producing a commodity from a biomass of increasing complexity. *Animal Frontiers*, 3(2), 6-11.
<https://doi.org/10.2527/af.2013-0010>
 56. Lehman, C., & Selin, N. E. (2020, March 21). *Biofuel*. Encyclopedia Britannica.
<https://www.britannica.com/technology/biofuel>
 57. Lehmann, J., & Joseph, S. (2008, December). Biochar for environmental management: An introduction. In *Biochar for environmental management* (1-14). Retrieved from
https://www.researchgate.net/publication/284398088_Biochar_for_environmental_management_An_introduction
 58. Li, Z., Ong, Y. L., Wu, J. C., & Zhang, D. (2013, March 15). Biological detoxification of furfural and 5-hydroxy methyl furfural in hydrolysate of oil palm empty fruit bunch by enterobacter sp. FDS8. *Biomedical engineering journal*, 72, 77-82. <https://doi.org/10.1016/j.bej.2013.01.003>
 59. Mabee, W., Saddler, J. N., Sims R. E. H., & Taylor, M. (2010, March). An overview of second generation biofuel technologies. *Bioresource Technology*, 101(6), 1570-1580.
<https://doi.org/10.1016/j.biortech.2009.11.046>
 60. Malmali, M. (2016, February). Membranes for the removal of fermentation inhibitors from biofuel production. In A. Basile, A. Cassano, & A. Figoli, *Membrane technologies for biorefining* (219-240). Doi: [10.1016/B978-0-08-100451-7.00009-8](https://doi.org/10.1016/B978-0-08-100451-7.00009-8)
 61. Manyà, J. J. (2012, July 9). Pyrolysis for biochar purposes: a review to establish current knowledge gaps and research needs. *Environmental science and technology*, 46(15), 7939-7954. <https://doi.org/10.1021/es301029g>
 62. Maues, J. (2015, August 19). Brazil, improving energy efficiency in Brazilian sugarcane industry for climate change mitigation and sustainable development. In *United Nations Development Account project, promoting energy efficiency investments for climate change mitigation and sustainable development*.
<https://www.unecce.org/fileadmin/DAM/energy/se/pdfs/gee21/projects/others/Brazil.pdf>
 63. Meyer, A. S., Rasmussen, H., & Sørensen, H. (2014, February 19). Formation of degradation compounds from lignocellulosic biomass in the biorefinery: sugar reaction mechanisms. *Carbohydrate research* 385, 45-57.
<https://doi.org/10.1016/j.carres.2013.08.029>
 64. Mussatto, S. I., & Roberto, I. C. (2004, May). Alternatives for detoxification of diluted-acid lignocellulosic hydrolyzates for use in fermentative processes: a review. *Bioresource technology* 93(1), 1-10.
<https://doi.org/10.1016/j.biortech.2003.10.005>
 65. Nasa. (2020, March 25). *The causes of climate change*. <https://climate.nasa.gov/causes/>
 66. Office of Energy Efficiency & Renewable Energy. *Biofuels Basics*.
<https://www.energy.gov/eere/bioenergy/biofuels-basics>

67. Popa, V., & Spiridon, L. (2018, December). Hemicelluloses: Major sources, properties and applications. In M. N. Belgacem, & A. Gandini (Eds.), *Monomers, polymers and composites from renewable resources* ((289-304). <https://doi.org/10.1016/B978-0-08-045316-3.00013-2>
68. Qian, E. W. (2014). Pretreatment and saccharification of lignocellulosic biomass. In T. Hirasaw, & S. Tojo (Eds.), *Research approaches to sustainable biomass systems*, 181-204. <https://doi.org/10.1016/B978-0-12-404609-2.00007-6>
69. Rapid Transition Alliance. (2018, December 2). *The rise of Brazil's sugarcane cars*. <https://www.rapidtransition.org/stories/the-rise-of-brazils-sugarcane-cars/>
70. Shalumova, T. (2010, December 19). 2D structure of 2,5-bis(hydroxymethyl)furan [Illustration]. Wikimedia Commons. https://commons.wikimedia.org/wiki/File:Hydroxymethylfurfural_2.png
71. U.S. Energy Information Administration. (2019, June 21). *Biofuels explained*. <https://www.eia.gov/energyexplained/biofuels/ethanol.php>
72. Wang, X., Xing, W., & Zhou, J. (2018). Carbon-based CO₂ adsorbents. In Q. Wang (Eds.), *Post-combustion carbon dioxide capture materials* (1-75). <https://doi.org/10.1039/9781788013352-00001>
73. Yamane, T. (2016, April). *Sugarcane*. Encyclopedia Britannica. <https://www.britannica.com/plant/sugarcane>

Appendix

Appendix A: Data

Data 1: Total and Volatile Solid Percentage

Total and Volatile Solid Percentage									
Adsorbent	Sample #	Crucible Weight (g)	Initial Sample Weight (g)	Mass of Dry Substrate (g)	Total Solids (%)	Average TS (%)	Mass of Incinerated Substrate	Volatile Solid (%)	Average Volatile Solid (%)
Biochar1	1	26.6121	1.0137	27.3853	76.275032	76.51443	26.6629	71.263687	70.819668
	2	23.2804	0.9604	24.0152	76.509788		23.3385	70.460225	
	3	30.7937	1.0094	31.5685	76.75847		30.8545	70.73509	
Biochar 2	1	33.4379	1.0262	33.8344	38.637692	45.144121	33.6137	21.506529	18.837307
	2	34.1338	0.9647	34.4893	36.850834		34.2827	21.415984	
	3	23.7488	0.9971	24.3465	59.943837		24.211	13.589409	
Biochar 3	1	27.7591	0.5452	28.2473	89.545121	90.273572	27.7952	82.923698	82.952329
	2	25.9272	0.4841	26.3637	90.167321		25.9644	82.482958	
	3	34.5164	0.4701	34.9447	91.108275		34.5524	83.45033	
Biochar 4	1	31.9478	0.9721	32.8687	94.733052	94.689309	31.9986	89.507252	89.312259
	2	38.0426	1.0629	39.0471	94.505598		38.0978	89.312259	
	3	37.4988	1.0192	38.4653	94.829278		37.5569	89.128728	
Biochar 5	1	30.2573	0.8234	31.0176	92.336653	88.095007	30.2777	89.859121	84.644748
	2	29.4061	0.6079	29.8916	79.865109		29.4412	74.091133	
	3	37.0239	0.5621	37.5415	92.083259		37.0357	89.983989	
Biochar 6	1	29.7621	0.9567	30.1466	40.190237	51.286155	29.7911	37.158984	46.330797
	2	41.1061	0.9395	41.651	57.998936		41.141	54.284194	
	3	45.4007	1.016	45.9663	55.669291		45.4832	47.549213	

Data 2: pH of the Adsorbent

pH of the Adsorbents, Tested with Ultrapure Water											
Adsorbent	Control pH	pH at 5 mL	pH at 10 mL	pH at 15 mL	pH at 20 mL	pH at 25 mL	pH at 30 mL	pH at 40 mL	pH at 50 mL	pH at 60 mL	pH at 70 mL
Activated Carbon	7.77	7.03	7.9	6.73	7.73	7.6	7.6	7.49	7.43	7.38	7.34
Biochar 1	7.77	6.01	6.54	6.9	7.2	7.3	7.22	7.37	7.53	7.53	7.51
Biochar 2	7.66	7.34	8.35	8.03	7.7	7.67	9.11	9.32	9.45	9.46	9.63
Biochar 3	7.2	9.76	10.58	9.44	10.59	10.57	10.57	10.53	10.48	10.45	10.37
Biochar 4	8.37	9.37	9.81	10.04	10.1	10.11	10.12	10.2	10.15	10.16	10.21
Biochar 5	6.97	8.32	7.59	7.33	7.38	7.56	7.61	7.69	7.73	7.56	7.74
Biochar 6	7.39	7.39	9.1	9.79	9.8	9.81	9.42	9.98	9.91	10.02	9.84

Data 3: Positive Displacement Pump Raw Data for Weight of Adsorbent, Weight of Residue, and Time

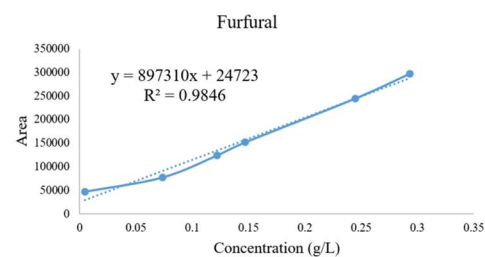
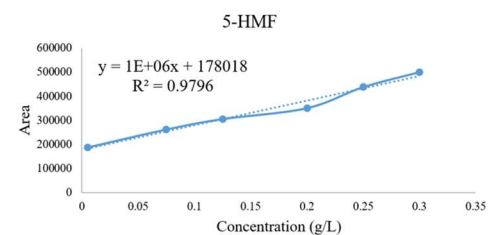
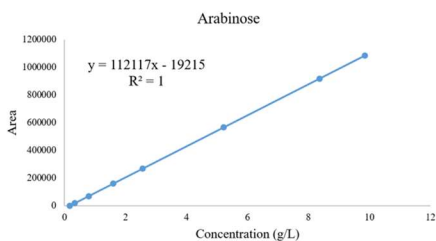
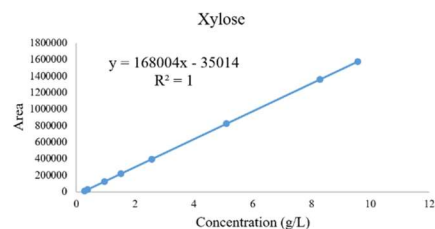
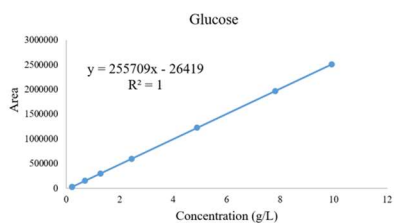
Weight of Adsorbent and Residue, and Study of the Amount of Time to Collect a Volume of Effluent, Positive Displacement Pump													
Adsorbent	Trial #	wt. of Adsorbent (g)	Residue (g)	Time for 5 mL (min)	Time for 10 mL (min)	Time for 15 mL (min)	Time for 20 mL (min)	Time for 25 mL (min)	Time for 30 mL (min)	Time for 35 mL (min)	Time for 40 mL (min)	Time for 45 mL (min)	Time for 50 mL (min)
Activated Carbon	1		0.9195	18.21	29.44	38.49	42.55	47.57	53.14	59.37	65.45	70.56	77.07
	2	1.0107	0.9761	22.55	30.93	37	42.25	46.64	53.03	58.59	65.76	71.03	75.25
	3	1.0109	0.9748	14.57	21.71	26.11	31.29	36.35	42.67	48.87	53.99	62.09	66.71
	4	1.0372	1.0744	9.57	18.91	31.25	38.57	45.91	50.5	55.08	59.14	66.19	72.55
Biochar 1	1	1.0137	0.7976	5.45	17.78	29.34	39.93	48.5	56.9	62.98	69.16	76.54	84.81
	2	1.0014	0.9231	14.34	21.39	33.75	47.03	67.31	86.73	92.05	97.16	102.22	108.72
	3	1.0413	0.817	14.17	47.57	57.67	75.25	92.82	100.09	105.46	111.48	118.85	126.85
Biochar 2	1	1.0781	0.3935	8.06	14.54	20.91	30.27	41.33	47.9	54.13	64.38	73.94	83.14
	2	1.02	0.3643	15.51	27.78	38.91	44.2	57.39	67.7	76.03	84.49	93.92	104.14

Data 4: CO₂ Peltier Pump Raw Data for Weight of Adsorbent, Weight of Residue, and Time

Weight of Adsorbent and Residue, and Study of the Amount of Time to Collect a Volume of Effluent, CO ₂ Peltier Pump													
Adsorbent	Trial #	wt. of Adsorbent (g)	Residue (g)	Time for 5 mL (min)	Time for 10 mL (min)	Time for 15 mL (min)	Time for 20 mL (min)	Time for 25 mL (min)	Time for 30 mL (min)	Time for 40 mL (min)	Time for 50 mL (min)	Time for 60 mL (min)	Time for 70 mL (min)
Activated Carbon	1	1.0016	0.9725	5.4	8.1	11.3	15	19.04	23.14	30.38	38.03	45.455	53.4
	2	1.0042	1.0356	4.37	7.23	11.2	16.3	20.08	22.51	29.2	36.4	43.1	50
Biochar 1	1	1.0038	0.901	16.51	20.13	23.46	27.06	30.36	33.4	40.57	47	53.15	59.28
	2	1.0052	0.8816	13.4	22.26	24.5	27.56	30.14	32.44	38.08	44.2	50.46	56.16
Biochar 2	1	1.0018	0.4018	10.45	12.55	15.28	17.55	20.16	23.23	28.45	34.45	40.56	46.33
	2	1.0018	0.3793	12.26	15.15	17.45	20.22	23.59	27.06	33.2	39.5	46.12	52.21
Biochar 3	1	1.0095	0.9536	15.57	19.18	21.57	24.27	27.08	29.58	35.56	41.37	47.42	53.45
	2	1.0048	0.9183	19.02	21.46	24.19	26.56	29.28	32.18	37.39	43.09	49.12	55.12
Biochar 4	1	1.0024	1.0022	10.57	13.59	17.14	20.26	23.41	26.56	33.29	39.38	46.1	52.03
	2	1.004	1.0124	11.24	14.06	17.26	20.45	23.16	26	31.47	37.25	43.22	48.48
Biochar 5	1	1.0045	0.9893	12.51	15.55	18.41	21.41	24.2	27.47	33.25	39.12	45	50.25
	2	1.0022	0.9408	10.14	13.52	19.09	22.04	25.07	28.02	34.38	41.05	46.53	53.51
Biochar 6	1	1.0093	0.8755	11.21	15.22	20.4	24.28	28.45	32.1	39.37	47.13	53.22	59.52
	2	1.0079	0.8523	14.14	18.59	24.19	27.27	30.08	32.42	38.34	44.03	50.11	57.07
Activated Biochar 4	1	1.0018	0.8056	11.21	15.22	20.4	24.28	28.45	32.1	39.37	47.13	53.22	59.52
	2	1.0008	0.7014	14.14	18.59	24.19	27.27	30.08	32.42	38.34	44.03	50.11	57.07

Data 5: HPLC Standard Curve for Carbohydrates and Inhibitors

Compound	Concentration (g/L)	Area
Glucose	0.1	27748
	0.2	28249
	0.5	151291
	1	302125
	2	599671
	5	1224467
	8	1972562
	10	2511523
Xylose	0.1	11662
	0.2	29901
	0.5	125065
	1	219515
	2	395645
	5	822525
	8	1356794
	10	1573863
Arabinose	0.1	0
	0.2	18273
	0.5	69388
	1	159891
	2	267238
	5	565287
	8	918546
	10	1084725
5-HMF	0.005	187661.5
	0.075	261980.5
	0.125	305178
	0.15	279871
	0.2	350502
	0.25	437862.5
Furfural	0.3	499687.5
	0.0048	47396
	0.07342	77426
	0.12209	124261
	0.14684	151682.5
	0.20016	161078
	0.2446	244539
	0.29328	297178



Data 6: HPLC Raw Data for Trials with the Positive Displacement Pump

HPLC Area, Positive Displacement Pump													
Adsorbent	Trial	Compound	Control	5 mL	10 mL	15 mL	20 mL	25 mL	30 mL	35 mL	40 mL	45 mL	50 mL
Activated Carbon	Trial 1	glucose	183442	33333	85135	162524	152942	171598	174356	206500	220065	202210	201036
		xylose	168533	43666	118682	186750	201420	162605	204023	234303	223627	236759	231527
		arabinose	144902	44298	89515	137462	144072	133380	147239	206500	220065	202210	201036
		5-HMF	3612265	8279.5	21852.5	0	2157	6099.5	40152.5	80949.5	122034.5	299100.5	496231
		furfural	3889884	0	0	0	0	17366.5	119811	276445.5	401789.5	1027136	1808858
	Trial 2	glucose	198857	0	0	52820	84949	147394	191808	209738	226334	226312	243733
		xylose	255131	0	0	92244	113552	197857	230918	242011	239372	236866	259636
		arabinose	174483	0	0	89808	130216	180822	190172	185231	184338	173783	196068
		5-HMF	4240666	7148.5	2092.5	2917	8579	52014	110688	252720.5	292426	423767	617806
		furfural	3894134	275855.5	3899	1035.5	13968	134932	340180	743439	661431	961437	1301474
	Trial 3	glucose	195458	0	111392	169954	183056	220322	163036	185364	171915	191165	171180
		xylose	211216	0	117855	201117	204536	211903	163666	207637	174211	215749	169874
		arabinose	163048	0	109870	186149	178261	183934	135836	178774	151518	162236	139742
		5-HMF	3849740	11963	171710	362624	391286	437441.5	1003084	888669	995663	1406456	1484123
		furfural	3927806	27820.5	185927.5	340312.5	687378.5	868421	1219852	1482323	1614349	1598131	2011189
	Trial 4	glucose	211143	0	80527	164763	217296	205478	218833	202638	222384	235064	207021
		xylose	191880	0	107828	188332	217852	207517	230501	200098	208727	219531	201374
		arabinose	179464	0	133224	175807	192273	191742	209513	204984	208727	210378	193303
		5-HMF	5125381	4687	2155.5	1183.5	0	0	2353.5	3626	103289	544294.5	667221
		furfural	4309639	131757	4293	1839	0	0	0	0	177288	699656.5	1105091
Biochar 1	Trial 1	glucose	185337	168253	169320		168241	173189	177553	167742	166048	173175	171578
		xylose	156033	154075	154076		145353	150956	153061	156032	152306	143735	144524
		arabinose	149313	153283	147266		139355	130025	135414	137502	140772	137847	144652
		5-HMF	4428780	4034343	3790351		4006864	4027782	4539491	4013821	4384741	3853450	3790948
		furfural	3895968	3639481	3693215		3790490	3624197	3910595	3904516	3867784	3887894	3908902
	Trial 2	glucose	200101	111025	238950	194676	152160	170251	190917	150860	184275	161724	158310
		xylose	172719	84065	186001	151946	128399	154970	161230	128404	163834	146453	149830
		arabinose	172322	91698	187694	151829	120010	156264	169743	125367	170944	144283	143730
		5-HMF	4769392	3427593	3963647	4326744	4411958	4157496	3718624	4221611	4284190	4113165	4020385
		furfural	4155518	3030388	3931733	3930456	3934848	3972855	3863355	3790698	3813230	3901765	4003991
	Trial 3	5-HMF	5173953	4503346	3884868	4295119	4335927	4437959	4536055	4727553	4586862	4811924	4938802
		furfural	4283907	3811545	3622590	3838839	3837172	3835986	3880196	4057413	3930710	4095061	4251821
	Trial 1	glucose	202719	172761	205288	218454	209179	207078	210101	228549	206122	210899	212197
		xylose	184244	148100	182486	184781	182656	182674	179972	186465	182705	184323	180794
		arabinose	184250	144865	188645	185114	183593	177320	179650	192740	178593	180313	180808
Biochar 2	Trial 1	glucose	199214	143746	177613	179329	217618	208395	212074	208820	211630	221200	205884
		xylose	173170	135543	170599	145227	188703	191959	182585	183126	194761	196637	169539
	Trial 2	arabinose	180548	138423	172750	146274	188742	194846	188245	192571	197861	204010	172987

Data 7: Concentration Profile for Trials with the Positive Displacement Pump

Concentration Profile, Positive Displacement Pump													
Adsorbent	Trial	Compound	Control	5 mL	10 mL	15 mL	20 mL	25 mL	30 mL	35 mL	40 mL	45 mL	50 mL
Activated Carbon	Trial 1	glucose	0.614069	0.027038548	0.22962	0.532265	0.494793	0.567751	0.578537	0.704242	0.757291	0.687465	0.682874
		xylose	0.794737	0.051498774	0.498012	0.903169	0.990488	0.759452	1.005982	1.186216	1.12267	1.200835	1.169692
		arabinose	1.121034	0.223721648	0.627024	1.054675	1.113631	1.018267	1.141879	1.670442	1.791432	1.632179	1.621708
		5-HMF	3.434247	-0.1697385	-0.15617	-0.17802	-0.17586	-0.17192	-0.13787	-0.09707	-0.05598	0.121083	0.318213
		furfural	4.307497	-0.02755235	-0.02755	-0.02755	-0.02755	-0.0082	0.10597	0.28053	0.420219	1.117131	1.988315
	Trial 2	glucose	0.674352	-0.10331666	-0.10332	0.103246	0.228893	0.473096	0.646786	0.716905	0.781807	0.781721	0.849849
		xylose	1.310189	-0.2084117	-0.20841	0.340647	0.467477	0.96928	1.166067	1.232096	1.216388	1.201471	1.337004
		arabinose	1.384875	-0.17138347	-0.17138	0.629637	0.990046	1.441414	1.524809	1.480739	1.472774	1.378631	1.577397
		5-HMF	4.062648	-0.1708695	-0.17593	-0.1751	-0.16944	-0.126	-0.06733	0.074703	0.114408	0.245749	0.439788
		furfural	4.312234	0.279872619	-0.02321	-0.0264	-0.01199	0.122822	0.351559	0.800967	0.709574	1.043913	1.422864
	Trial 3	glucose	0.66106	-0.10331666	0.332304	0.561322	0.61256	0.758296	0.534267	0.621585	0.568991	0.644271	0.566116
		xylose	1.048796	-0.2084117	0.493089	0.988685	1.009035	1.052886	0.765767	1.027493	0.828534	1.075778	0.802719
		arabinose	1.282883	-0.17138347	0.808575	1.488927	1.418572	1.469171	1.040172	1.423147	1.180044	1.275641	1.075011
		5-HMF	3.671722	-0.166055	-0.00631	0.184606	0.213268	0.259424	0.825066	0.710651	0.817645	1.228438	1.306105
		furfural	4.349759	0.003451984	0.179653	0.351706	0.738491	0.940253	1.331902	1.624411	1.771546	1.753472	2.213801
	Trial 4	glucose	0.722399	-0.10331666	0.2116	0.541021	0.746462	0.700245	0.752473	0.689139	0.766359	0.815947	0.706279
		xylose	0.933704	-0.2084117	0.433406	0.912585	1.088296	1.026779	1.163585	0.982619	1.033981	1.098289	0.990215
		arabinose	1.429302	-0.17138347	1.016875	1.396684	1.543548	1.538812	1.697316	1.656921	1.690306	1.705031	1.552735
		5-HMF	4.947363	-0.173331	-0.17586	-0.17683	-0.17802	-0.17802	-0.17566	-0.17439	-0.07473	0.366277	0.489203
		furfural	4.77529	0.119283191	-0.02277	-0.0255	-0.02755	-0.02755	-0.02755	-0.02755	0.170025	0.752174	1.204008
Biochar 1	Trial 1	glucose	0.62148	0.554669566	0.558842		0.554623	0.573973	0.591039	0.552671	0.546046	0.573918	0.567673
		xylose	0.720334	0.708679555	0.708686		0.656764	0.690115	0.702644	0.720328	0.69815	0.647133	0.65183
		arabinose	1.160377	1.195786544	1.142119		1.071559	0.988343	1.036408	1.055032	1.084198	1.058109	1.118804
		5-HMF	4164.556	3778.117958	3539.074		3751.196	3771.69	4273.021	3758.012	4121.41	3600.894	3539.659
		furfural	4143.44	3857.599938	3917.483		4025.891	3840.567	4159.741	4152.966	4112.03	4134.442	4157.854
	Trial 2	glucose	0.679217	0.330868292	0.831144	0.658002	0.491735	0.562483	0.643302	0.486651	0.617327	0.529137	0.515786
		xylose	0.819653	0.291963287	0.898711	0.696007	0.55585	0.714007	0.751268	0.55588	0.766767	0.663312	0.683412
		arabinose	1.3656	0.646494287	1.502707	1.182818	0.899016	1.222375	1.342597	0.946797	1.353309	1.115513	1.110581
		5-HMF	4498.26	3183.67297	3708.856	4064.589	4148.075	3898.773	3468.802	3961.588	4022.898	3855.341	3764.443
		furfural	4432.693	3178.801083	4183.298	4181.875	4186.769	4229.126	4107.095	4026.123	4051.233	4149.9	4263.825
	Trial 3	5-HMF	5243.432	4586.425002	3980.49	4382.421	4422.401	4522.364	4618.471	4806.085	4668.247	4888.745	5013.05
		furfural	4972.557	4446.136787	4235.557	4476.554	4474.697	4473.375	4522.644	4720.142	4578.939	4762.099	4936.799
	Trial 1	glucose	0.689456	0.57229898	0.699502	0.75099	0.714719	0.706502	0.718324	0.790469	0.702764	0.721445	0.726521
		xylose	0.888253	0.673114926	0.877789	0.891449	0.878801	0.878908	0.862825	0.901473	0.879092	0.888723	0.867717
		arabinose	1.471989	1.120704264	1.511189	1.479695	1.466129	1.410179	1.430961	1.547714	1.421533	1.436874	1.441289
Biochar 2	Trial 2	glucose	0.675749	0.458830155	0.591274	0.597984	0.747721	0.711653	0.72604	0.713315	0.724304	0.761729	0.701833
		xylose	0.822338	0.598372658	0.807034	0.656014	0.914794	0.934174	0.878378	0.881598	0.950852	0.962019	0.800725
		arabinose	1.43897	1.06324643	1.369418	1.133271	1.512054	1.566497	1.507622	1.546206	1.593389	1.648234	1.371532

Data 8: Positive Displacement Pump Cx/Co Values

Concentration in the Effluent (Cx) Divided by the Concentration in the Feed (Co), Positive Displacement Pump													
Adsorbent	Trial	Compound	Control	5 mL	10 mL	15 mL	20 mL	25 mL	30 mL	35 mL	40 mL	45 mL	50 mL
Activated Carbon	Trial 1	glucose	0	0.044031766	0.3739325	0.8667838	0.8057609	0.9245716	0.9421359	1.1468447	1.2332333	1.1195239	1.1120473
		xylose	0	0.064799766	0.6266374	1.1364375	1.2463095	0.9556018	1.2658049	1.4925891	1.4126304	1.5109835	1.471798
		arabinose	0	0.199567179	0.5593259	0.9408053	0.9933963	0.9083278	1.0185938	1.4900905	1.5980173	1.4559581	1.4466174
		5-HMF	0	0	0	0	0	0	0	0	0	0.0352574	0.0926587
		furfural	0	0	0	0	0	0	0	0.026517	0.0602855	0.2287576	0.4393586
	Trial 2	glucose	0	0	0	0.1531043	0.3394263	0.7015565	0.9591215	1.0631009	1.1593442	1.1592166	1.2602443
		xylose	0	0	0	0.2599981	0.3568012	0.739802	0.8899994	0.9403953	0.9284063	0.9170214	1.0204664
		arabinose	0	0	0	0.4546526	0.7148994	1.0408262	1.1010446	1.0692222	1.0634709	0.9954917	1.1390177
		5-HMF	0	0	0	0	0	0	0	0.0183876	0.0281609	0.0604899	0.1082516
		furfural	0	0	0	0	0	0	0.0436375	0.1521538	0.1300856	0.2108166	0.3023198
	Trial 3	glucose	0	0	0.5026828	0.8491236	0.9266323	1.1470903	0.8081981	0.940286	0.8607244	0.9746035	0.8563763
		xylose	0	0	0.4701479	0.9426851	0.962089	1.0038989	0.7301393	0.9796881	0.7899854	1.0257262	0.7653716
		arabinose	0	0	0.6302796	1.1606099	1.1057685	1.1452101	0.8108084	1.1093351	0.9198376	0.9943546	0.8379649
		5-HMF	0	0	0	0.0502778	0.0580839	0.0706545	0.2247082	0.1935471	0.2226871	0.3345673	0.3557201
		furfural	0	0	0.0021093	0.043281	0.1358372	0.1841179	0.2778381	0.3478344	0.3830432	0.3787183	0.4888733
	Trial 4	glucose	0	0	0.2929127	0.7489227	1.0333092	0.9693326	1.0416297	0.9539583	1.0608529	1.1294959	0.9776856
		xylose	0	0	0.4641796	0.977382	1.1655681	1.0996838	1.2462038	1.0523887	1.1073974	1.1762715	1.060523
		arabinose	0	0	0.7114491	0.9771793	1.0799319	1.0766183	1.1875144	1.1592522	1.1826096	1.1929123	1.0863594
		5-HMF	0	0	0	0	0	0	0	0	0	0.0740347	0.0988816
		furfural	0	0	0	0	0	0	0	0	0	0.1262552	0.2243848
Biochar 1	Trial 1	glucose	0	0.892498018	0.8992122		0.8924225	0.9235581	0.9510188	0.8892825	0.8786229	0.92347	0.9134208
		xylose	0	0.983820722	0.983829		0.9117494	0.9580479	0.9754419	0.9999917	0.9692032	0.8983796	0.9048992
		arabinose	0	1.030515458	0.9842657		0.9234577	0.8517425	0.8931652	0.9092146	0.9343495	0.9118664	0.9641732
		5-HMF	0	0.907207931	0.8498083		0.9007434	0.9056644	1.026045	0.9023801	0.9896397	0.8646525	0.8499488
		furfural	0	0.931013865	0.9454665		0.9716301	0.926903	1.0039342	1.0022991	0.9924195	0.9978284	1.0034788
	Trial 2	glucose	0	0.487131654	1.2236789	0.9687648	0.7239725	0.8281342	0.9471218	0.7164876	0.9088794	0.7790387	0.7593821
		xylose	0	0.356203478	1.0964526	0.8491485	0.6781526	0.8711085	0.916568	0.6781889	0.935478	0.8092589	0.8337824
		arabinose	0	0.473414018	1.1004004	0.8661524	0.6583304	0.8951191	0.9831556	0.6933191	0.9909998	0.8168666	0.8132548
		5-HMF	0	0.707756545	0.824509	0.9035914	0.922151	0.8667292	0.771143	0.8806934	0.8943231	0.8570739	0.8368665
		furfural	0	0.717126336	0.9437373	0.9434162	0.9445204	0.9540759	0.9265461	0.9082791	0.9139439	0.9362029	0.961904
	Trial 3	5-HMF	0	0.874699059	0.7591383	0.8357925	0.8434173	0.8624817	0.8808106	0.9165915	0.8903038	0.9323559	0.9560627
		furfural	0	0.894134931	0.8517866	0.900252	0.8998784	0.8996126	0.9095209	0.9492385	0.920842	0.9576761	0.9928089
	Trial 1	glucose	0	0.830073738	1.0145718	1.0892513	1.0366421	1.0247249	1.0418718	1.1465116	1.0193023	1.0463982	1.0537606
		xylose	0	0.75779669	0.9882195	1.0035985	0.9893587	0.9894793	0.971373	1.0148831	0.9896871	1.0005294	0.9768813
		arabinose	0	0.761353652	1.0266307	1.0052353	0.996019	0.9580089	0.9721271	1.0514436	0.9657224	0.9761445	0.9791438
		glucose	0	0.678995341	0.8749906	0.8849214	1.1065077	1.0531323	1.0744234	1.0555919	1.0718539	1.1272375	1.0386007
Biochar 2	Trial 2	xylose	0	0.727648455	0.9813906	0.7977431	1.1124309	1.1359984	1.0681476	1.0720635	1.1562799	1.1698587	0.9737181
		arabinose	0	0.738894089	0.9516652	0.7875574	1.0507894	1.0886242	1.0477088	1.0745229	1.1073122	1.1454259	0.9531342

Data 9: HPLC Raw Data for Trials with the CO₂ Peltier Pump

HPLC Area, CO ₂ Peltier Pump													
Adsorbent	Trial	Compound	Control	5 mL	10 mL	15 mL	20 mL	25 mL	30 mL	40 mL	50 mL	60 mL	70 mL
Activated Carbon	Trial 1	glucose	189417	0	44802	70714	143267	170044	198211	188988	188522	189825	186314
		xylose	192377	0	55710	80743	160307	181044	195242	180247	188201	177751	184409
		arabinose	165767	0	73387	83331	158823	158330	159101	141519	140231	149994	150737
	Trial 2	glucose	189417	0	0	21120	69295	123397	165627	189475	194333	206578	203562
		xylose	192377	0	0	22897	72473	143128	175668	155925	188019	191822	196340
		arabinose	165767	0	0	26504	79846	137736	155581	159853	153475	158918	152530
Biochar 1	Trial 1	glucose	192377	209840	184697	186136	177402	178015	193085	192943	191929	173744	194295
		xylose	165767	198848	199189	203328	191190	180909	204112	187423	189204	190432	211936
		arabinose	189417	162514	155258	162508	146589	159709	179832	155258	160836	157155	188263
	Trial 2	glucose	199240	170920	180923	159490	182888	174265	167950	173010	170729	172106	238858
		xylose	211450	173557	197626	164397	195401	179964	185780	192103	183843	191383	215080
		arabinose	179062	138216	157957	137490	158994	159327	153396	155213	150779	151431	188293
Biochar 2	Trial 1	glucose	147090	75170	112515	141843	171166	175444	183782	189322	182786	179113	178070
		xylose	157545	93884	126285	168054	180611	186656	193198	203824	200385	195310	194274
		arabinose	129276	70269	99326	130774	143866	151934	153185	159333	158993	155881	158262
		5-HMF	5241045		3861216	4058298	4117397	4308048	4391248	4852553			
		furfural	4382753		3325704	3739234	4159940	4252629	4288133	4313534			
		glucose	185205	72981	130300	149339	166370	171894	208656	184784	153758	156952	205929
	Trial 2	xylose	189813	72144	134346	155137	165088	178955	187330	181083	195053	228091	251892
		arabinose	158482	56411	124480	131707	152441	144363	160696	158612	160870	140911	164919
		5-HMF	4454223	3101789.5	3469251	4290570	4430600		4566051	4964324	3753503	4482066	4465542
		furfural	4344144	2713655.5	3571489	3852698	4085475		4301421	4356136	4129338	4443023	4407212
		glucose	182438	191985	172292								
		xylose	252478	236675	244881								
Biochar 3	Trial 1	arabinose	119933	125415	133627								
	Trial 1	5-HMF	6087543	153272.5	1709819	3358000	3852098	2734040	4467563	3355226	4370527	5046557	4882147
furfural		6148447	615769.5	3344158	4184721	4625929	5097923	2987252	5368730	5276538	5405795	5531943	
Biochar 4	Trial 2	5-HMF	3682667	108608	330802.5	1141858	2838698	3746767	3865302	3986512	3864951	3096953	5305159
		furfural	6143571	515624.5	1966334	3494896	4315817	4935739	5079001	5513254	5368724	5498315	5578089
Biochar 5	Trial 1	5-HMF	5075390	2817750.5		2869627		3534821	3710846	3480221	3420556	3933666	5274198
		furfural	5549833	5244544		4194268		5522828	2881746	5443761	5559198	5384213	5058374
	Trial 2	5-HMF	3834988	1263689	2517281	3008607	3070542	3950338	3823803	3236964	3485036	3224027	3440157
		furfural	5198295	2170327	3920887	4166658	4666167	4878845	5203793	5158638	5123975	5100006	5382223
	Trial 1	5-HMF	4081691	526243.5	1182568	1543380	2768522	3387153	2034670	2364513	2867497	3480600	3501532
		furfural	5435404	1428243.5	3219927	3706151	3989721	4116655	4508533	4504790	4595235	4922071	4987434
Biochar 6	Trial 2	5-HMF	4278277	204410.5	440283.5	731974.5	2076910	2076910	2318795	2812222	3108382	3403492	3544931
		furfural	5113241	673713.5	1529918	2683027	3754155	3754155	4105367	4373675	4723231	4851387	4967061
Activated Biochar 4	Trial 1	5-HMF	5745114	4873557	4712757	5425383	5655061	5390474	5400598	4804632	5338055	5355572	4848614
		furfural	4740398	4250070.5	4640008	5151577	4528975	4504852	4342087	4386111	3131655	4383059	4476300
	Trial 2	5-HMF	5556127	4570261.5	4626006	4854948	4834465	4916976	4935751	4943455	4842559	5179546	5072031
		furfural	4199242	4222612	4688683	4028887	3993089	4411475	4901538	2509224	3887399	4430561	4382609
	Trial 1	5-HMF	5745114	4873557	4712757	5425383	5655061	5390474	5400598	4804632	5338055	5355572	4848614
		furfural	4740398	4250070.5	4640008	5151577	4528975	4504852	4342087	4386111	3131655	4383059	4476300

Data 10: Concentration Profile for Trials with the CO₂ Peltier Pump

Concentration Profile, CO ₂ Peltier Pump													
Adsorbent	Trial	Compound	Control	5 mL	10 mL	15 mL	20 mL	25 mL	30 mL	40 mL	50 mL	60 mL	70 mL
Activated Carbon	Trial 1	glucose	0.637436	-0.103316661	0.07189	0.173224	0.456957	0.561674	0.671826	0.635758	0.633935	0.639031	0.625301
		xylose	0.936662	-0.208411704	0.123188	0.27219	0.745774	0.869205	0.953715	0.864462	0.911806	0.849605	0.889235
		arabinose	1.307135	-0.171383465	0.483174	0.571867	1.245199	1.240802	1.247679	1.09086	1.079372	1.166451	1.173078
	Trial 2	glucose	0.637436	-0.103316661	-0.10332	-0.02072	0.167675	0.379251	0.5444	0.637662	0.656661	0.704547	0.692752
		xylose	0.936662	-0.208411704	-0.20841	-0.07212	0.222965	0.64352	0.837206	0.719691	0.910722	0.933359	0.960251
		arabinose	1.307135	-0.171383465	-0.17138	0.065012	0.540783	1.057119	1.216283	1.254386	1.197499	1.246047	1.18907
Biochar 1	Trial 1	glucose	0.649011	0.717303654	0.618977	0.624605	0.590449	0.592846	0.65178	0.651225	0.647259	0.576143	0.656512
		xylose	0.778273	0.975179162	0.977209	1.001845	0.929597	0.868402	1.006512	0.907175	0.917776	0.925085	1.053082
		arabinose	1.518075	1.278120178	1.213402	1.278067	1.136081	1.253102	1.432584	1.213402	1.263154	1.230322	1.507782
	Trial 2	glucose	0.67585	0.56509939	0.604218	0.5204	0.611903	0.578181	0.553485	0.573273	0.564352	0.569737	0.830784
		xylose	1.050189	0.82464108	0.967906	0.770119	0.954662	0.862777	0.897395	0.935031	0.885866	0.930746	1.071796
		arabinose	1.425716	1.061400144	1.237475	1.054925	1.246724	1.249695	1.196794	1.213001	1.173453	1.179268	1.50805
Biochar 2	Trial 1	glucose	0.471908	0.19065031	0.336695	0.451388	0.566061	0.582791	0.615399	0.637064	0.611504	0.59714	0.593061
		xylose	0.729334	0.350408324	0.543267	0.791886	0.866628	0.902609	0.941549	1.004798	0.984328	0.95412	0.947954
		arabinose	0.981662	0.455363593	0.71453	0.995023	1.111794	1.183754	1.194912	1.249748	1.246715	1.218959	1.240196
	Trial 2	5-HMF	5.063027		3.683198	3.88028	3.939379	4.13003	4.21323	4.674535			
		furfural	4.856771		3.678752	4.139607	4.60846	4.711756	4.751323	4.779631			
		xylose	0.620964	0.182089797	0.406247	0.480703	0.547306	0.568908	0.712673	0.619317	0.497984	0.510475	0.702009
Biochar 3	Trial 1	xylose	0.921401	0.221006643	0.591248	0.715001	0.774232	0.856771	0.906621	0.869438	0.95259	1.14924	1.29091
		arabinose	1.242158	0.331760572	0.938885	1.003345	1.188277	1.116227	1.261905	1.243317	1.263457	1.085438	1.299571
		5-HMF	4.276205	2.9237715	3.291233	4.112552	4.252582		4.388033	4.786306	3.575485	4.304048	4.287524
	Trial 2	furfural	4.813744	2.99665946	3.952665	4.266056	4.525473		4.766132	4.827108	4.574355	4.923939	4.88403
		glucose	0.610143	0.647478188	0.570465								
		xylose	1.294398	1.200334516	1.249179								
Biochar 4	Trial 1	arabinose	0.898329	0.947224774	1.02047								
		5-HMF	5.909525	-0.0247455	1.531801	3.179982	3.67408	2.556022	4.289545	3.177208	4.192509	4.868539	4.704129
		furfural	6.824536	0.658687076	3.699317	4.636076	5.127777	5.653787	3.301567	5.955586	5.852843	5.996892	6.137477
	Trial 2	5-HMF	3.504649	-0.06941	0.152785	0.96384	2.66068	3.568749	3.687284	3.808494	3.686933	2.918935	5.127141
		furfural	6.819102	0.547081276	2.163813	3.867306	4.782176	5.473042	5.6327	6.116649	5.955579	6.100001	6.188905
		5-HMF	4.897372	2.6397325		2.691609		3.356803	3.532828	3.302203	3.242538	3.755648	5.09618
Biochar 5	Trial 1	furfural	6.157414	5.81718804		4.646716		6.127319	3.183987	6.039203	6.167852	5.97284	5.609712
		5-HMF	3.65697	1.085671	2.339263	2.830589	2.892524	3.77232	3.645785	3.058946	3.307018	3.046009	3.262139
		furfural	5.765646	2.39115133	4.342048	4.615946	5.17262	5.409637	5.771773	5.721451	5.68282	5.656109	5.970623
	Trial 2	5-HMF	3.903673	0.3482255	1.00455	1.365362	2.590504	3.209135	1.856652	2.186495	2.689479	3.302582	3.323514
		furfural	6.02989	1.56414227	3.560869	4.102738	4.418761	4.560221	4.996946	4.992775	5.09357	5.457811	5.530654
		5-HMF	4.100259	0.0263925	0.262266	0.553957	1.898892	1.898892	2.140777	2.634204	2.930364	3.225474	3.366913
Biochar 6	Trial 1	furfural	5.670858	0.723262306	1.677452	2.962526	4.156235	4.156236	4.547641	4.846654	5.236215	5.379037	5.507949
		5-HMF	5.567096	4.695539	4.534739	5.247365	5.477043	5.212456	5.22258	4.626614	5.160037	5.177554	4.670596
		furfural	5.255346	4.708904949	5.143468	5.713582	5.019727	4.992844	4.811452	4.860514	3.462495	4.857112	4.961024
	Trial 2	5-HMF	5.378109	4.3922435	4.447988	4.67693	4.656447	4.738958	4.757733	4.765437	4.664541	5.001528	4.894013
		furfural	4.65226	4.678304042	5.197713	4.462408	4.422513	4.88878	5.434928	2.768832	4.304728	4.910051	4.856611
		5-HMF											

Data 11: CO₂ Peltier Pump Cx/Co and Normalized Cx/Co Values

Concentration in the Effluent (Cx) Divided by the Concentration in the Feed (Co), CO ₂ Peltier Pump													
Adsorbent	Trial	Compound	Control	5 mL	10 mL	15 mL	20 mL	25 mL	30 mL	40 mL	50 mL	60 mL	70 mL
Activated Carbon	Trial 1	glucose	0	0	0.112781	0.271752	0.716868	0.881146	1.053952	0.997368	0.994509	1.002503	0.980963
		glucose norm.	0	0	0.107007	0.257841	0.680171	0.83604	1	0.946313	0.9436	0.951185	0.930748
		xylose	0	0	0.131518	0.290596	0.796204	0.927982	1.018206	0.922917	0.973463	0.907056	0.949365
		xylose norm.	0	0	0.129166	0.2854	0.781967	0.911389	1	0.906415	0.956056	0.890837	0.93239
		arabinose	0	0	0.369644	0.437497	0.952618	0.949254	0.954514	0.834543	0.825755	0.892373	0.897443
		arabinose norm.	0	0	0	0	0.263046	0.594964	0.854047	1.000356	1.03016	1.105284	1.08678
	Trial 2	glucose	0	0	0	0	0.23799	0.538291	0.772695	0.905067	0.932032	1	0.983259
		glucose norm.	0	0	0	0	0.238042	0.687036	0.893819	0.768357	0.972306	0.996473	1.025184
		xylose	0	0	0	0	0.232194	0.670159	0.871862	0.749482	0.948421	0.971995	1
		xylose norm.	0	0	0	0	0.232194	0.670159	0.871862	0.749482	0.948421	0.971995	1
		arabinose	0	0	0.049737	0.413717	0.80873	0.930496	0.959646	0.916125	0.953266	0.909677	
		arabinose norm.	0	0	0	0	0.049737	0.413717	0.80873	0.930496	0.959646	0.916125	0.909677
Biochar 1	Trial 1	glucose	0	1.105225418	0.953723	0.962394	0.909766	0.91346	1.004266	1.003411	0.997301	0.887725	1.011557
		glucose norm.	0	1	0.862922	0.870767	0.82315	0.826492	0.908653	0.907879	0.90235	0.803207	0.91525
		xylose	0	1.253003755	1.255612	1.287267	1.194435	1.115806	1.293263	1.165625	1.179246	1.188638	1.353101
		xylose norm.	0	0.926023898	0.927951	0.951346	0.882739	0.824629	0.955777	0.861447	0.871514	0.878455	1
		arabinose	0	0.841934877	0.799303	0.8419	0.74837	0.825454	0.943685	0.799303	0.832076	0.810449	0.99322
		arabinose norm.	0	0.836131026	0.894012	0.769993	0.905382	0.855486	0.818946	0.848224	0.835026	0.842994	1.229243
	Trial 2	glucose	0	0.680199963	0.727286	0.626396	0.736536	0.695946	0.666219	0.690038	0.679301	0.685783	1
		glucose norm.	0	0.785230905	0.921649	0.733314	0.909038	0.821544	0.854508	0.890346	0.84353	0.886265	1.020574
		xylose	0	0.76940122	0.903069	0.718531	0.890712	0.804983	0.837282	0.872397	0.826525	0.868398	1
		xylose norm.	0	0.744468148	0.867967	0.739926	0.874455	0.876538	0.839434	0.850801	0.823062	0.827141	1.057749
		arabinose	0	0.703823088	0.82058	0.699529	0.826713	0.828683	0.793604	0.804335	0.778126	0.781982	1
		arabinose norm.	0	0.403999304	0.713477	0.956518	1.199518	1.234969	1.304066	1.349976	1.295813	1.265374	1.256731
Biochar 2	Trial 1	glucose	0	0.299263979	0.528511	0.708544	0.888547	0.914808	0.965992	1	0.959878	0.937331	0.930928
		glucose norm.	0	0.480449845	0.744881	1.085766	1.188246	1.237581	1.290971	1.377692	1.349626	1.308208	1.299753
		xylose	0	0.348735264	0.540673	0.788105	0.86249	0.8983	0.937053	1	0.979628	0.949565	0.943428
		xylose norm.	0	0.463870036	0.727878	1.013611	1.132563	1.205868	1.217234	1.273094	1.270005	1.24173	1.263363
		arabinose	0	0.364364322	0.57174	0.796179	0.889614	0.947195	0.956123	1	0.997573	0.975364	0.992356
		arabinose norm.	0	0.736726	0.77433	0.785606	0.821983	0.837857	0.925875				
	Trial 2	glucose	0	0.293237439	0.65422	0.774124	0.881381	0.91617	1.147689	0.997349	0.801954	0.822069	1.130515
		glucose norm.	0	0.25550245	0.570032	0.674506	0.767962	0.798274	1	0.869006	0.698755	0.716282	0.985036
		xylose	0	0.239859431	0.641684	0.775993	0.840277	0.929857	0.98396	0.943604	1.03385	1.247275	1.40103
		xylose norm.	0	0.171202243	0.458009	0.553874	0.599757	0.663696	0.702312	0.673508	0.737922	0.890256	1
		arabinose	0	0.26708409	0.75585	0.807743	0.956623	0.898619	1.015898	1.000933	1.017147	0.873832	1.046221
		arabinose norm.	0	0.255284687	0.722458	0.772058	0.914361	0.858919	0.971017	0.956714	0.972211	0.835228	1
Biochar 3	Trial 1	5-HMF	0	0.696370501	0.778868	0.963259	0.994696		1.025106	1.114521	0.842684	1.006251	1.002541
		5-HMF norm.	0	0.624816151	0.698837	0.864281	0.892488		0.919773	1	0.756095	0.902855	0.899527
		furfural	0	0.624669785	0.822139	0.886871	0.940456		0.990165	1.00276	0.950553	1.022761	1.014518
		furfural norm.	0	0.615730648	0.810374	0.87418	0.926998		0.975996	0.988411	0.93695	1.008125	1
		glucose	0	1.061191265	0.934969								
		xylose	0	0.927330501	0.965065								
	Trial 2	5-HMF	0	0.259209	0.538111	0.621722	0.432526	0.72587	0.537642	0.709449	0.823846	0.796025	
		5-HMF norm.	0	0.096517495	0.542061	0.679325	0.751374	0.82845	0.483779	0.872673	0.857618	0.878725	0.899325
		furfural	0	0.043595	0.275017	0.759186	1.01829	1.052112	1.086698	1.052012	0.832875	1.462954	
		5-HMF norm.	0	0.029799	0.187988	0.51894	0.696051	0.71917	0.742811	0.719101	0.56931	1	
		furfural	0	0.080227765	0.317316	0.567128	0.701291	0.802605	0.826018	0.896988	0.873367	0.894546	0.907584
		5-HMF	0	0.539010004	0.549603		0.685429	0.721372	0.674281	0.662098	0.76687	1.040595	
Biochar 4	Trial 1	5-HMF norm.	0	0.517982587	0.528162		0.65869	0.693231	0.647976	0.636268	0.736954	1	
		furfural	0	0.944745258	0.754654		0.995112	0.517098	0.980802	1.001695	0.970024	0.91105	
		furfural norm.	0	0.94314655	0.753377		0.993428	0.516223	0.979142	1	0.968383	0.909508	
		5-HMF	0	0.296877196	0.639672	0.774026	0.790962	1.031542	0.996941	0.83647	0.904305	0.832932	0.892033
		5-HMF norm.	0	0.287799323	0.620113	0.750358	0.766776	1	0.966457	0.810893	0.876654	0.807463	0.864757
		furfural	0	0.414723948	0.75309	0.800595	0.897145	0.938253	1.001063	0.992335	0.985635	0.981002	1.035552
	Trial 2	furfural norm.	0	0.400486048	0.727235	0.77311	0.866345	0.906042	0.966695	0.958267	0.951797	0.947323	1
		5-HMF	0	0.089204577	0.257335	0.349763	0.663607	0.822081	0.475617	0.560112	0.688961	0.846019	0.851381
		furfural	0	0.259398148	0.590536	0.6804	0.732809	0.756269	0.828696	0.828004	0.84472	0.905126	0.917206
		5-HMF	0	0.006436789	0.063963	0.135103	0.463115	0.463115	0.522108	0.642448	0.714678	0.786651	0.821146
		furfural	0	0.127540192	0.295802	0.522412	0.732911	0.732911	0.801932	0.85466	0.923355	0.94854	0.971273
		5-HMF	0	0.843444949	0.814561	0.942568	0.983824	0.936297	0.938116	0.831064	0.926881	0.930028	0.838965
Biochar 5	Trial 1	furfural	0	0.896021873	0.978712	1.087194	0.955166	0.95005	0.915535	0.92487	0.658852	0.924223	0.943996
		furfural norm.	0	0.824159904	0.900218	1	0.878561	0.873855	0.842108	0.850695	0.606011	0.850099	0.868286
		5-HMF	0	0.816689269	0.827054	0.869624	0.865815	0.881157	0.884648	0.88608	0.86732	0.929979	0.909988
		furfural	0	1.00559825	1.117245	0.959192	0.950616	1.05084	1.168234	0.595159	0.925298	1.055412	1.043925
		furfural norm.	0	0.860784959	0.956354	0.821061	0.813721	0.899512	1	0.509451	0.792049	0.903425	0.893593
		furfural norm.	0	0.860784959	0.956354	0.821061	0.813721	0.899512	1	0.509451	0.792049	0.903425	0.893593

Data 12: pH of the Collected Effluents for the Positive Displacement Pump

pH of Collected Effluents, Positive Displacement Pump												
Adsorbent	Trial #	Control pH	pH at 5 mL	pH at 10 mL	pH at 15 mL	pH at 20 mL	pH at 25 mL	pH at 30 mL	pH at 35 mL	pH at 40 mL	pH at 45 mL	pH at 50 mL
Activated Carbon	1	3.3										
	2	3.31	7.05	7.22	5.4	4.53	4.26	4.1	4	3.93	3.75	3.62
	3	3.28	6.77	5.53	4.37	4.15	3.93	3.83	3.75	3.68	3.61	3.53
	4	3.4	7.57	7.5	4.8	4.18	3.88	3.71	2.42	2.33	3.43	3.45
Biochar 1	1	3.37	3.17	4.47		4.29	3.97	3.8	3.82	3.75	3.8	3.71
	2	3.38	4.63	4.21	4.03	4.02	4	4.03	3.91	3.7	2.15	2.54
	3	3.37	3.34	4.16	3.14	3.25	3.04	3	2.41	2.36	2.68	2.3
Biochar 2	1	3.34	6.45	6.49	3.8	4.56	5.88	3.34	4.55	4.28	4.26	4.32
	2	3.41	6.3	6.25	5.84	5.96	4.25	4.7	4.48	3.74	3.76	3.74

Data 13: pH of the Collected Effluents for the CO₂ Peltier Pump

pH of Collected Effluents, CO ₂ Peltier Pump												
Adsorbent	Trial #	Control pH	pH at 5 mL	pH at 10 mL	pH at 15 mL	pH at 20 mL	pH at 25 mL	pH at 30 mL	pH at 40 mL	pH at 50 mL	pH at 60 mL	pH at 70 mL
Activated Carbon	1	3.3	6.98	6.91	5.32	4.42	4.02	3.7	3.46	3.4	3.31	3.28
	2	3.34	6.7	7.03	6.35	4.63	4.21	4.06	3.77	3.51	3.34	3.29
Biochar 1	1	3.3	4.6	4.43	4.12	4	3.91	3.78	3.67	3.63	3.57	3.53
	2	3.29	4.55	4.43	4.17	3.95	3.8	3.71	3.69	3.58	3.5	3.48
Biochar 2	1	3.32	6.78	5.46	5.27	5.12	5.02	5.01	4.93	4.89	4.79	4.68
	2	3.54	6.09	5.28	5.14	5.03	4.97	4.94	4.84	4.77	4.74	4.66
Biochar 3	1	3.62	6.63	6.86	6.04	5.53	5.27	4.95	4.75	4.52	4.33	4.23
	2	3.5	7.89	7.43	6.66	5.63	5.14	4.88	4.69	4.44	4.29	4.18
Biochar 4	1	3.51	7.17	5.37	4.93	4.7	4.57	4.32	4.24	4.04	3.93	3.83
	2	3.53	7.49	6.65	5.27	4.86	4.66	4.42	4.18	3.99	3.9	3.81
Biochar 5	1	3.35	3.93	4.05	3.86	3.72	3.64	3.56	3.52	3.48	3.46	3.45
	2	3.39	4.4	4.09	4.06	3.89	3.7	3.58	3.55	3.52	3.47	3.46
Biochar 6	1	3.5	5.43	5.29	5.05	4.9	4.8	4.73	4.67	4.53	4.42	4.24
	2	3.38	7.39	6.81	5.81	5.31	4.88	4.76	4.57	4.36	4.22	4.07
Activated Biochar 4	1	3.38	8.72	8.89	8.42	7.47	6.82	6.27	5.5	4.99	4.86	4.71
	2	3.31	9.58	10.08	8.55	7.35	6.98	6.1	5.34	4.67	4.35	4.28

Data 14: Saturation and Breakthrough Capacity, Calculated from Results from the CO₂ Peltier Pump

Saturation and Breakthrough Capacity, CO ₂ Peltier Pump				
Adsorbent	Trial	Compound	Saturation Capacity (mg/g)	Breakthrough Capacity (mg/g)
Activated Carbon	Trial 1	glucose norm.	20.02997811	13.82036125
		xylose norm.	19.7653656	13.64067142
		arabinose	19.28216606	5
	Trial 2	glucose norm.	27.03609034	15
		xylose norm.	27.25028824	15
		arabinose	23.82161281	14.87565847
Biochar 1	Trial 1	glucose norm.	10.55784234	2.5
		xylose norm.	9.154062242	2.684940256
		arabinose	13.25317858	2.895162807
	Trial 2	glucose norm.	22.12031454	3.299500092
		xylose norm.	12.61370831	3.076496951
		arabinose norm.	16.00673949	3.240442281
Biochar 2	Trial 1	glucose norm.	12.42995832	4.251840052
		xylose norm.	11.77151827	4.128161839
		arabinose norm.	10.29246778	4.089089196
		5-HMF	8.86409509	5
		furfural	5.162561655	5
	Trial 2	glucose norm.	19.4030164	4.361243875
		xylose norm.	24.48311954	4.571994393
		arabinose norm.	12.46045064	4.361788283
		5-HMF norm.	12.08179977	3.437959623
		furfural norm.	7.451275319	3.46067338
Biochar 4	Trial 1	5-HMF	30.60864515	5
		furfural	21.29623575	4.758706263
	Trial 2	5-HMF norm.	32.13011814	9.92550209
		furfural	20.27509876	4.799430587
Biochar 5	Trial 1	5-HMF norm.	25.4821246	3.705043533
		furfural norm.	10.04745956	2.642133626
	Trial 2	5-HMF norm.	16.35246696	4.280501691
		furfural norm.	10.80982641	3.998784881
Biochar 6	Trial 1	5-HMF	30.31509619	4.776988557
		furfural	18.32317303	4.351504631
	Trial 2	5-HMF	34.88202331	14.31024327
		furfural	19.80571183	4.681149519
Activated Biochar 4	Trial 1	5-HMF	9.286105359	2.891387628
		furfural norm.	13.89073884	2.93960024
	Trial 2	5-HMF	10.67971411	2.958276827
		furfural norm.	14.22562215	2.848037602

Data 15: Percent Ethanol Produced from Detoxified Lignocellulose Biomass

Percent Ethanol Produced from Detoxified Lignocellulose Biomass								
Adsorbent	Average Saturation Capacity (mg/g)		Average Saturation Capacity (g/g)		Concentration in the Effluent (g/L)		Ethanol Produced (% of Control)	
	5-HMF	furfural	5-HMF	furfural	5-HMF	furfural	5-HMF	furfural
Biochar 2	10.5	6.3	0.0105	0.0063	0.85	0.91	29.9	25.061573
Biochar 4	31.4	20.8	0.0314	0.0208	0.5514286	0.7028571	31.691429	39.378231
Biochar 5	20.9	10.4	0.0209	0.0104	0.7014286	0.8514286	30.791429	28.732672
Biochar 6	32.6	19	0.0326	0.019	0.5342857	0.7285714	31.794286	37.398843
Activated Biochar 4	10	14.1	0.01	0.0141	0.8571429	0.7985714	29.857143	32.30082

Appendix B: Sample Calculations

Sample Calculation 1: Total and Volatile Solid

Calculating the Total and Volatile Solid Percentage: values shown below are from the first trial of testing biochar 1's total and volatile solid percentage

Known Values:

Crucible weight: 26.6121 g

Initial Sample Weight: 1.0137 g

Mass of Dry Substrate: 27.3853 g

Mass of Incinerated Substrate: 26.6629 g

$$TS = \frac{\text{mass of dry substrate}}{(\text{mass of wet substrate mix})} * 100$$

$$TS = \frac{(27.3853 \text{ g} - 26.6121 \text{ g})}{(1.0137 \text{ g})} * 100$$

$$TS = 76.28 \%$$

$$VS = TS - \left(\frac{\text{mass of incinerated substrate}}{\text{mass of dry substrate}} \right) * 100$$

$$VS = 76.28 - \left(\frac{26.6629 \text{ g} - 26.6121 \text{ g}}{1.0137 \text{ g}} \right) * 100$$

$$VS = 71.26\%$$

Sample Calculation 2: Ratio of Biochar to Hydrolysate

Determining the ratio of biochar to hydrolysate: The weight of the components from the synthetic sugarcane hydrolysate are from the first batch of hydrolysate made.

Known Values:

Mass of Glucose: 1.0197 g

Mass of Xylose: 1.0029 g

Mass of Arabinose: 1.0722 g

Mass of 5-HMF: 1.0072 g

Mass of Furfural: 1.0886 g

Mass of Acetic Acid: 1.0006 g

Mass of Water: 995.4 g

Calculating the Weight of the Hydrolysate:

$$\rho_{Mix} = \frac{m_{glucose} + m_{xylose} + m_{arabinose} + m_{5-HMF} + m_{furfural} + m_{acetic\ acid} + m_{water}}{volume}$$
$$\rho_{Mix} = \frac{1.0197\ g + 1.0029\ g + 1.0722\ g + 1.0072\ g + 1.0886\ g + 1.0006\ g + 995.3358\ g}{1000\ mL}$$

$$\rho_{Mix} = 1.001527\ \frac{g}{mL}$$

$$weight\ of\ hydrolysate = (\rho_{Mix})(Volume\ of\ Hydrolysate\ used\ in\ one\ trial)$$

$$weight\ of\ hydrolysate = (1.0\ \frac{g}{mL})(70\ mL)$$

$$weight\ of\ hydrolysate = 70\ g$$

If one gram of biochar was used in every trial the ratio of adsorbent to hydrolysate is

$$1\ g : 70\ g$$

$$Ratio = 0.0142 = 1.42\ \%$$

Sample Calculation 3: Ergun Equation

All equation variables are listed below:

ΔP = the pressure drop

μ = the fluid viscosity

L = the height of the bed

ϵ = the void space

v_s = superficial velocity

D_p = equivalent spherical diameter of the packing

ρ = the density of the fluid

The Ergun equation can be seen here:

$$\Delta p = \frac{150\mu L}{D_p^2} \frac{(1 - \epsilon)^2}{\epsilon^3} v_s + \frac{1.75L\rho}{D_p} \frac{(1 - \epsilon)}{\epsilon^3} v_s |v_s|$$

Sample Calculation 4: Interpretation of HPLC data of Glucose

Calculating the Concentration of Glucose: value shown below is from the first trial of testing the adsorption capacity biochar 1, using the CO₂ Peltier Pump.

Known Values:

Volume: 5 mL

HPLC Area of Glucose: 209840

Calibration Curve for Glucose: $y = 255709x + 26419$

Solving for Concentration of Glucose

$$(209840) = 255709x + 26419$$

$$x = 0.717$$

Sample Calculation 5: Normalizing a Breakthrough Curve

All breakthrough curves with concentrations above one were normalized. This is a sample calculation for normalizing a point in the breakthrough curve for glucose. The point is from trial one with biochar 1 as the adsorbent.

Known Values:

$$x_{\text{Maximum}} = 1.105225$$

$$x_{\text{Minimum}} = 0$$

$$x = 0.953$$

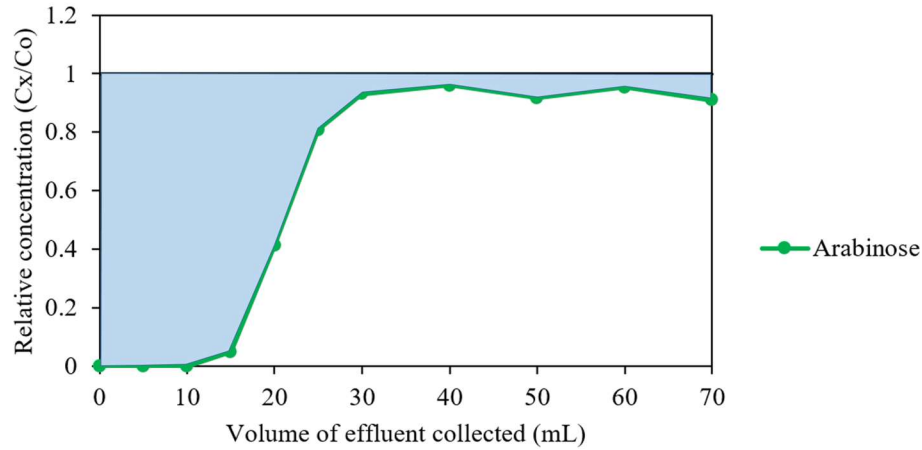
If a value of C_x/C_o was greater than one in a breakthrough curve, then all points on the curve were normalized using the equation shown below:

$$\begin{aligned} x_{\text{normalized}} &= \frac{(x - x_{\text{minimum}})}{(x_{\text{maximum}} - x_{\text{minimum}})} \\ x_{\text{normalized}} &= \frac{(0.9053 - 0)}{(1.105225 - 0)} \\ x_{\text{normalized}} &= 0.862 \end{aligned}$$

Sample Calculation 6: Saturation Capacity

Calculating the Saturation Capacity of arabinose: breakthrough curve shown below is from the second trial of testing activated carbon, while using the CO₂ Peltier Pump

Area in blue is the saturation capacity:



The blue area was found using Reimann sum and the equation below:

$$\frac{(x_{n+1} + x_n)}{2} (x_{n+1} - x_n)$$

Each point on the graph was plugged into the equation shown above and summed to find the total area.

Once the area was found it was subtracted from 70 to reveal the area of the blue: 23.82 mL

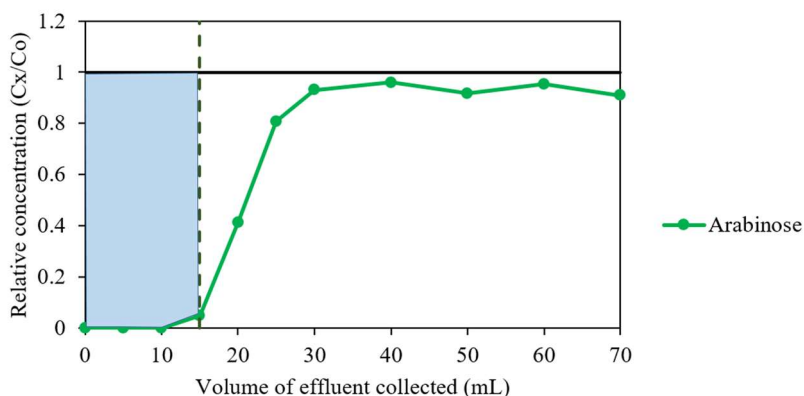
Then to calculate the saturation capacity the area was divided by the mass of the adsorbent and multiplied by the concentration of the compound in the feed.

$$\begin{aligned} \text{saturation capacity} &= 23.82 \text{ mL} \div 1 \text{ gram of biochar} \times \frac{1 \text{ g}}{1000 \text{ mL}} \\ \text{saturation capacity} &= 23.82 \text{ mg/g} \end{aligned}$$

Sample Calculation 7: Breakthrough Capacity

Calculating the breakthrough capacity of arabinose: breakthrough curve shown below is from the second trial of testing activated carbon, while using the CO₂ Peltier Pump

Area in blue is the breakthrough capacity:



The blue area was found using Reimann sum and the equation below:

$$\frac{(x_{n+1} + x_n)}{2} (x_{n+1} - x_n)$$

All points up to the breakthrough point were plugged into the equation shown above and summed to find the total area. Once the area was found it was subtracted from 15 to reveal the area of the blue: 14.87 mL

Then to calculate the breakthrough capacity the area was divided by the mass of the adsorbent and multiplied by the concentration of the compound in the feed.

$$\begin{aligned} \text{breakthrough capacity} &= 14.87 \text{ mL} \div 1 \text{ gram of biochar} \times \frac{1 \text{ g}}{1000 \text{ mL}} \\ \text{breakthrough capacity} &= 14.87 \text{ mg/g} \end{aligned}$$

Sample Calculation 8: Percent Ethanol Produced from Detoxified Lignocellulose Biomass

Calculating the percent of ethanol produced in the presence of inhibitors: shown below is biochar 4's saturation capacity of 5-HMF and furfural

Known Values;

Capacity for 5-HMF: 10.5 mg/g

Capacity for furfural: 6.3 mg/g

Calculating the concentration of 5-HMF remaining in Effluent:

$$\begin{aligned}10.5 \text{ mg/g} &= 0.0105 \text{ g/g} \\0.07 \text{ g} - 0.0105 \text{ g} &= 0.0595 \text{ g} \\ \frac{0.0595 \text{ g}}{70 \text{ mL}} * \frac{1000 \text{ mL}}{1 \text{ L}} &= 0.85 \text{ g/L}\end{aligned}$$

Calculating the concentration of furfural remaining in Effluent:

$$\begin{aligned}6.3 \text{ mg/g} &= 0.0064 \text{ g/g} \\0.07 \text{ g} - 0.0064 \text{ g} &= 0.0637 \text{ g} \\ \frac{0.0637 \text{ g}}{70 \text{ mL}} * \frac{1000 \text{ mL}}{1 \text{ L}} &= 0.91 \text{ g/L}\end{aligned}$$

Calculation of the amount of ethanol produced in the presence of 5-HMF, equation is based on research performed by Delgenes et al.

$$\begin{aligned}\% \text{ ethanol produced} &= 6(x) + 35 \\ \% \text{ ethanol produced} &= 6(0.85) + 35 \\ \% \text{ ethanol produced} &= 29.9 \%\end{aligned}$$

Calculation of the amount of ethanol produced in the presence of furfural, equation is based on research performed by Delgenes et al.

$$\begin{aligned}\% \text{ ethanol produced} &= 43.33x^2 - 139x + 115.67 \\ \% \text{ ethanol produced} &= 43.33(0.91)^2 - 139(0.91) + 115.67 \\ \% \text{ ethanol produced} &= 25.1 \%\end{aligned}$$

Appendix C: Images

Image 1: Biochar 1, Cool Terra

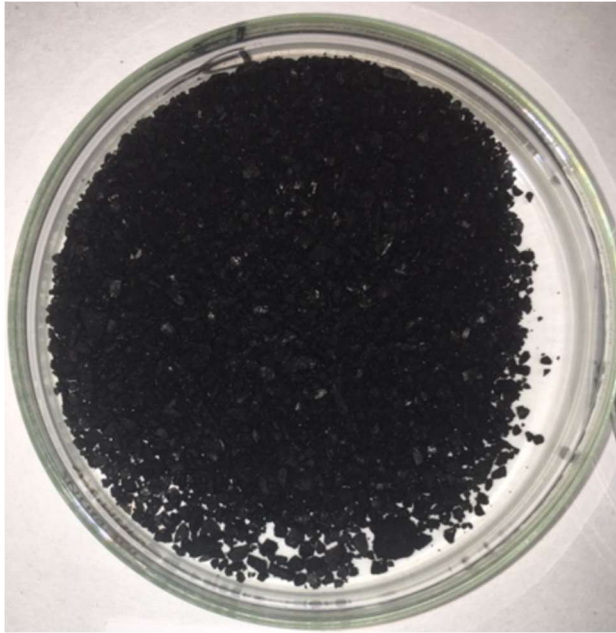


Image 2: Biochar 2, Blak 1



Image 3: Biochar 3, Rogue Biochar

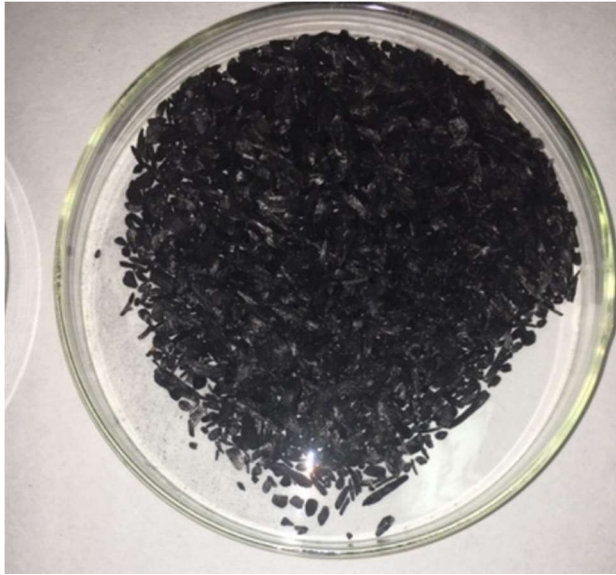


Image 4: Biochar 4, Gold Standard



Image 5: Biochar 5, Art 1



Image 6: Biochar 6, Wakefield

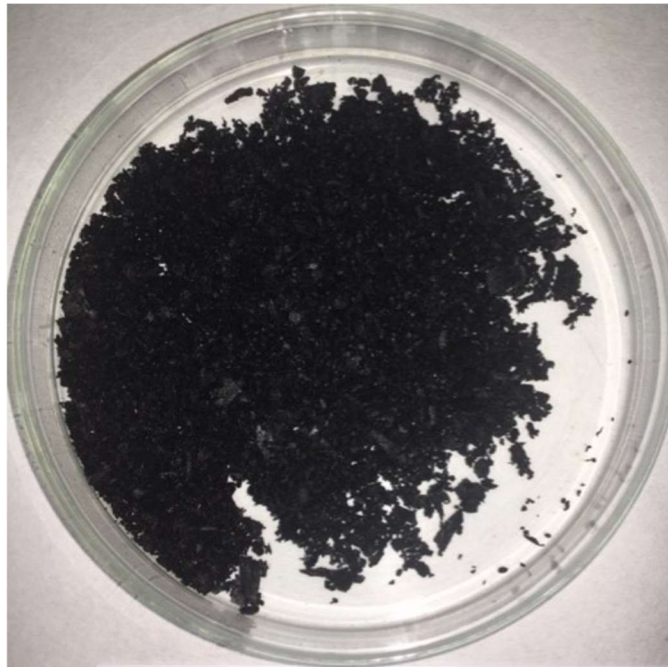


Image 7: Photograph of the Supercritical Peltier CO₂ Pump Display.

